The University of Alberta

Scintigraphic Imaging During Gene Therapy

by

Kevin Wayne Morin

A Thesis

Submitted to The Faculty of Graduate Studies and Research

in partial fulfilment of the requirements for the degree of

Doctor of Philosophy

in

Pharmaceutical Sciences

Faculty of Pharmacy and Pharmaceutical Sciences

Edmonton, Alberta

Spring 1997

The University of Alberta

Release Form

Name of Author Kevin Wayne Morin

Title of Thesis Scintigraphic Imaging During Gene Therapy

Degree for which thesis was presented Doctor of Philosophy

Year this degree granted 1997

Permanent Address:

12815-128 Street

Edmonton Alberta Canada

T5L-1E4

Date Mar. 25 1997

The University of Alberta

Faculty of Graduate Studies and Research

The undersigned certify that they have read, and recommend to the Faculty of Graduate Studies and Research, for acceptance, a thesis entitled Scintigraphic Imaging During Gene Therapy submitted by Kevin Wayne Morin in partial fulfilment of the requirements for the degree of Doctor of Philosophy in Pharmaceutical Sciences.

.....

Dr. Leonard Wiebe (Supervisor)

.....

Dr. Edward Knaus (Supervisor)

.....

Dr. John Samuel

.....

Dr. Carol Cass

.....

Dr. Juri Tjuvajev (External Examiner)

Date.....Mar 25 1997.....

Dedication

To

Wilma and Aime, who taught the most important lessons.....

Abstract

In vivo transduction of the herpes simplex virus type-1 thymidine kinase (HSV-1 TK) gene and subsequent administration of antiviral drugs such as ganciclovir has emerged as a promising gene therapy protocol for the treatment of cancer and other proliferative disorders. However, the evaluation of HSV-1 TK gene expression in transduced tissue has previously relied on invasive techniques for detection. This thesis describes an investigation that demonstrated that HSV-1 TK expression can be detected non-invasively using gamma scintigraphy.

Synthetic chemical methodologies were developed to synthesize and radiolabel a series of (*E*)-5-(2-iodovinyl)uracil nucleoside substrates for herpes simplex virus type-1 thymidine kinase (HSV-1 TK). (*E*)-5-(2-Iodovinyl)-2'-deoxyuridine (IVDU), (*E*)-5-(2-iodovinyl)-3'-*O*-(1-methyl-1,4-dihydropyridine-3-carbonyl)-2'-deoxyuridine (IVDU-CDS), (*E*)-5-(2-iodovinyl)-2'-fluoro-2'-deoxyuridine (IVFRU), (*E*)-5-(2-iodovinyl)-3'-*O*-(1-methyl-1,4-dihydropyridine-3-carbonyl)-2'-fluoro-2'-deoxyuridine (IVFRU-CDS), (*E*)-5-(2-iodovinyl)-2'-fluoro-2'-deoxyarabinouridine (IVFAU), (*E*)-5-(2-iodovinyl)-3'-*O*-(1-methyl-1,4-dihydropyridine-3-carbonyl)-2'-fluoro-2'-deoxyarabinouridine (IVFAU-CDS) and (*E*)-5-(2-iodovinyl)arabinouridine (IVAU) were synthesized and radiolabelled with isotopes of iodine ([^{125}I] and [^{131}I]) in 63-83% radiochemical yield.

The cytostatic activities of IVDU, IVFRU, IVFAU, IVDU-CDS, IVFRU-CDS and IVFAU-CDS in mammalian FM3A TK$^-$/HSV-1 TK$^+$ cells were substantially higher than in FM3A TK$^-$ or FM3A/0 cells. In HSV-1 TK expressing cells, the iodovinyl nucleoside derivatives displayed IC_{50} values varying from 0.005-0.093 μM. The cytostatic activity in FM3A TK$^-$/HSV-1 TK$^+$ cells was 1333-10423 times higher than in FM3A/0 cells which lack

HSV-1 TK expression. Thymidylate synthase inhibition after selective phosphorylation is implicated as the major mechanism for cytostatic activity.

Cellular uptake of these radiolabelled compounds was evaluated *in vitro*. All compounds showed minimal uptake in the KBALB cell line. However, increased uptake was observed for several compounds in KBALB-STK cells which were transduced with a replication incompetent Moloney murine leukemia virus vector encoding the HSV-1 TK gene. Because of its favorable properties and selective sequestering in HSV-1 TK-expressing cells, radiolabelled IVFRU emerged as the most promising candidate for further *in vivo* studies.

Transfection of KBALB cells with the pMLBKTK plasmid vector carrying the HSV-1 TK gene using calcium phosphate coprecipitation or cationic liposomes also resulted in transfectants that were capable of accumulating [^{125}I]IVFRU. Similarly, *in vitro* transduction of KBALB cells with the LSNtk retroviral vector resulted in cells that were capable of accumulating [^{125}I]IVFRU to a greater extent than non-transduced KBALB cells, indicating that the retroviral vector was capable of transferring the HSV-1 TK gene to KBALB cells. Intratumoral injection of LSNtk producer cell supernatant resulted in a statistically significant increase in tumor uptake of [^{131}I]IVFRU at 8 h after administration.

Biodistribution studies in Balb/c mice bearing subcutanous KBALB or KBALB-STK tumors demonstrated that the HSV-1 TK-expressing tumors were capable of selectively accumulating radiolabelled IVFRU *in vivo*. In animals bearing KBALB tumors, which lack HSV-1 TK-expression, mean tumor radioactivity accounted for only 0.23% dose/g while the blood radioactivity represented 0.81% dose/g 8 h after i.v. injection. In contrast, the KBALB-STK tumors, which expressed HSV-1 TK, accumulated much

more radioactivity than the KBALB tumors 8 h after administration of [^{131}I]IVFRU. A mean uptake of 1.77% dose/g of tissue in the HSV-1 TK-expressing tumors and a concurrent decrease in mean blood radioactivity resulted in a 10-fold increase in tumor/blood ratio compared to animals bearing KBALB tumors.

Planar scintigraphic images of mice with subcutaneous KBALB-STK tumors revealed the HSV-1 TK expressing tumors 8 h after intravenous injection of [^{131}I]IVFRU. Daily treatment with ganciclovir (100 mg/kg day) for 7 days resulted in complete regression of KBALB-STK tumors in all treated animals. Scintigraphic imaging of KBALB-STK tumor-bearing animals after 4 days of ganciclovir treatment failed to delineate the treated tumors which were approximately 4.5 mm in diameter. In contrast to the images obtained before ganciclovir treatment, there was a complete absence of [^{131}I]IVFRU in the tumor after 4 days of ganciclovir treatment. However, the images obtained before ganciclovir tretment were of excellent quality and illustrate that HSV-1 TK-expressing tissue can be clearly delineated with [^{131}I]IVFRU using planar scintigraphy before ganciclovir treatment.

Acknowledgements

My sincere thanks to:

Prof. Len Wiebe and Prof. Ed Knaus for their excellent supervision, guidance and mentoring. Their enthusiastic support made this investigation possible.

Prof. Jan Balzarini and Prof. Erik De Clercq for their collaborative efforts in this project.

Dr. Elena Atrazheva and Dr. Lung-Ji Chang for significant assistance.

Dr. James Diakur, Dr. Diane Jette, Dr. Majid Cheraghali, Dr. Debbie James, Mr. Gordon Haverland, Mr. Takashi Iwashina, Dr. John Mercer, Dr. Steve McQuarrie, Mr. Chris Ediss and Dr. Derrick Freitag for many helpful discussions during this work.

Prof. Yasuoki Murakami and Prof. Akita for their support and guidance during my 4 month visit at the School of Pharmaceutical Sciences, Toho University, Japan.

Special thanks to my family for their constant encouragement and support.

Alberta Heritage Foundation for Medical Research for financial support.

Table of Contents

List of Figures

List of Tables

List of Abbreviations

AAV	adeno-associated virus
ACV	acyclovir
ACV-CDS	acyclovir-chemical delivery system
AFP	alpha-fetoprotein
AMP	adenosine-5'-monophosphate
ara-ATP	adenine-arabinoside-5'-triphosphate
ara-IMP	inosine-arabinoside-5'-monophosphate
araM	6-methoxypurine-arabinoside
ATP	adenosine-5'-triphosphate
BBB	blood brain barrier
BCV	buciclovir
BVDC	(*E*)-5-(2-bromovinyl)-2'-deoxycytidine
BVDU	(*E*)-5-(2-bromovinyl)-2'-deoxyuridine
°C	degrees Celsius
CBG	cyclobutG
CD	cytosine deaminase
CDS	chemical delivery system
CEA	carcinoembyonic antigen
CMV	cytomegalovirus
CNS	central nervous system

cpm	counts per minute
dCMP	deoxycytidine-5'-monophosphate
dCyd	deoxycytidine
DMEM	Dulbecco's modified Eagle's media
DMF	dimethyl formamide
DMSO	dimethyl sulfoxide
DNA	deoxyribonucleic acid
DOTAP	N-[1-(2,3-dioleoyloxy)propyl]-N,N,N-trimethylammonium methylsulfate
dThd	deoxythymidine
dTMP	deoxythymidine-5'-monophosphate
DTT	dithiothreitol
dUMP	deoxyuridine-5'-monophosphate
EBNA-1	Epstein-Barr virus nuclear antigen-1
EDTA	ethylene diamine tetracetic acid
EBV	Epstein-Barr virus
E. coli	*Escherichia coli*
FBS	fetal bovine serum
FIAU	5-iodo-2'-fluoro-2'-deoxyarabinouridine
Fig.	figure
FIRU	5-iodo-2'-fluoro-2'-deoxyuridine
FMAU	5-methyl-2'-fluoro-2'-deoxyarabinouridine
g	gram(s)

G-418	geneticin
GBq	gigaBecquerel
GCV	ganciclovir
GCV-CDS	ganciclovir chemical delivery system
GFAP	glial fibrillary acidic protein
GM-CSF	ganulocyte macrophage colony stimulating factor
h	hour(s)
HMPAO	^{99m}Tc-hexamethylpropyleneamineoxime
HPLC	high performance liquid chromatography
HRMS	high resolution mass spectrometry
HSE	herpes simplex encephalitis
HSV-1	herpes simplex virus type-1
HSV-2	herpes simplex virus type-2
IC_{50}	inhibitory concentration-50
IL-2	interleukin-2
ip	intraperitoneal
iv	intravenous
IVAU	(*E*)-5-(2-iodovinyl)arabinouridine
IVDU	(*E*)-5-(2-iodovinyl)-2'-deoxyuridine
IVDU-CDS	(*E*)-5-(2-iodovinyl)-2'-deoxyuridine-chemical delivery system
IVDU-MP	(*E*)-5-(2-iodovinyl)-2'-deoxyuridine-5'-monophosphate
IVFAU	(*E*)-5-(2-iodovinyl)-2'-fluoro-2'-deoxyarabinouridine

IVFAU-CDS	(*E*)-5-(2-iodovinyl)-2'-fluoro-2'-deoxyarabinouridine-chemical delivery system
IVFRU	(*E*)-5-(2-iodovinyl)-2'-fluoro-2'-deoxyuridine
IVFRU-CDS	(*E*)-5-(2-iodovinyl)-2'-fluoro-2'-deoxyuridine-chemical delivery system
kb	kilobase(s)
kg	kilogram(s)
LTR	long terminal repeats
L	liter(s)
M	molar
MBP	myelin basic protein
MBq	megaBecquerel
mg	milligram(s)
min	minute(s)
mL	milliliter(s)
mm	millimeter(s)
mM	millimolar
mmol	millimole(s)
mol	mole(s)
MoMLV	Moloney murine leukemia virus
mp	melting point
µCi	microCurie(s)
µg	microgram(s)

µL	microliter(s)
µmol	micromole(s)
N	normal
NAD	nicotinamide adenine dinucleotide
NBMPR	S-(4-nitrobenzyl)-6-thioinosine
NCS	N-chlorosuccinimide
nm	nanometer(s)
NMR	nuclear magnetic resonance spectrometry
P	partition coefficient
PCV	penciclovir
PET	positron emission tomography
PLP	myelin proteolipid protein
pmol	picomole(s)
PNP	purine nucleoside phosphorylase
RNA	ribonucleic acid
S-BVDU	(E)-5-(2-bromovinyl)-4'-thio-2'-deoxyuridine
SPA	surfactant protein A
sp. act.	specific activity
SPECT	single photon emission computed tomography
SV-40	simian virus 40
t 1/2	half-life
TBAF	tetrabutyl ammonium fluoride

TBDMSCl	*tert*-butyldimethylsilyl chloride
TBq	teraBecquerel
TFT	5-trifluoromethyl-2'-deoxyuridine
TFT-CDS	5-trifluoromethyl-2'-deoxyuridine-chemical delivery system
THF	tetrahydrofuran
TK	thymidine kinase
TLC	thin layer chromatography
TS	thymidylate synthase
UV	ultraviolet
VZV	varicella zoster virus
VPC	vector producing cell(s)
XGPRT	xanthine-guanine phosphoribosyltransferase

I. Introduction

A. Suicide Genes in Cancer Gene Therapy

Although cancer chemotherapy has undergone intensive development over the last few decades, half of all cancers remain unresponsive to chemotherapeutic intervention. Considering that in Canada more than 100,000 new cases of cancer are diagnosed each year, it remains a major health problem.[1] However, with the advent of molecular biology, new treatment strategies have emerged which are based on transfer of genetic material. Historically, gene therapy has referred to the transfer of a normal gene to correct an aberrant gene defect. This traditional view of corrective gene transfer is applicable to a variety of genetic abnormalities including cancer.[2] However, introducing genes into neoplastic cells that are not normally present or expressed in these cells is a general strategy that encompasses most experimental approaches for cancer therapy. There are more than 100 human gene therapy clinical trials underway for the treatment of cancer.[3] These trials can be classified into 6 general categories: immunogene/cytokine, tumor suppressor, antioncogene/antisense, drug resistance, gene marking, and drug sensitivity. The latter category has also been referred to as metabolic suicide gene therapy.[4]

In principle, suicide genes function as negative selectable markers when introduced into cells. The protein products of suicide genes are capable of converting a prodrug into a toxic metabolite. Cells genetically modified to express these genes essentially commit metabolic suicide in the presence of a convertible prodrug. Ideally, the prodrugs will have minimal toxicity before conversion, leading to a selective toxic effect in cells

expressing the suicide gene. Since prodrug metabolism is a fundamental prerequisite for cytotoxic effect, basic medicinal chemistry is an integral component of the design of suicide gene therapy paradigms. In general, unique metabolic pathways that are not normally present in neoplastic cells represent the most attractive targets for selective prodrug activation. Metabolic pathways present in bacteria, viruses or fungi have been exploited as targets by medicinal chemists, with considerable success largely because they diverge from mammalian metabolic pathways. Therefore, it is not suprising that most prodrug-activating gene products used in suicide gene therapy are enzymes from non-mammalian organisms.[5]

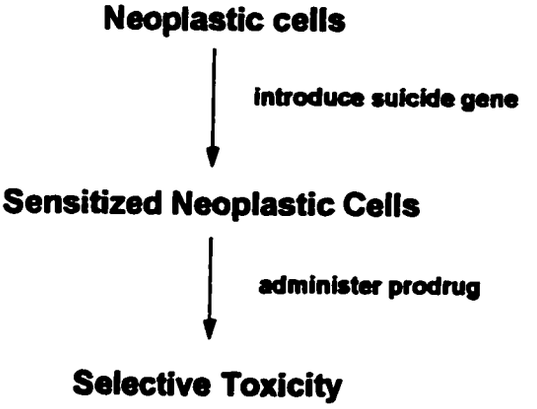

Fig. 1 Suicide gene therapy paradigm.

The cytosine deaminase (CD) gene from *Escherichia coli* is an example of a bacterial gene with potential applications in cancer gene therapy. In 1992, Mullen and co-workers first reported that murine fibroblasts could be sensitized to 5-fluorocytosine, with considerable cytotoxicity after transfection with an expression vector carrying the CD

gene.[6] The biochemical basis of toxicity is the selective conversion of 5-fluorocytosine, a relatively innocuous compound, to 5-fluorouracil by cytosine deaminase and then to cytotoxic derivatives by host enzymes.[7] Since mammalian cells lack cytosine deaminase or other metabolic pathways to convert cytosine to uracil, the conversion of 5-fluorocytosine will occur only in cells expressing CD. The clinical efficacy of 5-fluorouracil in colorectal cancer prompted several investgators to introduce the CD gene into experimental models of human and murine colorectal carcinoma.[8-10] *In vitro* and *in vivo* exposure of CD-expressing colorectal carcinoma cells to 5-fluorocytosine results in selective metabolism and toxicity.

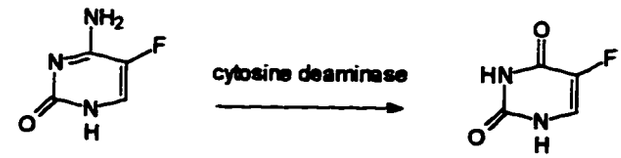

5-fluorocytosine 5-fluorouracil

Fig. 2 Conversion of 5-fluorocytosine to 5-fluorouracil by CD.

When CD-expressing cells are cultured in the presence of cells lacking CD expression, there is a cytotoxic effect conferred to these latter cells.[11] This cytotoxic effect on neighboring cells is commonly called the "bystander effect".[12] The bystander effect has been observed *in vivo* when as few as 4% of tumor cells engineered to express CD can lead to complete tumor regression after 5-fluorocytosine administration in a murine model.[13] The mechanisms responsible for the *in vitro* and *in vivo* bystander effect are poorly understood. However, it has been demonstrated *in vitro* that after selective conversion of 5-fluorocytosine in CD-expressing cells, 5-fluorouracil can diffuse out of the cells and exert cytotoxic effects on cells

lacking CD expression.[14] After *in vivo* treatment of CD-expressing experimental tumors with 5-fluorocytosine, an efficient immune response to wild type tumor can occur.[15,16] The immune response is tumor-specific and may be a contributing mechanism for *in vivo* tumor regression.

Attempts to target cellular CD expression have involved the incorporation of tissue-specific regulatory signals on CD expression vectors that function in neoplasms with cell-specific expression. For example, the carcinoembryonic antigen (CEA) is a tumor marker that is highly expressed in various carcinomas including colorectal carcinoma.[17] By ligating the CEA promoter to a promoterless CD gene, a chimeric gene capable of selective expression in CEA-expressing colorectal carcinoma was constructed.[18] Thus, human colorectal carcinoma cells overexpressing CEA are highly sensitive to 5-fluorocytosine when transfected with the construct possessing the CEA promoter and CD gene. A similar strategy was used to construct a retroviral vector with the erbB-1 promoter driving expression of the CD gene. This vector was constructed since one-third of breast and pancreatic cancers overexpress the erbB-1 oncogene.[19] High-level CD expression was present in breast and pancreatic cell lines overexpressing the erbB-1 protein, but not in cell lines lacking the oncogene product. The *trans*-activating properties of the Epstein-Barr virus nuclear antigen-1 (EBNA-1) has been exploited to regulate CD expression in cells transformed by Epstein-Barr virus (EBV).[20] This selectivity is achieved by incorporating the repeating sequences of the EBV replicon on a vector carrying the CD gene. Vector systems and regulatory elements used in suicide gene therapy will be discussed later in more detail.

The nfnB gene of *Escherichia coli,* which encodes for a nitroreductase, has recently been cloned and the product has been identified

as having potential utility as a prodrug-activating enzyme.[21] This nitroreductase can reduce nitro functionalities on aromatic compounds that are resistant to reduction by human reductases.[22] Consequently, compounds have been designed and synthesized that are selectively reduced by *E. coli* nitroreductase to yield cytotoxic derivatives.[23] In particular, nitroaromatics have been shown to be selectively reduced to bifunctional alkylating agents with considerable cytotoxicity. One compound, CB1954 ((5-aziridin-1-yl)-2,4-dinitrobenzamide), has been identified as a promising cytotoxic prodrug for clinical evaluation as part of a gene therapy protocol involving transfer of the *E. coli* nitroreductase gene into human neoplasms. Exposure of human tumor cells to CB1954 after nitroreductase gene transfer via a retroviral vector has been shown to be an effective and selective cytotoxic strategy.[24] Mixtures of transduced and non-transduced cells were exposed to CB1954 in vitro, and a bystander effect was observed since CB1954 toxicity was extended to neighboring, non-transduced cells in culture. However, the presence of 30-50% transduced cells was necessary for 90% cell killing after exposure to CB1954. Interstrand DNA cross linking appears to be the principle mechanism of cytotoxicity after nitroreductase-mediated reduction of CB1954 to a bifunctional alkylating derivative.[25]

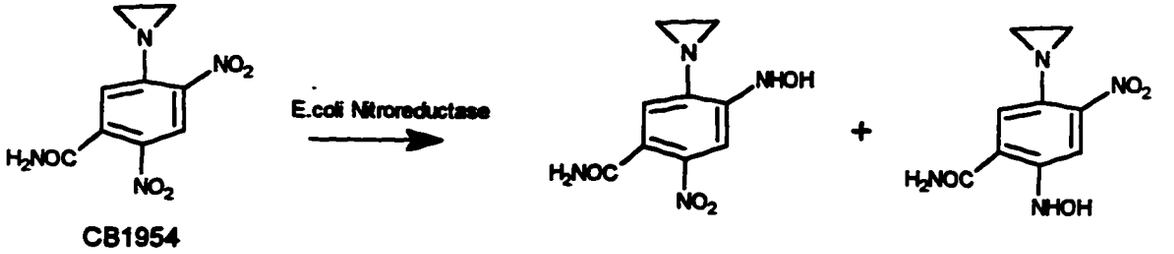

CB1954

Fig. 3 Reductive activation of CB1954 to cytotoxic derivatives.

The product of the *Escherichia coli* DeoD gene is a purine nucleoside phosphorylase (PNP) that differs from the mammalian enzyme in its substrate specificity and, unlike human purine nucleoside phosphorylase, is capable of catalyzing the conversion of the non-toxic prodrug 6-methylpurine-2'-deoxyriboside to the highly toxic 6-methylpurine.[26] This purine derivative exerts its toxicity by interfering with *de novo* nucleotide biosynthesis after metabolic processing by adenine phosphoribosyl transferase.[27,28] Because 6-methylpurine diffuses easily across membranes, it can mediate an effective bystander killing effect on neighboring cells that do not express *E. coli* PNP. In mixed cultures containing increasing percentages of cells with gene expression, 100% cancer cell growth arrest and total population killing of human melanoma cell cultures was demonstrated when as few as 1-2% of cells expressed *E. coli* PNP.[29] Similarly, expression of *E. coli* PNP in < 1% of a human colonic carcinoma cell line led to the death of virtually all bystander cells after treatment with 6-methylpurine-2'-deoxyriboside.[27] Minimal toxicity was observed in non-transfected or *E. coli* LacZ transfected cells that were treated with this compound. Bystander toxicity with DeoD gene transfer and 6-methylpurine-2'-deoxyriboside exposure *in vitro* is observed at a level substantially higher than that of other tumor sensitization strategies. However, *in vivo* studies have not yet appeared in the literature.

Fig. 4 Phosphorolytic conversion to 6-methylpurine.

Cyclophosphamide is used clinically as an alkylating prodrug that requires metabolism by liver cytochrome P450 enzymes for antitumor activity.[30] The principle human gene products CPY2B6, CYP3A4 and several CYP2C enzymes have been identified as the catalysts responsible for activation of cyclophosphamide.[31,32] The activation of cyclophosphamide involves metabolic hydroxylation to yield 4-hydroxy-cyclophosphamide which exists in equilibrium with the corresponding ring-opened aldophosphamide. Spontaneous β-elimination yields acrolein and the electrophilic phosphoramide mustard which is therapeutically active.[33] The rat liver CYP2B1 enzyme is also capable of hydroxylating cyclophosphamide in a manner identical to that observed in humans.[34]

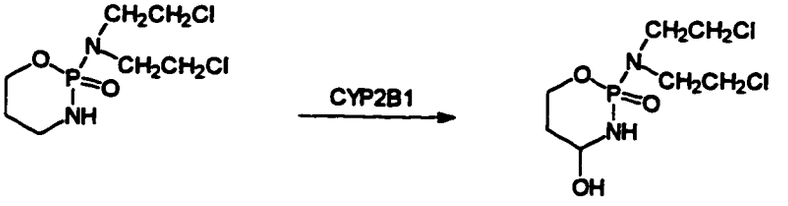

Fig. 5 Hydroxylation of cyclophosphamide by CYP2B1.

Introduction of the CYP2B1 gene into rat C6 glioma cells renders the cultured tumor cells sensitive to cyclophosphamide.[35] Furthermore, C6 cells bearing this gene are more sensitive than parental cells to the cytotoxic action of cyclophosphamide when grown subcutaneously in the flanks of athymic mice. Murine fibroblasts producing a retrovirus vector encoding CYP2B1 were grafted into the brains of athymic mice seeded with rat C6 gliomas. Administration of cyclophosphamide prevented the development of meningeal neoplasia and led to partial regression of the tumor mass. A similar study with the 9L gliosarcoma tumor model in rats also demonstrated

that CYP2B1 gene transfer can sensitize these tumors to the cytotoxic effects of cyclophosphamide.[36] A replication-defective adenoviral vector was used to indroduce the CYP2B1 gene into human breast MCF-7 tumors grown subcutaneously in nude mice.[37] These transduced tumors were found to be 15-20-fold more sensitive to the cytotoxic effects of cyclophosphamide compared to non-transduced tumors. However, since cyclophosphamide can be activated by normal host P450 isozymes, it is less selective than other prodrug-activating paradigms.

Xanthine-guanine phosphoribosyltransferase (XGPRT), an enzyme found in *Escherichia coli,* catalyzes the conversion of xanthine to its ribonucleotide form, which can contribute to purine synthesis via the salvage pathway.[38] However, unlike mammalian hypoxanthine-guanine phosphotransferases, XGPRT is capable of efficiently converting 6-thioxanthine to 6-thioxanthine ribonucleotide monophosphate, the principle cytotoxic metabolite which interferes with *de novo* synthesis of purine nucleotides in a manner analogous to 6-mercaptopurine ribonucleotide monophosphate.[39] Introducing the XGPRT gene into teratocarcinoma cells has been shown to sensitize these cells to 6-thioxanthine.[40] Similar results were observed when the XGPRT gene was indroduced into murine K3T3 sarcoma cells on a retroviral vector.[41] Transduced cells were up to 86-fold more sensitive to 6-thioxanthine than non-transduced cells. Moreover, 19 out of 20 mice bearing XGPRT-expressing K3T3 sarcomas had durable tumor regressions after *in vivo* treatment with 6-thioxanthine.

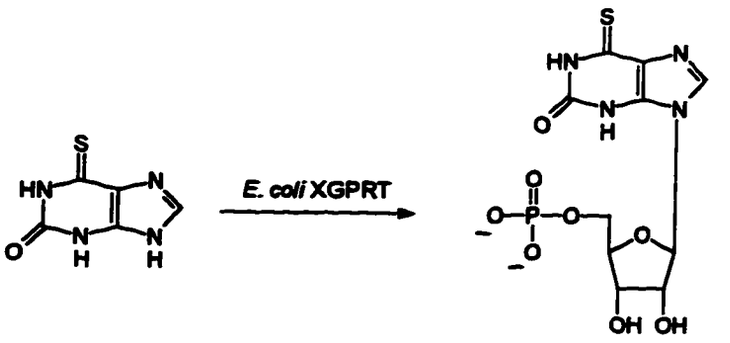

Fig. 6 Activation of 6-thioxanthine by *E. coli* XGPRT.

Varicella zoster virus (VZV) is a herpes virus that encodes a unique thymidine kinase (VZV TK) that, unlike mammalian thymidine kinases, can selectively activate prodrug derivatives structurally related to 6-methoxypurine arabinoside (araM).[42] Following initial phosphorylation by VZV TK, araM-monophosphate is demethoxylated by AMP deaminase to form ara-IMP, which is converted to ara-ATP, a cytotoxic derivative, by the sequential actions of the cellular adenylosuccinate synthetase, adenylosuccinate lyase, and nucleotide kinases.[43,44] In a study by Huber and coworkers, replication-defective, amphotrophic retroviruses were constructed containing a chimeric VZV TK gene that is transcriptionally regulated by either the hepatoma-associated alpha-fetoprotein or liver-associated albumin transcriptional regulatory sequences.[45] Subsequent to retroviral infection, expression of VZV TK was limited to either alpha-fetoprotein- or albumin-positive cells, respectively. Cells that selectively expressed VZV TK became selectively sensitive to araM due to the VZV TK-dependent anabolism of araM to araATP. In HepG2 cells, which express both alpha-fetoprotein and albumin, an IC_{50} < 0.5 μM was observed. Hence, these retrovirus-delivered chimeric genes generated tissue-specific

expression of VZV TK, tissue-specific anabolism of araM to araATP, and tissue-specific cytotoxicity due to araM exposure. However, *in vivo* studies examining the potential of this strategy are lacking at present.

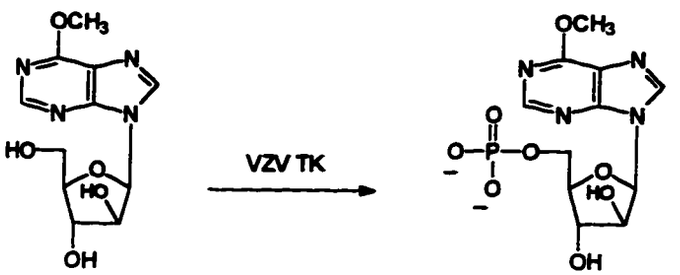

Fig. 7 Activation of 6-methoxypurine arabinoside by VZV TK.

B. HSV-1 Thymidine Kinase

Herpes simplex virus type-1 thymidine kinase (HSV-1 TK) is a virus-specific enzyme that has been extensively studied for more than two decades. Unlike mammalian thymidine kinases which catalyze the transfer of the γ-phosphate from ATP to deoxythymidine to produce deoxythymidine monophosphate (dTMP), HSV-1 TK has a broad substrate specificity and is capable of phosphorylating pyrimidine and purine nucleoside derivatives.[46,47] Recently, x-ray crystallographic evidence has shown that purine and pyrimidine nucleosides interact with the active site of HSV-1 TK in a similar manner.[48,49] However, HSV-1 TK is capable of sequential phosphorylation of pyrimidine nucleoside monophosphates to their corresponding diphosphate derivatives.[50,51] The unique properties of this virus-specific kinase have been exploited in the design of highly selective and potent antiherpetic compounds. Elion and coworkers discovered the acycloguanosine class of compounds, of which 9-(2-hydroxyethoxymethyl)guanine (acyclovir, ACV) is the prototype.[52] ACV has

extremely selective antiherpes activity due to selective initial phosphorylation by HSV-1 TK but not by host cellular kinases.[53] Further phosphorylation to the triphosphate derivative occurs by the action of host kinases.[54,55] ACV-triphosphate is the active anabolite of ACV and exerts its antiviral activity by preferential inhibition of virus-encoded DNA polymerase and by acting as a DNA chain terminator after incorporation into nascent DNA.[56,57] The specific metabolism of ACV to ACV-triphosphate has been shown to occur with cytotoxic effects in LM cells transfected with the HSV-1 TK gene.[58] In this study, a 53-fold increase in sensitivity to ACV was observed in murine LM cells expressing HSV-1 TK relative to wild type LM cells.

9-[[2-Hydroxy-1-(hydroxymethyl)ethoxy]methyl]guanine (ganciclovir, GCV) is an acycloguanosine analogue closely related to ACV. The antiviral activity and mechanism of activation of GCV are similar to ACV.[59,60] However, when GCV was evaluated for cytotoxic effect in murine LM cells transformed with UV inactivated HSV-1, it was found to be 120-fold more cytotoxic to HSV-1 TK expressing LM cells than wild type LM cells.[61] In contrast, cells transformed with UV inactivated HSV-1 were only 25-fold more sensitive to ACV than non-transformed cells.[62,63] The enhanced cytotoxicity of GCV in HSV-1-expressing cells has been attributed to its higher affinity for HSV-1 TK compared to ACV.

In 1986, Moolten first demonstrated that transfer of the HSV-1 TK gene into neoplasms followed by ganciclovir treatment could be exploited as a sensitization strategy for *in vivo* tumor treatment.[64] Murine K3T3 sarcoma cells transfected with the HSV-1 TK gene were 200 to 1000 times more sensitive to the cytotoxic effects of ganciclovir *in vitro* compared to non-transfected cells. Moreover, when Balb/c mice bearing HSV-1 TK-

expressing K3T3 sarcomas were treated with intraperitoneal administration of ganciclovir, complete tumor regression in all animals was observed. Based on these results, Moolten postulated that employing retroviral vectors for gene delivery would be more effective in the HSV-1 TK sensitization paradigm.[65]

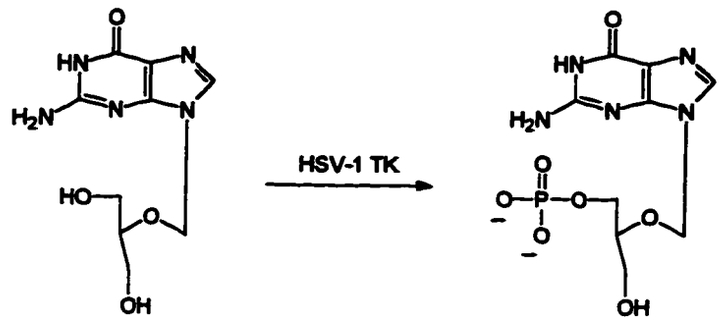

Fig. 8 Phosphorylation of ganciclovir by HSV-1 TK.

The most common type of retroviral vector used in gene therapy, including HSV-1 TK gene transfer, is based on the Moloney murine leukemia virus (MoMLV). The virus particle contains two identical copies of single-stranded RNA and is composed of a centrally located nucleoprotein core surrounded by a glycoprotein membrane coat. A wild type provirus contains three structural genes which encode for internal core proteins (*gag*), DNA polymerase and endonuclease (*pol*), and envelope glycoprotein (*env*). Like other retroviruses, MoMLV is packaged with its RNA-dependent DNA polymerase (reverse transcriptase). The provirus also contains two long terminal repeat (LTR) sequences that function as viral promoter, enhancer, repressor and polyadenylation signal.[66] The potential of MoMLV as a vector was realized with the advent of replication-defective vectors that could be propagated in producer cells with the absence of infectious helper virus. Mann and coworkers identified viral sequences (ψ packaging signal) located

5' to the *gag* coding region that were crucial for packaging of genomic RNA into MoMLV particles.[67] They created a packaging cell line (ψ-2 cells) that are murine fibroblasts transfected with a construct containing a MoMLV mutant that lacks the ψ sequences and therefore is incapable of packaging functions. However, this cell line can provide *trans*-complementation of structural components necessary for assembly of virus particles. Thus, when the ψ-2 cell line is transfected with a MoMLV construct containing the ψ signal, then the RNA of this construct is efficiently packaged. Of course, because of *trans*-complementation in the ψ-2 cells, it is possible to completely delete the *gag*, *pol* and *env* genes on the packaged construct and replace them with foreign genes.

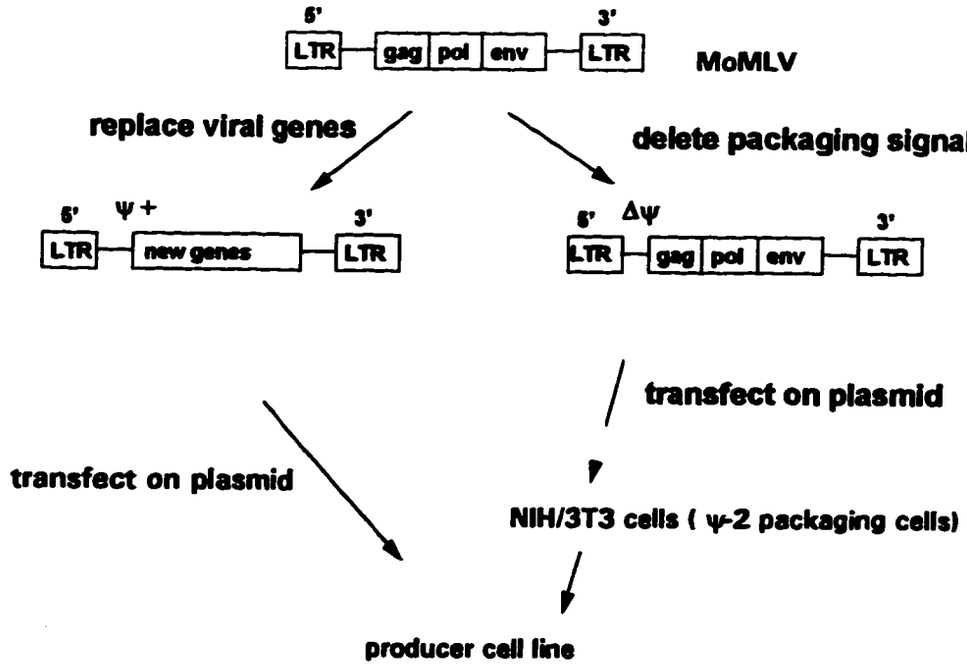

Fig. 9 Construction of ecotropic replication-incompetent MoMLV vector producer cells (based on ref. 67).

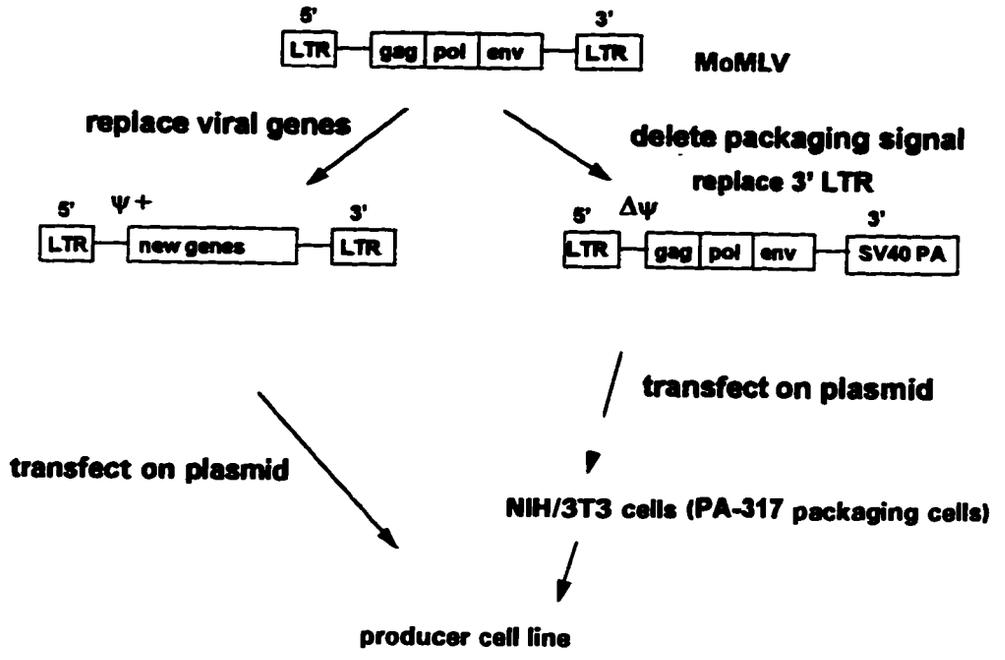

Fig. 10 Construction of amphotropic replication-incompetent MoMLV vector producer cells.

A limitation of retroviral vectors packaged in ψ-2 cells is that they retain a ecotropic host range where they are capable of transducing only rodent cells. However, by using *trans*-complementing MoMLV genomes that encode mutant envelope glycoproteins, packaging cells lines with an amphotropic or broad host range have been developed.[68,69] Most importantly, these latter packaging cell lines are capable of efficiently transducing human cells. Miller and coworkers further refined MoMLV packaging by constructing an amphotropic packaging cell line that was virtually incapable of homologous recombination events between the vector and packaging system.[70] By replacing the 3'-LTR with a SV-40 polyadenylation signal and deleting a portion of the 5'-LTR, they produced a MoMLV construct that is the *trans*-complementing component of the PA-

317 cell line. In addition, MoMLV packaging cell lines with amphotropic host range have been developed by using portions of the ψ- MoMLV genome on two separate plasmids as a strategy to eliminate recombination events.[71,72] These helper-free amphotropic retrovirus packaging cell lines are now used routinely in human gene therapy to safely produce replication-incompetent MoMLV vectors.

Replication-incompetent MoMLV vectors have some features that make them attractive for gene transfer in proliferative tissues. They are small vectors that can be easily manipulated with recombinant DNA techniques, provide long-term expression after efficient transduction and provide a degree of selectivity since integration into the host genome will only occur in cells that are replicating.[73] Therefore, many investigators have used this vector to introduce the HSV-1 gene into a variety of experimental neoplasms. In 1990, Moolten and Wells performed the first HSV-1 TK gene transfer into a murine K2 sarcoma cells with a replication-incompetent MoMLV vector derived from ψ-2 cells.[74] They found that transduced cells were sensitive to ganciclovir *in vitro* and that transduced tumors in mice could be completely eradicated after a short course of ganciclovir. However, in 37% of animals, tumor recurrence was observed and was associated with a loss of HSV-1 TK expression. Multiple transductions of the K2 cell line *in vitro* was subsequently found to produce cell lines that, after transplantation in Balb/c mice and treatment with ganciclovir could result in durable regressions in 100% of animals.[75] In contrast to K2 sarcomas, when rat C6 gliomas transduced *in vitro* with a retrovirus carrying the HSV-1 TK gene were grown in nude mice and treated with ganciclovir, all animals had durable regressions.[76] This latter scenario is more frequently observed when tumor cell lines are transduced with

retroviral vectors prior to implantation. *In vitro* transduction with MoMLV carrying the HSV-1 TK gene has also been performed on a variety of other cell lines with diverse properties including murine KBALB sarcoma, murine P388 leukemia cells, 9L rat glioma, rat XC hepatoma, rat Walker 256 meningeal carcinoma, human leukemia cells, human plasma cells, human lung carcinoma, human head and neck squamous carcinoma and human gastric carcinoma.[77-87] Invariably, introduction of the HSV-1 TK gene sensitizes cells to ganciclovir *in vitro* and *in vivo* after transplantation. A bystander effect is often seen. In general, cell cultures containing as few as 10% transduced cells can be completely killed *in vitro* following exposure to ganciclovir. Only one report has described complete ganciclovir resistance despite confirmed HSV-1 TK gene transfer and expression.[88]

Although *in vitro* transduction with MoMLV vectors and implantation of transduced neoplastic cells in experimental animals are useful models, the approach is not representative of an ideal *in vivo* sensitization strategy where the HSV-1 TK gene is introduced into a pre-existing tumor before ganciclovir treatment. Short and coworkers addressed this concern by developing an ingenious technique where vector producing cells (VPC) are grafted by stereotaxis directly into the brain of animals bearing gliomas.[89] The grafted packaging cells continually release retroviral vectors that transduce nearby replicating glioma cells. Since most adult brain cells are quiescent, the transduction of glioma cells is a selective process due to integration that only occurs in replicating cells. This technique was adapted for HSV-1 TK gene delivery to gliomas by Culver and colleagues with astonishing success.[90] In rats bearing 9L gliomas, they stereotactically injected VPC derived from PA-317 cells which secreted amphotropic vectors carrying the HSV-1 TK gene. Complete tumor regression was observed in

11 of 14 rats after ganciclovir treatment. These results were corroborated by others using glioma models and *in situ* VPC engraftment.[91-95] Bystander effects appeared to play a crucial role in tumor regression since tumor transduction efficiency is less than 50%, as determined by reporter gene expression, after producer cells are implanted.

Although *in situ* VPC-mediated gene delivery is effective, there is a theoretical possibility that retroviral vectors could escape the local brain environment and transduce other proliferating tissues. Since MoMLV integration could lead to insertional mutagenesis in normal tissues, toxicity studies were undertaken in rats and primates.[96] Proliferation of the VPC did not occur after intracerebral injection and VPC survival was limited to 7 to 14 days. No significant inflammatory response was observed in the meninges or brain parenchyma but endothelial cells were occasionally transduced in brain capillaries adjacent to the injected site of the VPC. No neurological deficits were observed in the rats or primates treated with the HSV- TK vector-producer cells, with or without ganciclovir. In primates injected with producer cells in the absence of brain tumors, magnetic resonance imaging before, during, and after ganciclovir administration showed minimal and localized breakdown of the blood-brain barrier without significant edema. Similarly, histological examination of the monkeys' brains showed no damage to neurons, astroglia, or myelin. Long-term clinical (> 9 months) and radiological (3 months) assessment of the primates revealed no evidence of toxicity. Therefore, several clinical trials were initiated involving stereotactic implantation of VPC secreting amphotropic retroviral vectors carrying the HSV-1 TK gene followed by ganciclovir treatment in humans with inoperable brain tumors.[97-100]

The successful application of VPC as vector delivery systems for experimental gliomas has prompted investigations with other tumor models. A rat model of leptomeningeal carcinomatosis has been shown to be efficiently transduced with intrathecal VPC resulting in eradication of neoplasia after treatment with ganciclovir.[101] Toxicity studies in rats and monkeys revealed that intrathecal or intraventricular administration of VPC did not result in adverse toxicity or transduction of normal brain tissue.[102] Thus, a clinical trial was initiated in patients with leptomeningeal carcinomatosis.[103] Similarly, a rat model of liver metastatic disease was found to be sensitive to ganciclovir after intratumoral injection of VPC with a 60-fold reduction in tumor mass compared to controls.[104] An evaluation of the toxicities associated with injecting VPC in the liver revealed that normal rat liver parenchyma is not transduced and clinical or histological evidence of toxicity is lacking.[105] Since VPC are xenogeneic, they are evenutally rejected by a non-murine host. Although it may be expected that VPC may be more efficiently eliminated by the host immune system if they are located at a hepatic site, it appears that the survival time of VPC at this site is similar (7-14 days) to that observed with stereotactic implantation in the brain. A phase 1 clinical trial is underway in patients with liver metasases of malignant melanoma.[106] An *in vivo* toxicity study in nude mice bearing a human breast carcinoma also demonstrated that implantation of VPC was not associated with overt systemic toxicity however, when exposed to ganciclovir, transduced cells were eradicated with a potent bystander effect.[107]

Although VPC are promising vehicles for efficient HSV-1 TK gene delivery, effort has been directed toward the development of other vector systems. Adenoviral vectors are large (38 kb) DNA viral vectors that offer

several important advantages over retroviral vectors. Unlike retroviral vectors, adenoviral vectors are capable of transducing both replicating and nondividing cells. They can be isolated in extremely high titer (10^{11} pfu/mL) obviating the need for VPC engraftment and they do not integrate their genetic material into recipient cells. A disadvantage of adenoviral vectors is the transient nature of gene expression, however this point may be less important for HSV-1 TK gene therapy applications since ganciclovir is usually administered within a few days after transduction.

Like retroviruses, adenoviral vectors are modified for use in gene therapy which renders them replication-defective. Vector constructs lack one or more early genes of the wild-type virus. Most frequently, the E1a gene , which encodes a transcriptional activator that is crucial for activation of other early genes, is deleted from adenoviral vector constructs.[108] *Trans*-complementation occurs when these constructs are introduced into the 293 human kidney packaging cell line which constitutively express the E1a protein product.[109] The E2a and E3 regions, which are not required for viral replication, are also deleted in some vector constructs which allow an increased packaging capacity and appears to decrease host immune response after infection.[110,111] Propagation of vector particles in 293 cells is usually followed by purification by ultracentifugation. The stability of adenoviral vectors to standard purification techniques is an important advantage over retroviral vectors which are highly sensitive to these manipulations due to facile degradation of the glycoprotein envelope during purification.

Initial studies of *in vivo* adenovirus-mediated HSV-1 TK gene transfer was performed in rat 9L and C6 glioma models.[112,113] Administration of ip ganciclovir after stereotactic injection of adenovirus vector resulted in

complete regression of 9L gliomas implanted in the brains of syngeneic Fischer 344 rats. The C6 glioma was slightly less sensitive *in vivo* but led to significant reductions of tumor volume. A comparison of the efficacy of *in vivo* HSV-1 TK gene transfer with an adenoviral vector and retroviral VPC in 9L gliomas indicated that there was no significant difference in the ability to induce tumor regression after treatment with ganciclovir.[114] However, it has been shown that some cell lines are more susceptible to adenoviral infection than others. In one comparative study, a human mesothelioma cell line was found to be much more sensitive to ganciclovir *in vitro* than human non-small cell lung carcinoma or ovarian carcinoma.[115] It was suggested that this differential sensitivity to ganciclovir may be related to expression of the vitronectin receptor which is neccesary for adenovirus internalization. *In vitro* and *in vivo* models of human and rat mesothelioma have been shown to be particularly sensitive to ganciclovir after adenoviral transduction.[116-120] Although human ovarian carcinoma is less susceptible to *in vivo* adenoviral transduction, significant prolongation of survival has been observed in a nude mouse model after adenoviral vector and ganciclovir administration.[121] Other *in vitro* and *in vivo* models of human and rodent tumors that respond to adenoviral delivery of the HSV-1 TK gene followed by ganciclovir include squamous cell carcinoma of the head and neck, melanoma, breast carcinoma, hepatocellular carcinoma, spinal cord tumors and prostate cancer.[122-128]

Adeno-associated virus (AAV) is a small single-stranded DNA virus that integrates into a specific site on chromosome 19 in non-dividing cells.[129] An AAV vector carrying the HSV-1 TK gene has been shown to sensitize human hepatocellular carcinoma cells to ganciclovir *in vitro*.[130] In addition, a replication-deficient, ribonucleotide reductase gene-deleted

herpes simplex type-1 virus (HSV-1) vector carrying an intact HSV-1 TK gene sensitized 9L gliomas in rats leading to prolonged surivival after treatment with ganciclovir.[131] Although AAV and HSV-1 vectors for gene delivery are still in developmental stages, they are promising viral vector systems for gene delivery to neoplasms. Non-viral gene delivery systems can also mediate HSV-1 TK gene delivery to tumors *in vivo*. Sugaya and coworkers could transfect a mouse tumor model with repeated administrations of plasmid-cationic liposome complexes.[132] However, as with most *in vivo* cationic liposome-mediated transfections, the efficiency of gene transfer was low. Plasmid conjugates that target certain internalized receptors could offer improved efficiency of gene transfer. One study reported the efficient *in vitro* transfection of squamous cell carcinoma cells using a plasmid carrying the HSV-1 TK gene complexed with a polylysine-anti-erythrocyte growth factor receptor antibody conjugate.[133] Tumor cells overexpressing the erythrocyte growth factor receptor were efficiently transfected and sensitized to ganciclovir.

Effort has been devoted to the development of vectors that have improved targeting to neoplastic cells. As mentioned earlier, cell-specific gene expression can be achieved using tissue-specific regulatory sequences to drive expression of other suicide genes. This concept is also applicable for the tissue-specific expression of the HSV-1 TK gene. The first experiment demonstrating the application of tissue-specific expression of HSV-1 TK was performed in mouse glioma cells.[134] The HSV-1 TK gene could be specifically controlled in mouse glioma cells by glial-specific promoters, including the 2.5 kb 5' flanking region of the mouse glial fibrillary acidic protein (GFAP) gene, the 1.3 kb 5' flanking region of the myelin basic protein (MBP) gene, and the 1.5 kb 5' flanking region of the

myelin proteolipid protein (PLP) gene. Various fibroblast, myeloma, and glioma cell lines were transduced with retrovirus vectors carrying each promoter. Only glioma cells were capable of expressing HSV-1 TK with the highest expression observed with the vector carrying the MBP promoter. These transduced cells were highly susceptible to the cytotoxic effects of ganciclovir.

A variety of other regulatory sequences have been exploited to promote HSV-1 TK gene expression. The CEA promoter has been used to specifically drive HSV-1 TK expression in animal models of pancreatic, gastric and lung cancer that overexpress CEA.[135-137] The alpha-fetoprotein (AFP) promoter, a liver-specific regulatory element that is only active in fetal liver tissue or liver neoplasms, has been incorporated in vectors to direct HSV-1 TK expression in hepatoma and hepatocellular carcinoma expressing this tumor-associated protein.[138-141] Similarly, enhanced expression of tyrosinase in melanoma cells has been exploited in a vector strategy where the tyrosinase promoter is ligated to the HSV-1 TK gene to direct melanoma-specific expression of the kinase.[142] Regulatory elements of the *myc* oncogene (*myc-max* response elements) have proven to be useful for cell-specific expression of HSV-1 TK in small cell lung carcinoma with high-level expression of the *myc* oncogene.[143] Human surfactant protein A (SPA) expression is considered a marker of respiratory epithelial differentiation and non-small cell lung carcinoma, therefore its regulatory sequences have been used on a plasmid construct to promote HSV-1 TK expression in non-small cell lung carcinoma.[144] Since the DF3/MUC1 gene encodes a mucin-like glycoprotein that is overexpressed in the majority of human breast cancers, its promoter sequences have been

used for tissue-specific regulation of HSV-1 TK gene expression in breast carcinoma.[145,146]

The rapid advancement of cytokine gene therapy in cancer has important implications in suicide gene therapy, including the HSV-1 TK/ganciclovir paradigm. Combination gene therapy where a cytokine gene is transferred with the HSV-1 TK gene followed by ganciclovir has yielded exciting results. The first report of combining the interleukin-2 (IL-2) gene with HSV-1 TK gene indicated that the IL-2 gene did not enhance tumoricidal effects in the rat 9L glioma model after ganciclovir treatment.[147] However, in a murine squamous cell carcinoma model, mice receiving both HSV-1 TK and IL-2 genes by intratumoral administration of adenoviral vectors had a significantly greater number of regressions of tumors compared to those treated with the HSV-1 TK gene and ganciclovir alone.[148] This synergism was confirmed in survival studies because mice treated with the combination therapy survived longer than mice receiving only HSV-1 TK gene and ganciclovir. In a murine model of colon carcinoma, adenoviral transfer of the IL-2 gene in combination with the HSV-1 TK gene led to an effective systemic antitumoral immunity against challenges of tumorigenic doses of parental tumor cells inoculated at distant sites.[149] The antitumoral immunity was associated with the presence of tumor-specific cytolytic CD8+ T lymphocytes. Longer-term immunity was observed with co-administration of the granulocyte-macrophage colony stimulating factor (GM-CSF) gene carried on an adenoviral vector in the same mouse model of colon carcinoma.[150] Thus, the combination of cytokine and HSV-1 TK gene transfer with ganciclovir administration is effective for inducing tumor regression and potentiating antitumor immunity.

A crucial component of the HSV-1 TK/ganciclovir gene therapy paradigm is the potent bystander effect that is elicited *in vivo*. This effect is necessary for successful suicide gene therapy since it is impossible to transduce every neoplastic cell *in vivo* within a tumor, even with highly efficient viral vectors. *In vitro* experiments have confirmed that metabolic cooperation between cells is an important mechanism contributing to the bystander effect.[151-155] Phosphorylated ganciclovir metabolites can be transferred through gap junctions from cells expressing HSV-1 TK to cells that do not express this kinase. Gap junctions are composed of connexin proteins which can allow cellular transfer of a variety of small molecules.[156] Moreover, enhanced connexin expression in HSV-1 TK-expressing neoplastic cells is correlated with a potent bystander effect *in vitro* after exposure to ganciclovir.[156,157] Another mechanism contributing to the bystander effect is the transfer of phosphorylated ganciclovir metabolites by phagocytosis of apoptotic vesicles. Apoptotic cell death is characterized by cell chromatin condensation, DNA fragmentation, cell shrinkage and formation of apoptotic vesicles.[158] Thus, when HSV-1 TK-expressing cells undergo apoptosis after exposure to ganciclovir, they break up into apoptotic vesicles that can be phagocytosed by nearby cells that lack HSV-1 TK expression.[77,159,160] The presence of phosphorylated ganciclovir metabolites in the apoptotic vesicles can then exert cytotoxic effects in non-transduced cells. However, like gap junction transfer, most evidence for metabolite transfer by apoptotic vesicle phagocytosis is from *in vitro* studies.

In vivo studies have confirmed that the HSV-1 TK/ganciclovir paradigm can induce potent anti-tumor immunity.[161,162] Tumor-infiltrating lymphocytes have been identified in some experimental models and release

of T-cell activating cytokines has been observed after ganciclovir treatment of HSV-1 TK-expressing tumors.[104,163] Moreover, the decreased efficacy of the gene therapy in immunocompromised animal models is indicative of the importance of an immunological component for anti-tumor effect. An additional mechanism of cytotoxicity is through disruption of tumor vasculature during ganciclovir administration. Intratumoral injection of VPC does not influence tumor growth or intratumoral vasculature. However, tumor vasculature decreases after initiation of ganciclovir therapy in HSV-1 TK transduced tumors with evidence of intratumoral hemorrhage. The transduction of endothelial cells during *in situ* gene therapy has been observed and is postulated to contribute to the multifocal hemorrhages after ganciclovir treatment.[93,164] Therefore, the vascular changes during this gene therapy protocol may induce tumor ischemia which may, in turn, contribute to the overall *in vivo* bystander effect.

The large number of investigations into the potential of the HSV-1 TK/ganciclovir therapy approach in cancer treatment has stimulated interest in other potential applications. A very provocative approach to controlling cell proliferation after transluminal coronary angioplasty has been described. Angioplasty is associated with cellular proliferation leading to occulsion of coronary vessels undergoing the procedure. Essentially, the technique involves adenovirus-mediated transduction of coronary endothelium by means of a modified balloon catheter. After angioplasty and transduction, ganciclovir is administered leading to cytotoxity in the proliferating endothelium and prevention of reocclusion.[165-167] Another potential use of the HSV-1 TK gene is as a "safety switch" during gene therapy. Incorporation of the HSV-1 TK gene on a vector as an *in vivo* negative selectable marker secondary to a therapeutic gene is thought to improve the

safety of gene transfer.[168] Complications of gene transfer could include, for example, overexpression of introduced genes for growth or angiogenic factors or insertional mutagenesis, both of which could cause uncontrolled cell growth. Therefore, the presence of the HSV-1 TK gene as a safety marker could be used, with ganciclovir, to eliminate cells that proliferate as a result of gene transfer.

C. Nucleoside derivatives with cytostatic activity against HSV-1 TK-expressing cells.

It is obvious, from the majority of the literature on HSV-1 TK gene therapy, that ganciclovir has been the drug of choice for most investigators. Ganciclovir is in wide clinical use as an antiviral for cytomegalovirus (CMV) infections and therefore it is logical that this clinically-acceptable compound should be used extensively.[169,170] However, other anti-herpetic compounds that are selectively phosphorylated by HSV-1 TK have a great deal of potential in the HSV-1 TK gene therapy paradigm. Balzarini, De Clercq and coworkers have conducted several comparative studies that indicate that potent antiherpetic pyrimidine nucleoside derivatives can function as surrogates of ganciclovir *in vitro* with greater potency. However, a comparative sudy involving a series of acycloguanosine derivatives (acyclovir, ganciclovir, penciclovir, buciclovir and cyclobutG) found that ganciclovir was the most potent in the series with an IC_{50} of 1.0 μM in the FM3A TK^-/HSV-1 TK^+ murine mammary carcinoma cell line which is transfected with the HSV-1 TK gene.[171] These results support the observations mentioned previously in HSV-1 TK-expressing LM cells.

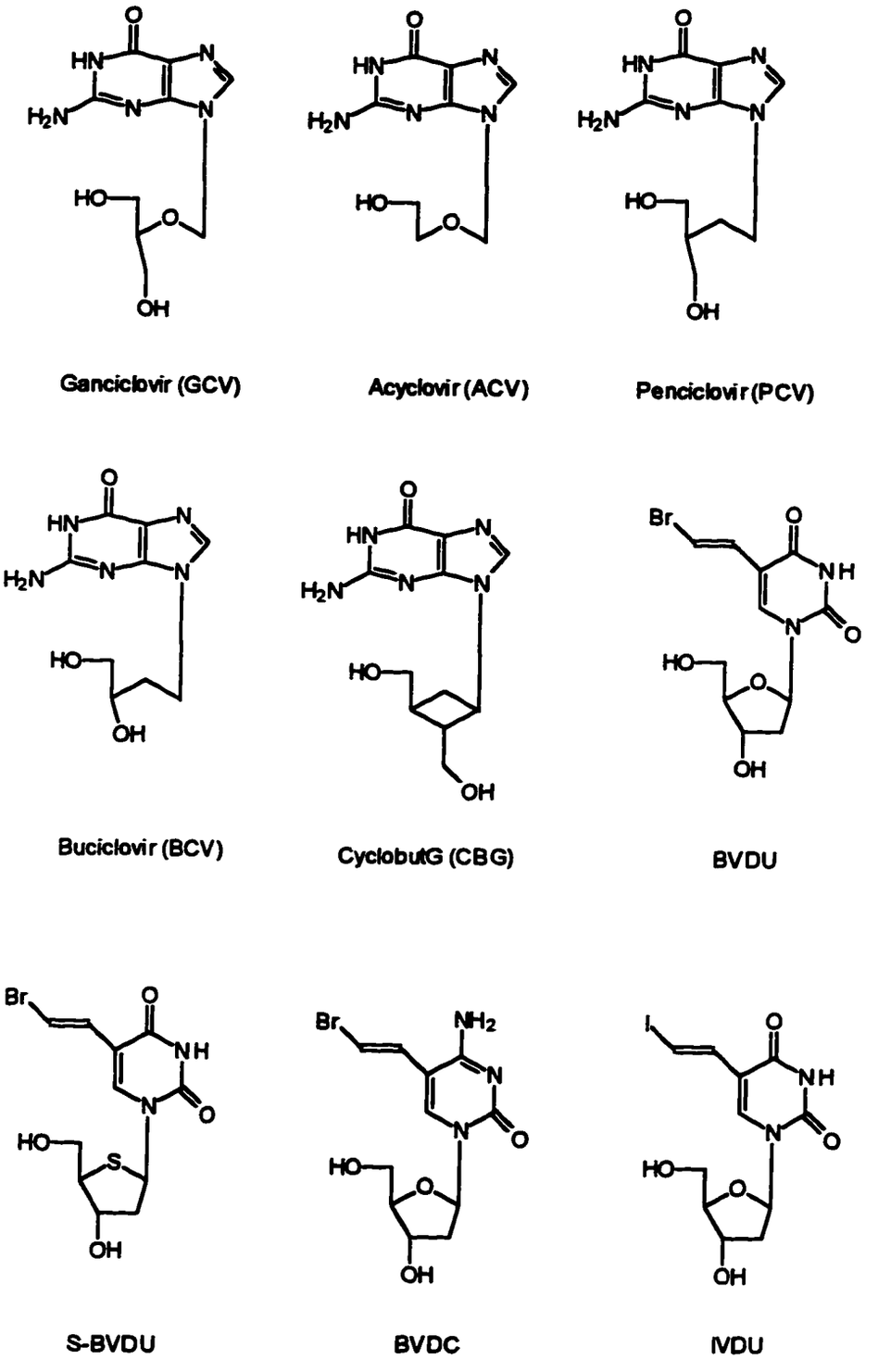

Fig. 11 Examples of acycloguanosine and (*E*)-5-(2-halovinyl)-nucleosides with cytostatic activity against FM3A TK^-/HSV-1 TK^+ cells.

Several 5-substituted compounds related to (*E*)-5-(2-bromovinyl)-2'-deoxyuridine (BVDU) are extremely potent *in vitro* against FM3A TK$^-$/HSV-1 TK$^+$ cells. (*E*)-5-(2-bromovinyl)-2'-deoxycytidine (BVDC), (*E*)-5-(2-iodovinyl)-2'-deoxyuridine (IVDU), BVDU and the 4'-thio derivative of BVDU (S-BVDU) possess IC_{50} values in the range of 0.002-0.007 μM against FM3A TK$^-$/HSV-1 TK$^+$ cells.[171-174] The concentrations required for 50% inhibition of proliferation of cells lacking HSV-1 TK expression is 10,000-50,000-fold higher than for HSV-1 TK$^+$ cells. Other structurally related 5-substituted-2'-deoxyuridine compounds have been evaluated for their inhibitory activity against FM3A TK$^-$/HSV-1 TK$^+$ cells.[172,175] However, in general, they are less potent and/or less selective than the (*E*)-5-(2-halovinyl)-2'-deoxyuridine derivatives in their anti-proliferative activity against HSV-1 TK-expressing cells.

The principle mechanisms of cytotoxicity for 5-substituted-2'-deoxyuridine derivatives are different than the mechanisms responsible for the toxicity of acycloguanosine compounds. As mentioned earlier, acycloguanosine derivatives exert their toxicity after phosphorylation to the triphosphate derivative which can inhibit DNA polymerases and terminate DNA elongation after incorporation. These mechanisms have been shown to be responsible for ganciclovir toxicity in FM3A TK$^-$/HSV-1 TK$^+$ cells.[176] In contrast, several 5-substituted-2'-deoxyuridine derivatives are potent inhibitors of thymidylate synthase (TS) after selective phosphorylation by HSV-1 TK. TS catalyzes the methylation of 2'-deoxyuridine monophosphate (dUMP) to thymidine monophosphate (dTMP) and can be inhibited by a variety of 5-substituted-2'-deoxyuridylate derivatives.[177] In detailed studies examining the metabolism of IVDU and BVDU in FM3A TK$^-$/HSV-1 TK$^+$ cells, phosphorylation to the 5'-mono, 5'-di, and 5'-triphosphate

derivatives was detected and there was a close correlation between TS inhibition and cytostatic activity.[178,179,180] Although the triphosphate derivatives are substrates for DNA polymerases, the toxicity associated with polymerase inhibition or incorporation into DNA appears to be minor compared to that associated with TS inhibition. These results are supported by the observation that IVDU is phosphorylated in FM3A TK^-/HSV-2 TK^+ cells only to the monophosphate derivative (IVDU-MP) and retains potent cytostatic activity in these cells. Unlike HSV-1 TK, HSV-2 TK is incapable of phosphorylating pyrimidine nucleoside-monophosphates to their diphosphate derivatives. Therefore, cytostatic effects of IVDU in FM3A TK^-/HSV-2 TK^+ cells is a consequence of anabolism to IVDU-MP which can inhibit TS.

D. Scintigraphic detection of HSV-1 TK expression

The concept of imaging HSV-1 TK gene expression using radiolabelled nucleoside analogues was first proposed over a decade ago.[181-183] The technique was thought to be useful for non-invasive diagnosis of herpes simplex encephalitis (HSE), a relatively uncommon form of herpes infection in the brain. However, HSE is the most common form of sporadic fatal encephalitis of viral origin. Without treatment, mortality approaches 70% and neurological deficits among survivors occur frequently. Early diagnosis and initiation of antiviral therapy is crucial in order to avoid serious morbidity.[184] Consequently, a sensitive and specific non-invasive method of virus detection was thought to be useful for unambiguous diagnosis of HSE. Quantitative autoradiographic mapping of experimental HSE in rats was first demonstrated using ^{14}C-labelled 5-methyl-2'-fluoroarabinouridine (FMAU).[181] This compound, which is selectively phosphorylated by HSV-1 TK, demonstrated enhanced and selective uptake in tissues infected with

HSV-1 due to intracellular metabolic trapping of phosphorylated metabolites. Similarly, radiolabelled IVDU was proposed to be a radioligand with potential as a scintigraphic imaging agent for diagnosis of HSE.[185] IVDU has potent and selective activity against HSV-1, the principle etiologic agent of HSE.[186] The selectivity of IVDU is attributed to selective phosphorylation by herpes simplex type-1 thymidine kinase (HSV-1 TK) in infected cells.[187] In contrast, human thymidine kinase does not recognize IVDU as a substrate for phosphorylation. Selective phosphorylation of IVDU leads to metabolic trapping of nucleotide derivatives of IVDU in HSV-1 infected cells.

Quantitative uptake studies of [^{131}I]IVDU *in vitro* revealed that the compound displays preferential uptake in HSV-1 infected cells while uptake in uninfected cells is extremely low.[188] However, intracarotid administration of [^{131}I]IVDU to rabbits with HSE results in very low uptake of radioactivity in regions of brain infected with HSV-1 compared to blood activity.[189] The extremely rapid catabolic deglycosylation of IVDU, catalyzed by pyrimidine phosphorylases, is a mechanism of inactivation of the nucleoside before reaching its site of action.[190] However, it has been proposed that imaging HSV-1 infected brain with radiolabelled IVDU is hindered by limited permeation across the blood-brain barrier (BBB).[191] Disruption of the BBB followed by intracarotid administration of [^{131}I]IVDU has been shown to allow specific scintigraphic imaging and autoradiography of infected brain in a HSE rat model.[192] However, since FMAU is stable to phosphorolysis and can traverse intact BBB to allow selective accumulation in HSV-1 infected brain, it is likely that stability to phosphorylase-catalyzed deglycosylation is more important for reaching the site of specific phosphorylation.

The metabolic trapping of several phosphorylase-resistant congeners of FMAU and IVDU in HSV-1 infected cells has been observed.[193,194] In these studies, 5-iodo-2'-fluoroarabinouridine (FIAU) and (*E*)-5-(2-iodovinyl)-2'-fluoro-2'-deoxyuridine (IVFRU) emerged as promising compounds for imaging HSE. Both compounds accumulate rapidly in HSV-1 infected cells and can be labelled with isotopes of iodine that permit non-invasive scintigraphic imaging (^{123}I, ^{124}I, ^{131}I). However, shortly after these *in vitro* studies were performed, interest in the scintigraphic imaging of HSE with radioiodinated nucleosides decreased because of the advent of new diagnostic procedures using magnetic resonance imaging (MRI) and single photon emission computed tomography (SPECT) with ^{99m}Tc-hexamethylpropyleneamineoxime (HMPAO).[195-197]

Recently, Tjuvajev and coworkers proposed that radiolabelled nucleosides can be used to detect HSV-1 TK gene expression during suicide gene therapy.[198] Moreover, they suggested that the HSV-1 TK gene could be used, with radiolabelled nucleosides, as a reporter system which could yield important information during gene therapy. In this latter approach, the HSV-1 TK gene would be incorporated on vectors carrying other therapeutic genes (ie. cytokines). The HSV-1 TK gene would be a marker that could be detected non-invasively with scintigraphic imaging. The most useful information from scintigraphic imaging of HSV-1 TK gene expression would be related to the localization and extent of vector delivery and gene expression. Since gene delivery and expression are the most important issues in the area of gene therapy, Tjuvajev and coworkers suggested that radiolabelled nucleosides could function as probes to ascertain whether vector delivery is optimal for therapeutic effect. Similarly, vector delivery to

undesired sites could be detected with a sensitive scintigraphic reporter system.

Quantitative autoradiography after administration of ^{14}C-labelled FIAU detected HSV-1 TK gene expression in the brains of rats with experimental RG2 gliomas that were engrafted with VPC secreting retroviral vectors carrying the HSV-1 TK gene.[198] The magnitude of FIAU uptake in HSV-1 TK expressing glioma cells corresponded to the level of HSV-1 TK mRNA expression. A subsequent study with [^{131}I]FIAU confirmed the results observed with [^{14}C]FIAU but also allowed non-invasive planar scintigraphy and SPECT imaging of tumors transduced *in vivo* with VPC.[199] Very impressive images of tumors expressing HSV-1 TK were obtained. In rats bearing subcutaneous RG2 gliomas, *in vitro* and *in vivo* transduction led to different levels of [^{131}I]FIAU uptake that was correlated to the proportion of tumor transduced (100% vs <50%). Thus, *in vivo* scintigraphic imaging of HSV-1 TK gene transfer and expression in neoplasms appears to be a realistic goal with radioiodinated nucleoside analogues.

E. Anti-herpes nucleosides conjugated to the dihydropyridine chemical delivery system (CDS)

The inability of some antiherpetic nucleoside derivatives to easily traverse the BBB is a consequence of their relatively low lipophilicity. Increasing the lipophilic character of highly polar nucleoside analogues while retaining their selective antiviral properties would be desirable to improve brain uptake. Among the more successful approaches currently being applied in the design of lipophilic prodrugs, the dihydropyridine ⇔ pyridinium salt redox chemical delivery system (CDS) as proposed by Bodor and

coworkers is unique.[200] This brain-directed prodrug approach involves coupling a lipophilic 1-methyl-1,4-dihydropyridyl promoiety to a drug molecule through an amide or ester linkage. The derivatized prodrug can gain entry to the brain due to increased lipophilicity. Following distribution after administration, the 1-methyl-1,4-dihydropyridine promoeity can undergo oxidation in a manner analogous to the NAD ⇔ NADH redox system. The 1-methyl-pyridinium salt derivative is highly polar which results in cerebral trapping of the prodrug intermediate. Clearance from the central compartment is facilitated since oxidation occurs in the periphery in addition to the brain. Hydrolysis of the ester linkage releases the intact drug and the oxidized promoiety, trigonelline. The net result is a reservoir effect leading to an elevated and sustained concentration of hydrolyzed active drug within the brain.

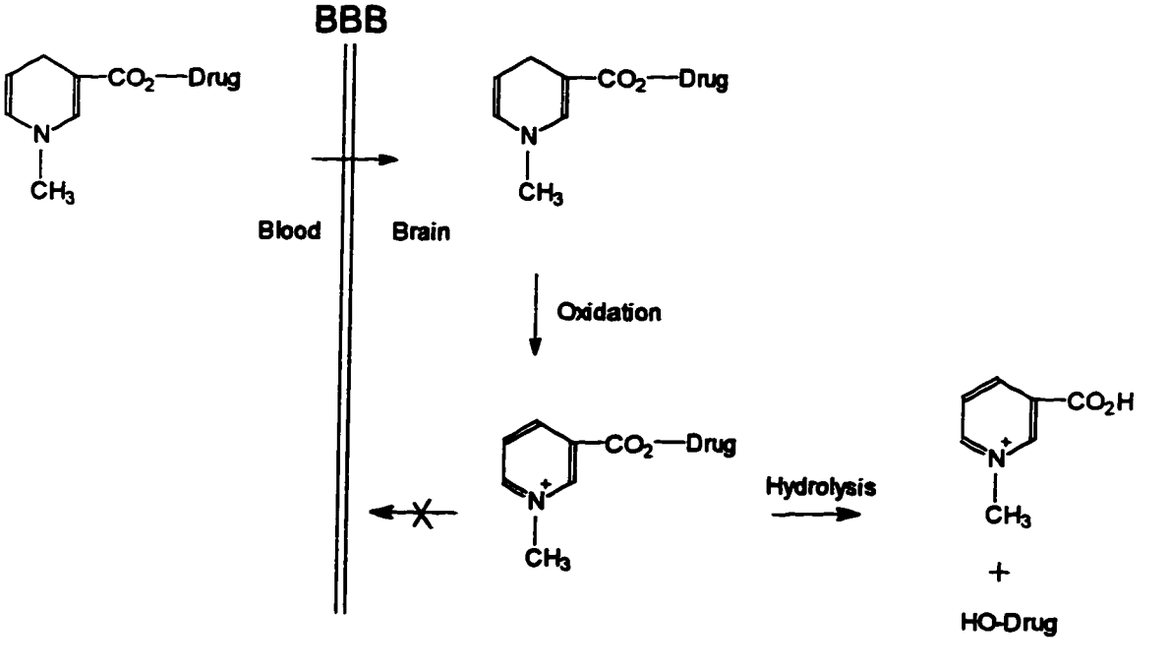

Fig. 12 Dihydropyridine ⇔ Pyridinium salt redox chemical delivery system. (CDS).

Several antiherpetic nucleoside derivatives have been synthesized that incorporate the CDS promoiety in their structure as a cleavable ester functionality. A series of 5-trifluorothymidine (TFT) derivatives were synthesized and evaluated *in vitro* and *in vivo* as potential prodrugs for TFT, a potent antiviral nucleoside analogue.[201,202] The CDS-ester prodrug derivatives of TFT were substantially more lipophilic than the parent compound. In addition, the 1-methyl-1,4-dihydropyridine underwent rapid oxidation to the 1-methylpyridinium salt in rat blood, liver and brain homogenates before hydrolysis of the ester linkage. *In vivo* experiments demonstrated enhanced CNS delivery of CDS-derivatives compared to TFT and a significant decrease in viral titer in rats with experimental HSE. A similar study was carried out with a CDS-derivative of ganciclovir (GCV-CDS). Like TFT-CDS derivatives, GCV-CDS possessed a 55-fold greater lipophilicity than ganciclovir and enhanced delivery of the active principle to the brain in rats.[203] A CDS-derivative of acyclovir (ACV-CDS) was found to be approximately 30 times more lipophilic than acyclovir and improved delivery to the skin after application on hairless mice.[204]

Kumar and coworkers synthesized (*E*)-5-(2-iodovinyl)-3'-*O*-(1-methyl-1,4-dihydropyridine-3-carbonyl)-2'-deoxyuridine (IVDU-CDS) as a putative radiopharmaceutical for scintigraphic imaging of HSE.[205] However, the synthetic approach was not amenable to radiolabelling and therefore *in vitro* and *in vivo* data was lacking. It is conceivable that IVDU-CDS may enhance lipophilicity and delivery to the brain. If delivered to brain tissue infected with HSV-1, one would expect rapid uptake of liberated IVDU after oxidation and hydrolysis of the CDS-prodrug in the brain. Similarly, if delivered to brain tumor tissue transduced with a vector carrying the HSV-1 TK gene, radiolabelled derivatives of IVDU-CDS could undergo oxidation and

hydrolysis. Selective uptake of the parent compound in the transduced tissue could occur. Further study of this latter concept will require additional development of chemical and radiochemical syntheses of appropriate compounds and biological investigation in suitable *in vitro* and *in vivo* models. The objectives of this work are to develop synthetic and radiosynthetic methods for nucleoside derivatives chemically related to IVDU including related CDS-derivatives. These compounds are evaluated in appropriate *in vitro* and *in vivo* models of HSV-1 TK gene therapy to ascertain if scintigraphic detection of HSV-1 TK-expressing tumors can be achieved.

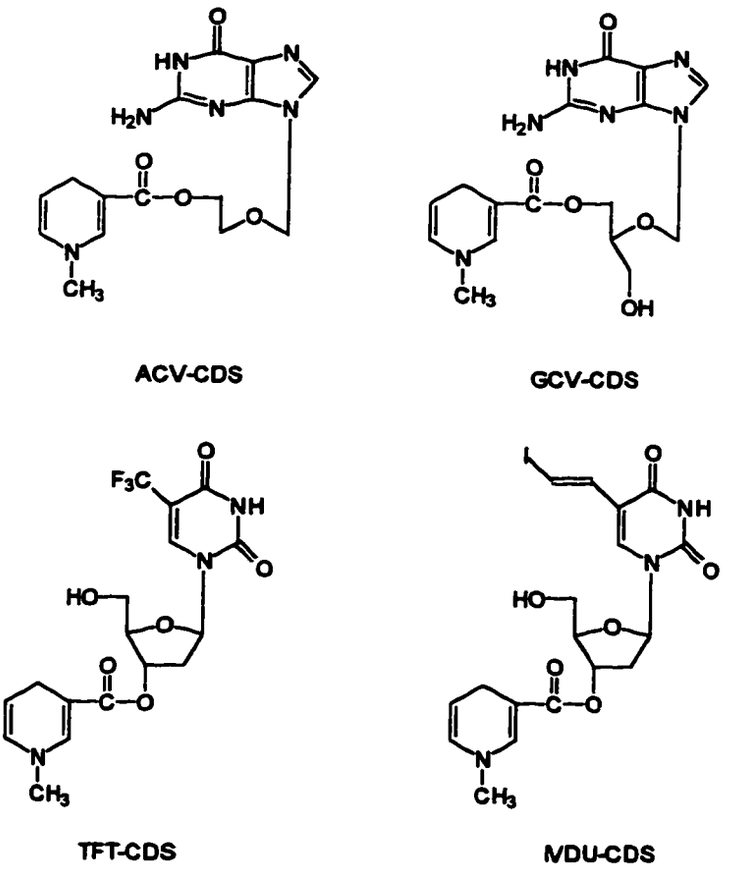

Fig. 13 CDS-derivatives of antiherpetic nucleosides.

II. Materials and Methods

A. Materials

Solvents and reagents used were of reagent quality. Solvents were dried using standard methods and were freshly distilled prior to use. 5-Iodo-2'-deoxyuridine and O^2,2-anhydrouridine were purchased from the Aldrich Chemical Company. 2'-Fluoro-2'-deoxyuridine, 5-iodo-2'-fluoro-2'-deoxyuridine and 2',3',5'-tri-*O*-acetyl-5-iodoarabinouridine were prepared using literature procedures.[206,207,208] 5-Iodo-2'-fluoro-2'-deoxyarabinouridine was obtained as a generous gift from Bristol Meyers Squibb. (*E*)-2-Tri-butylstannyl-1-trimethylsilylethene was prepared as previously described.[209] Radiochemical quality $Na^{125}I$ and $Na^{131}I$ were obtained in dilute aqueous NaOH solution from the Edmonton Radiopharmaceutical Centre.

Dulbecco's modified Eagle's media (DMEM), geneticin (G-418), trypsin, penicillin and streptomycin were obtained from Sigma. Fetal bovine serum (FBS) was purchased from Gibco. N-[1-(2,3-Dioleoyloxy)propyl]-N,N,N-trimethylammonium methylsulfate (DOTAP) cationic liposomes and a luciferase reporter gene assay kit (reaction buffer, luciferin, and lysis buffer) were purchased from Boehringer Mannheim.

B. Chromatography and Instrumental Analysis

Melting points were determined on a Buchi capillary apparatus and are uncorrected. Nuclear magnetic resonance (NMR) spectra were acquired on a Bruker AM-300 spectrometer or a JEOL 400 MHz spectrometer. The assignments of exchangeable protons (N*H*, O*H*) were confirmed by addition of D_2O. ^{13}C NMR spectra were acquired using the J modulated spin echo technique where methyl and methine carbon resonances appear as positive

peaks, and methylene and quaternary carbon resonances appear as negative peaks. High resolution mass spectrometry was performed on a A.E.I. MS-50 mass spectrometer. Thin layer chromatography (TLC) analysis was performed using Whatman MK6F silica gel microslides. Column chromatography was performed on Merck 7734 silica gel (60-200 μ particle size). Aluminum oxide column chromatography was performed using Camag 507-C neutral alumina. High performance liquid chromatography (HPLC) separations were performed on a preparative Whatman Partisil M9 10/25 ODS reverse phase column using a Waters HPLC system consisting of Model 510 solvent pumps, Model 860 gradient controller, Model U6K injector unit, and a Hewlett Packard Model 1040A diode array ultraviolet detector. "No carrier added" product was detected during HPLC purification using an in-line NaI(Tl) gamma detector. Analytical HPLC separations were performed on a C_{18} Radial-Pak column obtained from Waters. Gamma radioactivity (^{125}I and ^{131}I decay) determinations were obtained by photon counting using a Beckman Gamma 8000 scintillation counter. A Beckman LS 9000 scintillation counter in single photon counting mode was used to detect luminescence in the luciferase detection assay.

C. Cell Lines

The KBALB cell line, a Kirsten virus-transformed sarcoma cell line, was obtained from the American Type Culture Collection. The KBALB-LNL and KBALB-STK cell line was obtained from Dr. Scott Freeman (Tulane University). The KBALB-STK cell line was derived by exposing KBALB cells to supernatants from an ecotropic ψ-2 producer cell line transfected with a construct possessing the HSV-1 TK gene under direction of the SV-40 early promoter/enhancer and *neo*^{R} gene driven by the 5'-LTR. This rapidly

growing sarcoma cell line has been characterized extensively and does not produce retrovirus particles.[77] The KBALB-LNL cell line is transduced with the LNL6 retroviral vector which contains only the neomycin phosphotransferase (*neo*^{R}) gene. Cell lines were maintained in DMEM supplemented with 10% fetal bovine serum, penicillin (100 U/mL) and streptomycin (100 μg/mL). Transduced KBALB cells were maintained in media that had 1 mg/mL geneticin (G-418) added in addition to FBS and antibiotics. Cells were cultured at 37° C in 5% CO_2 atmosphere.

FM3A cells (designated FM3A/0), derived from a spontaneous murine mammary carcinoma in a C3H/He mouse, and FM3A/TK$^-$, selected for resistance against 5-bromo-2'-deoxyuridine and lacking cytosolic TK activity, were maintained by Dr. Jan Balzarini (Rega Institute, Belgium) in RPMI 1640 culture medium containing 10% fetal calf serum and 2 mM L-glutamine. The FM3A TK$^-$/HSV-1 TK$^+$ and FM3A TK$^-$/HSV-2 TK$^+$ cell lines, lacking cellular TK activity and containing the HSV-1 and HSV-2 thymidine kinase genes, respectively, were derived from FM3A TK$^-$ cells as reported earlier.[210,211]

D. Plasmid and Retroviral Vectors

E. coli clones harboring plasmids pMLBKTK and pSluc2 were obtained from the American Type Culture Collection (ATCC 39369 and ATCC 37574). The clones were cultured in LB medium supplemented with ampicillin (50 μg/mL). Overnight cultures at 37° C were subjected to alkaline lysis mini-prep purification procedures for isolation of plasmids as previously described.[237] The plasmid vectors were used in transfection experiments immediately after purification.

The replication incompetent Moloney murine leukemia virus vector, LSNtk, was obtained in PA-317 producer cell supernatants from Dr. Lung-Ji Chang (University of Alberta) with a titre of approximately 1 x 10^6 colony-forming units/mL. The LSNtk vector possesses the HSV-1 TK gene under influence of the 5'-LTR and the neomycin phosphotransferase gene driven by the SV-40 early promoter/enhancer regulatory elements. Supernatants were used for *in vitro* and *in vivo* transduction immediately after removal from producer cell culture.

E. Chemical Synthesis

2',3',5'-Tri-*O*-acetyl-(*E*)-5-(2-trimethylsilylvinyl)arabinouridine (2). *(E)*-$Bu_3SnCH=CH\text{-}SiMe_3$ (10.3 g, 26.2 mmol) was added to a stirred solution of (*E*)-5-(2-trimethylsilylvinyl)arabinouridine (1)(5.2 g, 9.9 mmol) and $(Ph_3P)_2Pd(II)Cl_2$ (0.99 g, 1.41 mmol) in dry acetonitrile (300 mL) under an argon atmosphere and the reaction was allowed to proceed for 16 h at 50 ° C with stirring. Removal of the solvent *in vacuo* gave a residue that was purified by silica gel column chromatography using hexane-ethyl acetate (1.5:1, v/v) as eluent to yield 2',3',5'-tri-*O*-acetyl-(*E*)-5-(2-trimethylsilylvinyl)arabinouridine (2)(3.32 g, 64%) as a white crystalline product: mp 159-160 °C; The ^1H and ^{13}C NMR spectra were identical to those reported previously.[208]

^1H NMR ($CDCl_3$) δ 0.12 (s, 9H, $SiMe_3$), 2.15, 2.13 and 1.99 (three s, 3H each, OAc), 4.20 (dt, 1H, $J_{3',4'}$=3.4 Hz, H-4'), 4.40 (dd,1H, J_{gem}=12 Hz, $J_{5',4'}$=3.8 Hz, H-5'), 4.50 (dd, 1H, J_{gem}=12 Hz, $J_{5'',4'}$=6.2 Hz, H-5''), 5.13 (dd, 1H, $J_{2',3'}$=1.6 Hz, $J_{3',4'}$= 3.4 Hz, H-3'), 5.42 (dd, 1H, $J_{2',3'}$=1.6 Hz, $J_{1',2'}$=4.0 Hz, H-2'), 6.32 (d, 1H, $J_{1',2'}$=4.0 Hz, H-1'),

6.67 and 6.56 (two d, 1H each, J_{trans}=19.3 Hz, C*H*=C*H*SiMe$_3$), 7.6 (s, 1H, uracil H-6); 9.29 (br s, 1H, NH).

^{13}C NMR ($CDCl_3$) δ: 170.30, 169.60 and 168.41 (acetyl CO); 161.80 (C-4); 149.15 (C-2); 136.41 (C-6); 133.43 and 131.33 (vinyl C-1 and C-2); 112.84 (C-5); 84.39 (C-1'); 80.63 (C-4'); 76.27 (C-2'); 74.51 (C-3'); 62.50 (C-5'); 20.70, 20.59 and 20.33 (acetyl's Me); -1.39 ($SiMe_3$).

(*E*)-5-(2-Trimethylsilylvinyl)arabinouridine (9). 2',3',5'-Tri-*O*-acetyl-(*E*)-5-(2-trimethylsilylvinyl)arabinouridine (**2**)(0.18 g, 0.34 mmol) was added to a 2% suspension of LiOH in dry benzene (200 mL), and the reaction was allowed to proceed for 80 h at 25 °C with stirring. After filteration to remove solid LiOH, and removal of the solvent *in vacuo,* the residue obtained was purified by silica gel column chromatography using methanol-chloroform (12:88, v/v) as eluent. Recrystallization of (*E*)-5-(2-trimethylsilylvinyl)arabinouridine (**9**) from methanol gave white crystals (51 mg, 39%): mp 103-105 °C; UV (CH_3OH) λ_{max} 246, 296 nm; ^{1}H NMR (CD_3OD) δ 0.10 (s, 9H, Si*Me*$_3$), 3.79-3.92 (m, 3H, H-5', H-4;), 4.10 (dd, 1H, $J_{3',4'}$=4.2, $J_{2',3'}$=3.9 Hz, H-3'), 4.19 (dd,1H, $J_{1',2'}$=4.5, $J_{2',3'}$=3.9 Hz, H-2'), 6.16 (d, 1H, $J_{1',2'}$=4.5 Hz, H-1'), 6.69 and 6.53 (two d, 1H each, J_{trans}=19.4 Hz, C*H*=C*H*SiMe$_3$), 8.07 (s, 1H, uracil H-6); ^{13}C NMR (CD_3OD) δ: 164.70 (C-4 *C*=O), 151.60 (C-2 *C*=O), 140.56 (C-6), 135.71 and 130.19 (vinyl C-1 and C-2), 112.78 (C-5), 87.12 (C-1'), 85.82 (C-4'), 77.19 (C-2'), 76.93 (C-3'), 61.99 (C-5'), -1.20 (Si*Me*$_3$). Exact Mass calculated for $C_{14}H_{22}N_2O_6Si$ 342.1247, Found (HRMS), 342.1243 (M^+, 1.74%)

(*E*)-5-(2-Trimethylsilylvinyl)-2'-deoxyuridine (6). (*E*)-Bu_3SnCH=$CHSiMe_3$ (220 mg, 0.56 mmol) and $(Ph_3P)_2Pd(II)Cl_2$ (20 mg, 0.028 mmol) were added to a solution of 5-iodo-2'-deoxyuridine (**3**)(100

mg, 0.28 mmol) in dry acetonitrile (10 mL) and the reaction was allowed to proceed at 60 °C for 16 hours under an argon atmosphere with stirring. Removal of the solvent *in vacuo* gave a residue that was purified by silica gel column chromatography. Elution with methanol-chloroform (3:20 v/v) afforded (*E*)-5-(2-trimethylsilylvinyl)-2'-deoxyuridine (6) which was recrystallized from ethyl acetate as a colorless solid (67 mg, 73% yield): mp 108-110 °C; ^{1}H NMR (DMSO-d_6) δ 0.09 (s, 9H, SiMe_3), 2.08-2.22 (m, 2H, H-2'), 3.56-3.64 (m, 2H, H-5'), 3.78-3.79 (m, 1H, H-4'), 4.22-4.30 (m, 1H, H-3'), 5.17 (t, 1H, $J_{OH,5'}$=5.0 Hz, C-5' OH), 5.27 (d, 1H, $J_{OH,3'}$=4.4 Hz, C-3' OH), 6.16 (t, 1H, $J_{1',2'}$=6.1 Hz, H-1'), 6.59 (s (A_2), 2H, C*H*=C*H*SiMe$_3$), 8.18 (s, 1H, H-6), 11.42 (s, 1H, NH). Exact mass calculated for $C_{14}H_{22}N_2O_5Si$ 326.1298, found (HRMS) 326.1301 (M^+, 2.39%). Anal. calc'd for $C_{14}H_{22}N_2O_6Si$: C, 51.51; H, 6.79; N, 8.58. Found: C, 51.33 ; H, 6.49 ; N, 8.18 .

(*E*)-5-(2-Trimethylsilylvinyl)-2'-fluoro-2'-deoxyuridine (7). $(Ph_3P)_2PdCl_2$ (37 mg, 0.05 mmol) and (*E*)-Bu_3SnCH=$CHSiMe_3$ (412 mg, 1.06 mmol) were added with stirring to a solution of 5-iodo-2'-fluoro-2'-deoxyuridine (4)(197 mg, 0.53 mmol) in dry THF (5 mL) at 50°, and the reaction mixture was stirred for 16 h at 50 °C under an atmosphere of argon at which time TLC analysis indicated the reaction was completed. Removal of the solvent *in vacuo* and purification of the residue by silica gel column chromatography with methanol-dichloromethane (1:25, v/v) as eluent afforded (*E*)-5-(2-trimethylsilylvinyl)-2'-fluoro-2'-deoxyuridine (7) as a white solid (146 mg, 80% yield) after recrystallization from ethyl acetate: mp 164-165 °C; ^{1}H NMR (DMSO-d_6) δ 0.08 (s, 9H, SiMe_3), 3.62-3.65 (m, 1H, J_{gem}=9.9 Hz, H-5'), 3.84-3.88 (m, 1H, H-5''), 3.89 (d, 1H, $J_{3',4'}$=8.8 Hz, H-4'), 4.14-4.25 (m, 1H, $J_{3',F}$=24.2, $J_{2',3'}$=3.8 Hz, H-3'), 5.04 (dd,

1H, $J_{2',F}$=53.3, $J_{2',3'}$=3.8 Hz, H-2'), 5.43 (t, 1H, $J_{OH,5'}$=4.8 Hz, C-5' OH), 5.63 (d, 1H, $J_{OH,3'}$=6.6 Hz, C-3' OH), 5.92 (d, 1H, $J_{1',F}$=17.0 Hz, H-1'), 6.52 and 6.59 (two d,1H each, J_{trans}=19.8 Hz, C*H*=C*H*SiMe$_3$), 8.33 (s, 1H, uracil H-6), 11.51 (s, 1H, NH). Exact mass calculated for $C_{14}H_{21}FN_2O_5Si$ 344.1204, found (HRMS) 344.1208 (M^+, 2.2%). Anal. calc'd for $C_{14}H_{21}FN_2O_5Si$: C, 48.82; H, 6.15; N, 8.13. Found: C, 48.68; H, 6.16; N, 7.86.

(*E*)-5-(2-Trimethylsilylvinyl)-2'-fluoro-2'-deoxyarabinouridine (8). (*E*)-$Bu_3SnCH=CHSiMe_3$ (220 mg, 0.56 mmol) was added to a solution of 5-iodo-2'-fluoro-2'-deoxyarabinouridine (5)(100 mg, 0.27 mmol) and $(Ph_3P)_2Pd(II)Cl_2$ (20 mg, 0.028 mmol) in dry acetonitrile (10 mL) and the reaction was allowed to proceed at 60 °C for 16 h under an argon atmosphere with stirring. Removal of the solvent *in vacuo*, purification of the residue by silica gel column chromatgraphy with methanol-chloroform (1:10 v/v) as eluent and recrystallization of the product from EtOAc gave (*E*)-5-(2-trimethylsilylvinyl)-2'-fluoro-2'-deoxyarabinouridine (8) as a white solid (59 mg, 64% yield): mp 182-183 °C; ^{1}H NMR (DMSO-d_6) δ 0.09 (s, 9H, Si*Me*$_3$), 3.60-3.70 (m, 2H, H-5'), 3.78-3.80 (m, 1H, H-4'), 4.24-4.31 (m, 1H, $J_{3',F}$=20.9 Hz, H-3'), 5.11 (dt, 1H, $J_{2',F}$=52.8, $J_{1',2'}$=4.4, $J_{2',3'}$=4.4 Hz, H-2'), 5.27 (t, 1H, $J_{OH,5'}$=5.5 Hz, C-5' OH), 5.90 (d, 1H, $J_{OH,3'}$=5.0 Hz, C-3' OH), 6.15 (dd, 1H, $J_{1',F}$=13.2, $J_{1',2'}$=4.4 Hz, H-1'), 6.59 (two d, 1H each, J_{trans}=19.2 Hz, C*H*=C*H*SiMe$_3$), 8.04 (s, 1H, uracil H-6), 11.58 (s, 1H, NH) Exact mass calculated for $C_{14}H_{21}FN_2O_5Si$ 344.1204, found (HRMS) 344.1202 (M^+, 3.53%). Anal. calc'd for $C_{14}H_{21}FN_2O_5Si$: C, 48.82; H, 6.15; N, 8.13. Found: C, 48.77; H, 6.32; N, 7.72.

(*E*)-5-(2-Iodovinyl)-2'-deoxyuridine (10). After dissolution of (*E*)-5-(2-trimethylsilylvinyl)-2'-deoxyuridine (**6**)(39 mg, 0.116 mmol) in dry acetonitrile (2 mL), iodine monochloride (19 mg, 0.116 mmol) was added immediately, and the reaction was allowed to proceed at 25 °C for 30 minutes with stirring. The solvent was removed *in vacuo*, and the residue was purified by silica gel column chromatography using methanol:chloroform (1:9 v/v) as eluent. The solvent from pooled fractions was removed *in vacuo* and (*E*)-5-(2-iodovinyl)-2'-deoxyuridine (**10**) was isolated in 77% yield (34 mg) after recrystallization from methanol: mp 167-169 °C; ^{1}H NMR (DMSO-d_6) δ 2.10-2.16 (m, 2H, H-2'), 3.52-3.68 (m, 2H, H-5'), 3.76-3.80 (m, 1H, H-4'), 4.20-4.26 (m, 1H, H-3'), 5.10 (t, 1H, $J_{OH,5'}$=4.0 Hz, C-5' OH), 5.27 (d, 1H, $J_{OH,3'}$=3.0 Hz, C-3' OH), 6.13 (t, 1H, $J_{1',2'}$=4.0 Hz, H-1'), 7.12 (d, J_{trans}=14.3 Hz, 1H, C*H*=CHI), 7.20 (d, J_{trans}=14.3 Hz, 1H, CH=C*H*I), 8.07 (s, 1H, H-6); 11.55 (s, 1H, NH).

(*E*)-5-(2-Iodovinyl)-2'-fluoro-2'-deoxyuridine (11). After dissolution of (*E*)-5-(2-trimethylsilylvinyl)-2'-fluoro-2'-deoxyuridine (**7**)(40 mg, 0.116 mmol) in dry acetonitrile (2 mL), iodine monochloride (19 mg, 0.116 mmol) was added immediately, and the reaction was allowed to proceed at 25 °C for 30 minutes with stirring. The solvent was removed *in vacuo*, and the residue was purified by silica gel column chromatography using methanol:chloroform (7:93 v/v) as eluent. The solvent from pooled fractions was removed *in vacuo* and (*E*)-5-(2-iodovinyl)-2'-fluoro-2'-deoxyuridine (**11**)(IVFRU) was isolated in 78% yield (36 mg) after recrystallization from methanol as a white solid: mp 107-109 °C (lit. mp 108-110 °C);[194] ^{1}H NMR (DMSO-d_6) δ 3.65 (d, 1H, J_{gem}=12 Hz, H-5'), 3.82-3.96 (m, 2H, H-4', H-5''), 4.20 (dd, 1H, $J_{3',F}$=23, $J_{2',3'}$=6 Hz, H-3'), 5.06 (dd, 1H, $J_{2',F}$=54, $J_{2',3'}$=6 Hz, H-2'), 5.47 (br s, 1H, C-5' OH)

5.72 (br s, 1H, C-3' OH), 5.92 (d, 1H, $J_{1',F}$=18 Hz, H-1'), 7.09 (d, 1H, J_{trans}=16 Hz, C*H*=CHI), 7.20 (d, 1H, J_{trans}=16 Hz, CH=C*H*I), 8.23 (s, 1H, uracil H-6), 11.60 (br s, 1H, NH).

(*E*)-5-(2-Iodovinyl)-2'-fluoro-2'-deoxyarabinouridine (12). After dissolution of (*E*)-5-(2-trimethylsilylvinyl)-2'-fluoro-2'-deoxyarabinouridine (8)(40 mg, 0.116 mmol) in dry acetonitrile (2 mL), iodine monochloride (19 mg, 0.116 mmol) was added immediately, and the reaction was allowed to proceed at 25 °C for 30 minutes with stirring. The solvent was removed *in vacuo*, and the residue was purified by silica gel column chromatography using methanol:chloroform (8:92 v/v) as eluent. The solvent from pooled fractions was removed *in vacuo* and (*E*)-5-(2-iodovinyl)-2'-fluoro-2'-deoxyarabinouridine (12)(IVFAU) was isolated in 64% yield (30 mg) after recrystallization from methanol: mp 178 °C (lit. mp 178-179 °C);[212] ^{1}H NMR (DMSO-d_6) δ 3.61-3.71 (m, 2H, H-5'), 3.79-3.80 (m, 1H, H-4'), 4.17-4.27 (m, 1H, $J_{3',F}$=20 Hz, H-3'), 5.06 (dt, 1H, $J_{2',F}$= 54, $J_{1',2'}$ =3.0 Hz, H-2'), 5.20 (t, 1H, $J_{OH,5'}$=6.0 Hz, C-5' OH), 5.94 (d, 1H, $J_{OH,3'}$=4.9 Hz, C-3' OH), 6.10 (dd, 1H, $J_{1',F}$=10, $J_{1',2'}$=4.9 Hz, H-1'), 7.15 (d, 1H, J_{trans}=14.8 Hz, C*H*=CHI), 7.23 (d, 1H, J_{trans}=14.8 Hz, CH=C*H*I), 7.98 (s, 1H, uracil H-6), 11.73 (s, 1H, NH).

(*E*)-5-(2-Iodovinyl)arabinouridine (13). After dissolution of (*E*)-5-(2-trimethylsilylvinyl)arabinouridine (9)(40 mg, 0.116 mmol) in dry acetonitrile (2 mL), iodine monochloride (19 mg, 0.116 mmol) was added immediately, and the reaction was allowed to proceed at 25 °C for 30 minutes with stirring. The solvent was removed *in vacuo*, and the residue was purified by silica gel column chromatography using methanol:chloroform (1:9 v/v) as eluent. The solvent from pooled fractions was removed *in vacuo* and (*E*)-5-(2-iodovinyl)arabinouridine (13) was isolated in 75% yield (34 mg) after

recrystallization from methanol: mp. 171-175 °C (lit. mp 170-175 °C);[208] ^{1}H NMR (DMSO-d_6) δ 3.62-3.65 (m, 2H, H-5'), 3.72-3.76 (m, 1H, H-4'), 3.90-3.93 (m, 1H, H-3'), 4.00-4.05 (m, 1H, H-2'), 5.13 (t, 1H, $J_{OH,5'}$=5.5 Hz, C-5' OH), 5.46 (d, 1H, $J_{OH,3'}$=4.4 Hz, C-3' OH), 5.56 (d, 1H, $J_{OH,2'}$=5.3 Hz, C-2' OH), 5.98 (d, 1H, $J_{1',2'}$=4.7 Hz, H-1'), 7.13 (d, 1H, J_{trans}=14.6 Hz, C*H*=CHI); 7.19 (d,1H, J_{trans}=14.6 Hz, CH=C*H*I); 7.88 (s, 1H, uracil H-6); 11.54 (s, 1H, NH).

5'-*O*-*t*-Butyldimethylsilyl-2'-fluoro-2'-deoxyuridine (16). Imidazole (1.0 g, 14.69 mmol) and *t*-butyldimethylsilyl chloride (1.0 g, 6.63 mmol) were added to a solution of 2'-fluoro-2'-deoxyuridine (15)(1.46 g, 5.93 mmol) in dry DMF (20 mL) and the reaction was allowed to proceed with stirring for 48 hrs at 25 °C. Removal of the solvent *in vacuo* gave a residue which was purified by elution from a silica gel column using chloroform:methanol (96:4 v/v), as eluant to afford the desired compound (16)(1.42 g, 67%) as a white solid after recrystallization from methanol: mp 58-60 °C; ^{1}H NMR ($CDCl_3$) d 0.13 (s, 6H, Si*Me*$_2$), 0.93 (s, 9H, *Me*$_3$C), 2.44 (br s, 1H, 3'-OH, exchanges with deuterium oxide), 3.88 (d, 1H, J_{gem}=10.6 Hz, H-5'), 4.06-4.12 (m, 2H, H-4, H-5"), 4.30-4.42 (m, 1H, $J_{3',F}$=18 Hz, H-3'), 4.96 (dt, 1H, $J_{2',F}$=51, $J_{2',3'}$=4.3 , $J_{1',2'}$=2.0 Hz, H-2'), 5.70 (d, 1H, $J_{5,6}$=7.0 Hz, uracil H-5), 6.12 (dd, 1H, $J_{1',F}$=14.7, $J_{1',2'}$=2.0 Hz, H-1'), 7.94 (d,1H, $J_{5,6}$=7.0 Hz, uracil H-6), 8.86 (br s, 1H, NH, exchanges with deuterium oxide). Anal. calcd. for $C_{15}H_{25}FN_2O_5Si.1/2H_2O$: C, 48.76; H, 7.11; N, 7.58. Found: C, 48.90; H, 7.03; N, 7.50.

3'-*O*-(3-Pyridylcarbonyl)-5'-*O*-*t*-butyldimethylsilyl-2'-fluoro-2'-deoxyuridine (17). 5'-*O*-*t*-butyldimethylsilyl-2'-fluoro-2'-deoxyuridine (16)(1.32 g, 3.65 mmol) was added to a solution of nicotinoyl chloride hydrochloride (1.24 g, 7.0 mmol) in dry pyridine (50 mL) and the reaction

was allowed to proceed for 48 hrs at 25 °C with stirring. Removal of the solvent *in vacuo* and purification of the residue obtained by elution from a silica gel column using chloroform:methanol (97:3 v/v) as eluant afforded the desired product (17)(1.236 g, 73%) after recrystallization from methanol as a white solid: mp 212-214 °C; ^{1}H NMR ($CDCl_3$) d 0.13 (s, 6H, SiMe_2), 0.93 (s, 9H, Me_3C), 3.90 (d, 1H, J_{gem}=10.6 Hz, H-5'), 4.12 (d, 1H, J_{gem}=10.6 Hz, H-5"), 4.48 (d,1H, $J_{3',4'}$=5 Hz, H-4'), 5.28 (ddd, 1H, $J_{2',F}$=51.0, $J_{2',3'}$=3.0, $J_{1',2'}$=2.7 Hz, H-2'), 5.49 (ddd, 1H, $J_{3',F}$=13.7, $J_{3',4'}$=5.0, $J_{2',3'}$=3.0 Hz, H-3'), 5.76 (d, 1H, $J_{5,6}$=7.0 Hz, uracil H-5), 6.25 (dd, 1H, $J_{1',F}$=14.0, $J_{1',2'}$=2.7 Hz, H-1'), 7.46 (dd, 1H, $J_{4,5}$=8.0, $J_{5,6}$=5.0 Hz, pyridyl H-5), 7.90 (d, 1H, $J_{5,6}$=7.0 Hz, uracil H-6), 8.34 (ddd, 1H, $J_{4,5}$=8.0, $J_{2,4}$=$J_{4,6}$=1.6 Hz, pyridyl H-4), 8.46 (br s, 1H, NH, exchanges with deuterium oxide), 8.86 (dd, 1H, $J_{5,6}$=5.0, $J_{4,6}$=1.6 Hz, pyridine H-6), 9.27 (d, 1H, $J_{2,4}$=1.6 Hz, pyridyl H-2). Anal. calcd. for $C_{21}H_{28}FN_3O_6Si$: C, 54.53; H, 5.46; N, 9.08. Found: C, 54.33; H, 5.85; N, 8.99

5-Iodo-3'-*O*-(3-pyridylcarbonyl)-2'-fluoro-2'-deoxyuridine (18). Iodine monochloride (52 mg, 0.32 mmol) was added to a solution of 3'-*O*-(3-pyridylcarbonyl)-5'-*O*-*t*-butyldimethylsilyl-2'-fluoro-2'-deoxyuridine (17)(0.12 g, 0.26 mmol) in methanol (6 mL) and the reaction mixture was stirred at reflux temperature for 24 h. Removal of the solvent *in vacuo*, purification of the residue obtained by elution from a silica gel column using chloroform:methanol (93:7 v/v) as eluant and recrystallization of the product obtained from methanol gave the desired compound (18)(46 mg, 41 %) as colorless crystals: mp 202-203 °C; ^{1}H NMR (CD_3OD) d 3.84 (dd, 1H, J_{gem}=12.2, $J_{4',5'}$=2.3 Hz, H-5'), 4.00 (dd, 1H, J_{gem}=12.2, $J_{4',5"}$=1.8 Hz, H-5"), 4.48 (ddd,1H, $J_{3',4'}$=6.5, $J_{4',5'}$=2.3, $J_{4',5"}$=1.8

Hz, H-4'), 5.59 (ddd, 1H, $J_{2',F}$=52.0, $J_{2',3'}$=4.5, $J_{1',2'}$=1.7 Hz, H-2'), 5.64 (ddd, 1H, $J_{3',F}$=13.3 , $J_{3',4'}$=6.5, $J_{2',3'}$=4.5 Hz, H-3'), 6.12 (dd, 1H, $J_{1',F}$=19.8, $J_{1',2'}$=1.7 Hz, H-1'), 7.64 (dd, 1H, $J_{4,5}$=7.5 , $J_{5,6}$=5.0 Hz, pyridyl H-5), 8.45 (d, 1H, $J_{4,5}$=7.5 Hz, pyridyl H-4), 8.56 (s, 1H, uracil H-6), 8.86 (d, 1H, $J_{5,6}$=5.0 Hz, pyridyl H-6), 9.22 (s, 1H, pyridyl H-2). ^{19}F NMR (CD_3OD): δ 37.67 (ddd, $J_{2',F}$=52.0, $J_{1',F}$=19.8, $J_{3',F}$=13.3 Hz, F-2). Anal. calcd. for $C_{15}H_{13}FIN_3O_6$: C, 35.65; H, 2.60; N, 8.32. Found: C, 36.05; H, 2.45; N, 8.09.

(*E*)-5-(2-Trimethylsilylvinyl)-3'-O-(3-pyridylcarbonyl)-2'-fluoro-2'-deoxyuridine (19). (*E*)-Bu_3SnCH=$CHSiMe_3$ (41 mg, 0.106 mmol) was added to a solution of 5-iodo-3'-*O*-(3-pyridylcarbonyl)-2'-fluoro-2'-deoxyuridine (18)(20 mg, 0.04 mmol) and $(Ph_3P)_2Pd(II)Cl_2$ (4 mg, 0.0057 mmol) in dry THF (30 mL) and the mixture was stirred at 50 °C for 16 h under an argon atmosphere. Removal of the solvent *in vacuo* and purification of the residue obtained by elution from a silica gel column using chloroform:methanol (95:5 v/v) as eluant afforded the desired compound (19)(9 mg, 50 %) as colorless crystals after recrystallization from ethyl acetate: mp 112-114 °C; ^{1}H NMR ($CDCl_3$) d 0.1 (s, 9H, SiMe_3), 3.92 and 4.12 (two d, 1H each, J_{gem}=12.5 Hz, H-5'), 4.45 (d,1H, $J_{3',4'}$=5.0 Hz, H-4'), 5.58 (m, 1H, $J_{2',F}$=51 Hz, H-2'), 5.68 (d, 1H, $J_{3',4'}$=5.0 Hz, H-3'), 5.93 (dd, 1H, $J_{1',F}$=18.0, $J_{1',2'}$=2.0 Hz, H-1'), 6.55 and 6.62 (two d, 1H each, J_{trans}=19 Hz, C*H*=C*H*$SiMe_3$), 7.44 (dd, 1H, $J_{4,5}$=8.0, $J_{5,6}$=5.0 Hz, pyridyl H-5), 7.78 (s, 1H, uracil H-6), 8.32 (ddd, 1H, $J_{4,5}$=8.0, $J_{4,6}$=$J_{2,4}$=1.6 Hz, pyridyl H-4), 8.82 (dd, 1H, $J_{5,6}$=5.0, $J_{4,6}$=1.6 Hz, pyridyl H-6), 9.24 (d, 1H, $J_{2,4}$=2.0 Hz, pyridyl H-2). Anal. calcd. for $C_{20}H_{24}FN_3O_6Si$: C, 53.44; H, 5.38; N, 9.35. Found: C, 53.11; H, 5.16; N, 9.03.

(*E*)-5-(2-Trimethylsilylvinyl)-3'-*O*-(1-methylpyridinium-3-carbonyl)-2'-fluoro-2'-deoxyuridine iodide (20). Iodomethane (165 mg, 1.16 mmol) was added to a solution of (*E*)-5-(2-trimethylsilylvinyl)-3'-*O*-(3-pyridylcarbonyl)-2'-fluoro-2'-deoxyuridine (19)(26 mg, 0.058 mmol) in acetone (3 mL) and the reaction mixture was heated at reflux for 16 h. Removal of the solvent *in vacuo* and trituration of the residue obtained with ether (3 x 10 mL) gave the pyridinium salt (20)(31 mg, 90 %) as yellow crystals: mp 172-174 °C; ^{1}H NMR (DMSO-d_6) d 0.1 (s, 9H, SiMe_3), 3.70-3.90 (m, 2H, H-5'), 4.44 (br s, 4H, N*Me*, H-4'), 5.44 (t, 1H, $J_{OH,5'}$=3 Hz, C-5' OH, exchanges with deuterium oxide), 5.55-5.58 (m, 1H, H-3'), 5.58-5.80 (m, 1H, H-2'), 6.12 (dd, 1H, $J_{1',F}$=17.0, $J_{1',2'}$=1.8 Hz, H-1'), 6.60 (s (A_2), 2H, C*H*=C*H*SiMe$_3$), 8.22 (s, 1H, uracil H-6), 8.29 (dd, 1H, $J_{4,5}$=7.6, $J_{5,6}$=5.0 Hz, pyridinium H-5), , 9.06 (d, 1H, $J_{4,5}$=7.6 Hz, pyridinium H-4), 9.23 (d, 1H, $J_{5,6}$=5.0 Hz, pyridinium H-6), 9.66 (s, 1H, pyridinium H-2), 11.62 (s,1H, NH, exchanges with deuterium oxide). Anal. calcd. for $C_{21}H_{27}FIN_3O_6Si.1/2\ H_2O$: C, 42.00; H, 4.71; N, 6.99. Found: C, 42.37; H, 4.57; N, 6.57.

(*E*)-5-(2-Trimethylsilylvinyl)-3'-*O*-(1-methylpyridinium-3-carbonyl)-2'-fluoro-2'-deoxyuridine bromide (21). (*E*)-5-(2-Trimethylsilylvinyl)-3'-*O*-(3-pyridylcarbonyl)-2'-fluoro-2'-deoxyuridine (19)(30 mg, 0.067 mmol) was dissolved in acetone (5 mL). A solution of 2N bromomethane in diethylether (1.16 mL, 220 mg, 2.316 mmol) was added and the reaction mixture stiirred at 22 °C for 72 hrs. The solvent was evaporated and the residue triturated with ether (3 x 10 ml) to yield the bromide salt (21)(26 mg, 71%) as colorless crystals: mp 176-178 °C; The ^{1}H NMR was identical to that observed for (*E*)-5-(2-trimethylsilylvinyl)-3'-*O*-(1-methylpyridinium-3-carbonyl)-2'-fluoro-2'-deoxyuridine iodide. Anal. calcd. for

$C_{21}H_{27}BrFN_3O_6Si$: C, 46.33; H, 5.00; N, 7.72. Found: C, 46.56; H, 5.19; N, 7.24.

(*E*)-5-(2-Iodovinyl)-3'-*O*-(1-methyl-1,4-dihydropyridine-3-carbonyl)-2'-fluoro-2'-deoxyuridine (22). Iodine monochloride (1.7 mg, 0.01 mmol) was added to a solution of (*E*)-5-(2-trimethylsilylvinyl)-3'-*O*-(1-methylpyridinium-3-carbonyl)-2'-fluoro-2'-deoxyuridine iodide (20)(6 mg, 0.0101 mmol) in acetonitrile (1 mL), immediately after its preparation, and the reaction mixture was stirred at 25 °C for 15 min. Removal of the solvent *in vacuo* gave the corresponding iodovinyl salt as a yellow solid which was used immediately without further purification. The iodovinyl nucleoside precursor was dissolved in a two phase solvent system comprised of water: ethyl acetate (1 mL each). Sodium dithionite (10 mg, 0.057 mmol) and sodium bicarbonate (4 mg, 0.048 mmol) were added and the reaction was allowed to proceed at 25 °C with stirring for 15 min. The ethyl acetate fraction was washed with water (1 mL) and the ethyl acetate solution was dried (Na_2SO_4). The solvent was removed *in vacuo* and the product was purified using a short neutral aluminum oxide column. Elution with chloroform:methanol (9:1 v/v) afforded the desired product (22)(3 mg, 59%) as a yellow solid after recrystallization from methanol: mp 131-133 °C; ^1H NMR ($CDCl_3$) d 3.02 (s, 3H, N*Me*), 3.11 (br s, 2H, dihydropyridyl H-4), 3.86 and 4.10 (two d, 1H each, J_{gem}=12.5 Hz, H-5'), 4.27 (d,1H, $J_{3',4'}$=7.5 Hz, H-4'), 4.87 (dt, 1H, $J_{5,6}$=8.0, $J_{4,5}$=3.8 Hz, dihydropyridyl H-5), 5.18 (dd, 1H, $J_{2',F}$=51 Hz, H-2'), 5.29-5.35 (m, 1H, H-3'), 5.68 (d, 1H, $J_{5,6}$=8.0 Hz, dihydropyridyl H-6), 6.05 (d, 1H, $J_{1',F}$=16 Hz, H-1'), 7.06 (d, 1H, J_{trans}=15 Hz, C*H*=CHI), 7.11 (s, 1H, dihydropyridyl H-2), 7.40 (d, 1H, J_{trans}=15 Hz, CH=C*H*I), 8.12 (s, 1H,

uracil H-6). Anal. calcd. for $C_{18}H_{19}FIN_3O_6 \cdot H_2O$: C, 40.24; H, 3.94; N, 7.82. Found: C, 40.52; H, 4.09; N, 7.61.

5-Iodo-5'-*O*-*t*-butyldimethylsilyl-2'-deoxyuridine (24). Imidazole (0.9 g, 14.5 mmol) and *t*-butyldimethylsilyl chloride (0.9 g, 6 mmol) were added to a solution of 5-iodo-2'-deoxyuridine (**23**)(2.0 g, 5.7 mmol) in dry DMF (10 ml). The reaction was stirred for 36 hrs at room temperature. The solvent was removed *in vacuo* and the residue chromatographed on a column of silica gel. Elution with chloroform:methanol (95:5 v/v) afforded the 5'-*O*-*t*-butyldimethylsilyl derivative (**24**)(2.13 g, 80%) after recrystallization from methanol: mp 206-208 °C; ^{1}H NMR (DMSO-d_6) δ 0.08 (s, 6H, SiMe_2), 0.86 (s, 9H, Me_3C), 1.98-2.16 (m, 2H, H-2'), 3.66-3.82 (m, 2H, H-5'), 3.83-3.88 (m, 1H, H-4'), 4.12-4.16 (m,1H, H-3'), 5.35 (d, 1H, C-3' OH), 6.02-6.08 (m, 1H, H-1'), 7.97 (s, 1H, uracil H-6). Anal. calc'd for $C_{15}H_{25}IN_2O_5Si$: C, 38.46; H, 5.39; N, 5.98. Found: C, 38.47; H, 5.27; N, 5.87.

5-Iodo-3'-*O*-(3-pyridylcarbonyl)-5'-*O*-*t*-butyldimethylsilyl-2'-deoxyuridine (25). 5-Iodo-5'-*O*-*t*-butyldimethylsilyl-2'-deoxyuridine (**24**)(1.9 g, 4.06 mmol) was added to a solution of nicotinoyl chloride hydrochloride (1 g, 5.63 mmol) in 50 ml dry pyridine for 6 hrs at 25 °C. The solvent was evaporated and purification by silica gel column chromatography using chloroform:methanol (95:5 v/v) yielded the 3'-*O*-nicotinoyl nucleoside (**25**)(1.76 g, 76%) after recrystallization from methanol: mp 216-217 °C; ^{1}H NMR (DMSO-d_6) δ 0.16 (s, 6H, SiMe_2), 0.93 (s, 9H, Me_3C), 2.30-2.42 (m, 1H, H-2'), 2.48-2.60 (m, 1H, H-2''), 3.90-3.98 (m, 2H, H-5'), 4.30-4.34 (m, 1H, H-4'), 5.44-5.48 (m, 1H, H-3'), 6.24 (dd, 1H, $J_{1',2'}$=6 Hz, H-1'), 7.60 (dd, 1H, $J_{4,5}$=8.2 Hz, $J_{5,6}$=5.0 Hz, pyridyl H-5), 8.07 (s, 1H, uracil H-6), 8.35 (ddd, 1H, $J_{4,5}$=8.2 Hz, $J_{4,6}$=1.6 Hz, $J_{2,4}$=1.6 Hz, pyridyl H-

4), 8.84 (dd, 1H, $J_{5,6}$=5.0 Hz, $J_{4,6}$=1.6 Hz, pyridyl H-6), 9.15 (d, 1H, $J_{2,4}$=1.6 Hz, pyridyl H-2). Anal. calc'd for $C_{21}H_{28}IN_3O_6Si$: C, 43.98; H, 4.92; N, 7.32. Found: C, 43.72; H, 4.71; N, 7.15.

5-Iodo-3'-*O*-(3-pyridylcarbonyl)-2'-deoxyuridine (26). 5-Iodo-5'-*O*-*t*-butyldimethylsilyl-3'-*O*-(3-pyridylcarbonyl)-2'-deoxyuridine (25)(600 mg, 1.046 mmol) was dissolved in 20 ml THF. A 1 M solution of *n*-Bu_4N^+ F^- in THF (3 mL) was added with stirring. The reaction was allowed to proceed for 90 minutes at 25 °C. The solvent was then evaporated and the mixture chromatographed on a column of silica gel using chloroform:methanol (93:7 v/v). Recrystallization from methanol gave the deprotected analog as colorless crystals (26)(346 mg, 72 %): mp 212-215 °C; ^{1}H NMR (DMSO-d_6) δ 2.38-2.56 (m, 2H, H-2'), 3.68-3.74 (m, 2H, H-5'), 4.22-4.26 (m, 1H, H-4'), 5.36 (t, 1H, $J_{OH,5'}$=4.5 Hz, C-5' OH, exchanges with deuterium oxide), 5.48-5.51 (m, 1H, H-3'), 6.24 (dd, 1H, $J_{1',2'}$=6 Hz, H-1'), 7.58 (dd, 1H, $J_{4,5}$=8.2 Hz, $J_{5,6}$=5.0 Hz, pyridyl H-5), 8.33 (ddd, 1H, $J_{4,5}$=8.2 Hz, $J_{4,6}$=1.6 Hz, $J_{2,4}$=1.6 Hz, pyridyl H-4), 8.42 (s, 1H, uracil H-6), 8.84 (dd, 1H, $J_{5,6}$=5.0 Hz, $J_{4,6}$=1.6 Hz, pyridyl H-6), 9.13 (d, 1H, $J_{2,4}$=1.6 Hz, pyridyl H-2), 11.72 (s, 1H, NH, exchanges with deuterium oxide). Anal. calc'd for $C_{15}H_{14}IN_3O_6$: C, 39.23; H, 3.08; N, 9.15. Found: C, 39.09; H, 3.06; N, 8.88.

(*E*)-5-(2-Trimethylsilylvinyl)-3'-*O*-(3-pyridylcarbonyl)-2'-deoxyuridine (27). 5-Iodo-3'-*O*-(3-pyridylcarbonyl)-2'-deoxyuridine (26)(300 mg, 0.65 mmol) and $(Ph_3P)_2Pd(II)Cl_2$ (46 mg, 0.065 mmol) was dissolved in dry THF (30 mL). (*E*)-$Bu_3SnCH{=}CHSiMe_3$ (506 mg, 1.30 mmol) was added and the mixture stirred under nitrogen at 50 °C for 16 hrs. The solvent was removed *in vacuo* and the residue purified by silica gel chromatography using chloroform:methanol (95:5 v/v) as eluant. The product was

recrystallized from ethyl acetate to give the (*E*)-5-(2-trimethylsilylvinyl) nucleoside (**27**)(233 mg, 83%): mp 178-180 °C; ^{1}H NMR (DMSO-d_6) δ 0.10 (s, 9H, Si*Me*$_3$), 2.46-2.51 (m, 2H, H-2'), 3.72-3.74 (m, 2H, H-5'), 4.22-4.26 (m, 1H, H-4'), 5.34 (t, 1H, $J_{OH,5'}$=4.5 Hz, C-5' OH, exchanges with deuterium oxide), 5.48-5.52 (m, 1H, H-3'), 6.30 (t, 1H, $J_{1',2'}$=6.2 Hz, H-1'), 6.60 (s (A_2), 2H, C*H*=C*H*SiMe$_3$), 7.58 (dd, 1H, $J_{4,5}$=8.0 Hz, $J_{5,6}$=5.0 Hz, pyridyl H-5), 8.20 (s, 1H, uracil H-6), 8.33 (ddd, 1H, $J_{4,5}$=8.0 Hz, $J_{4,6}$=1.6 Hz, $J_{2,4}$=1.6 Hz, pyridyl H-4), 8.82 (dd, 1H, $J_{5,6}$=5.0 Hz, $J_{4,6}$=1.6 Hz, pyridyl H-6), 9.12 (d, 1H, $J_{2,4}$=1.6 Hz, pyridyl H-2), 11.46 (s, 1H, NH, exchanges with deuterium oxide). Anal. calc'd for $C_{20}H_{25}N_3O_6Si.1/2\ H_2O$: C, 54.52; H, 5.96; N, 9.54. Found: C, 54.37; H, 5.79; N, 9.38.

(*E*)-5-(2-Trimethylsilylvinyl)-3'-*O*-(1-methylpyridinium-3-carbonyl)-2'-deoxyuridine iodide (28). (*E*)-5-(2-Trimethylsilylvinyl)-3'-*O*-(3-pyridylcarbonyl)-2'-deoxyuridine (**27**)(200 mg, 0.46 mmol) was dissolved in acetone (25 mL). Iodomethane (1.32 g, 9.27 mmol) was added and the reaction mixture refluxed for 16 hrs. The solvent was evaporated and the residue triturated with ether (3 x 10 ml) to yield the pure pyridinium iodide salt (**28**)(210 mg, 80%) as yellow crystals: mp 164-165 °C; ^{1}H NMR (DMSO-d_6) δ 0.08 (s, 9H, Si*Me*$_3$), 2.48-2.53 (m, 2H, H-2'), 3.71-3.75 (m, 2H, H-5'), 4.27-4.29 (m, 1H, H-4'), 4.41 (s, 3H, N*Me*), 5.40 (t, 1H, $J_{OH,5'}$=4.5 Hz, C-5' OH, exchanges with deuterium oxide), 5.54-5.58 (m, 1H, H-3'), 6.35 (t, 1H, $J_{1',2'}$=6.0 Hz, H-1'), 6.58 (s (A_2), 2H, C*H*=C*H*SiMe$_3$), 8.20 (s, 1H, uracil H-6), 8.24 (dd, 1H, $J_{4,5}$=8.2 Hz, $J_{5,6}$=5.0 Hz, pyridyl H-5), 9.00 (d, 1H, $J_{4,5}$=8.2 Hz, pyridyl H-4), 9.16 (d, 1H, $J_{5,6}$=5.0 Hz, pyridyl H-6), 9.61 (s,1H, pyridyl H-2), 11.48 (s, 1H,

NH, exchanges with deuterium oxide). Anal. calc'd for $C_{21}H_{28}IN_3O_6Si.1/2$ H_2O: C, 43.30; H, 5.03; N, 7.22. Found: C, 43.34; H, 4.93; N, 6.96.

(*E*)-5-(2-Trimethylsilylvinyl)-3'-*O*-(1-methylpyridinium-3-carbonyl)-2'-deoxyuridine bromide (29). (*E*)-5-(2-Trimethylsilylvinyl)-3'-*O*-(3-pyridylcarbonyl)-2'-deoxyuridine (**27**)(25 mg, 0.0579 mmol) was dissolved in acetone (1.5 mL). A solution of 2N bromomethane in diethylether (1.16 mL, 220 mg, 2.316 mmol) was added and the reaction mixture stiirred at 22 °C for 24 hrs. An additional aliquot of bromomethane was added (220 mg, 2.316 mmol) and the mixture stirred for an additional 24 hrs. The solvent was evaporated and the residue triturated with acetone (3 x 10 ml) to yield the pure pyridinium bromide salt (**29**)(22 mg, 72%) as colorless crystals: mp 166-168 °C; The ^1H NMR was identical to that observed for (*E*)-5-(2-trimethylsilylvinyl)-3'-*O*-(1-methylpyridinium-3-carbonyl)-2'-deoxyuridine iodide. Anal. calcd. for $C_{21}H_{28}BrN_3O_6Si$: C, 47.91; H, 5.36; N, 7.98. Found: C, 48.29; H, 5.04; N, 7.65.

(*E*)-5-(2-Iodovinyl)-3'-*O*-(1-methyl-1,4-dihydropyridine-3-carbonyl)-2'-deoxyuridine (30). (*E*)-5-(2-Trimethylsilylvinyl)-3'-*O*-(1-methylpyridinium-3-carbonyl)-2'-deoxyuridine iodide (**28**)(25 mg, 0.044 mmol) was dissolved in acetonitrile (5 mL). Iodine monochloride (7.1 mg, 0.044 mmol) was added and the reaction mixture stirred at 25 °C for 15 minutes. The solvent was evaporated and the crude iodide salt was obtained as a yellow solid and used without further purification. The yellow residue was dissolved in a two phase solvent system consisting of water:ethyl acetate (5 mL each). Sodium dithionite (50 mg, 0.285 mmol) and sodium bicarbonate (20 mg, 0.24 mmol) were added and the reaction was allowed to proceed at room temperature for 15 minutes with vigorous stirring. The ethyl acetate fraction was washed with water and then dried using sodium sulfate. The

solvent was removed *in vacuo* and the compound purified by chromatography using a short column of neutral aluminum oxide. Elution with chloroform:methanol (9:1 v/v) afforded the title compound (**30**)(12 mg, 56%) as a yellow solid: mp 165-168 °C; ^{1}H NMR (DMSO-d_6) δ 2.26-2.34 (m, 2H, H-2'), 2.96-3.00 (m, 5H, N*Me*, dihydropyridyl H-4) 3.64-3.69 (m, 2H, H-5'), 4.00-4.03 (m, 1H, H-4'), 4.72-4.77 (m, 1H, dihydropyridyl H-5), 5.20 (bs, 1H, C-5' OH, exchanges with deuterium oxide), 5.21-5.26 (m, 1H, H-3'), 5.86 (d, 1H, $J_{5,6}$=8.0 Hz, dihydropyridyl H-6), 6.18 (t, 1H, $J_{1',2'}$=6.0 Hz, H-1'), 7.12 (d, 1H, J_{trans}=15 Hz, C*H*=CHI), 7.15 (s,1H, dihydropyridyl H-2), 7.24 (d, 1H, J_{trans}=15 Hz, CH=C*H*I), 8.09 (s, 1H, uracil H-6), 11.60 (s, 1H, NH, exchanges with deuterium oxide). Anal. calc'd for $C_{18}H_{20}IN_3O_6$: C, 43.13; H, 4.02; N, 8.38. Found: C, 43.16; H, 3.67; N, 7.95.

5-Iodo-5'-*O*-*t*-butyldimethylsilyl-2'-fluoro-2'-deoxyarabinouridine (32). Imidazole (0.97 g, 14.3 mmol) and *t*-butyldimethylsilyl chloride (0.97 g, 6.44 mmol) were added to a solution of 5-iodo-2'-fluoro-2'-deoxyarabinouridine (**31**)(2.0 g, 5.37 mmol) in dry DMF (10 mL). The reaction was stirred for 16 hrs at room temperature. Water (20 mL) was added and the solid precipitate recovered by filtration. The residue was dissolved in dichloromethane and dried over $MgSO_4$. The residue was purified by silica gel column chromatography. Elution with dichloromethane:methanol (95:5 v/v) afforded the 5'-*O*-*t*-butyldimethylsilyl derivative (**32**)(2.14 g, 82%) after recrystallization from dichloromethane: mp 236-238 °C; ^{1}H NMR ($CDCl_3$) δ 0.16 (s, 6H, SiMe_2), 0.96 (s, 9H, Me_3C), 2.27 (d, 1H, $J_{OH,3'}$=4.4 Hz, C-3' OH), 3.87-3.92 (m, 2H, H-5'), 3.96-3.99 (m, 1H, $J_{3',4'}$=4.4 Hz, H-4'), 4.52 (dddd,1H, $J_{3',F}$=19.5, $J_{3',4'}$=4.4, $J_{OH,3'}$=4.4 Hz, $J_{2',3'}$=1.5 Hz, H-3'), 5.05 (ddd, 1H,

$J_{2',F}$=51.8, $J_{1',2'}$=3.9, $J_{2',3'}$=1.5 Hz, H-2'), 6.19 (dd, 1H, $J_{1',F}$=18.1, $J_{1',2'}$=3.9 Hz, H-1'), 7.92 (s, 1H, uracil H-6) 8.20 (bs, 1H, NH). Anal. calc'd for $C_{15}H_{24}FIN_2O_5Si$. 1/4 H_2O: C, 36.74; H, 5.03; N, 5.71. Found: C, 36.49; H, 5.03; N, 5.69.

5-Iodo-3'-*O*-(3-pyridylcarbonyl)-5'-*O*-*t*-butyldimethylsilyl-2'-fluoro-2'-deoxyarabinouridine (33). 5-Iodo-5'-*O*-*t*-butyldimethylsilyl-2'-fluoro-2'-deoxyarabinouridine (32)(1.0 g, 2.06 mmol) was added to a solution of nicotinoyl chloride hydrochloride (0.50 g, 2.81 mmol) and 4-dimethylaminopyridine (0.25 g, 2.05 mmol) in 10 ml dry pyridine and stirred for 16 hrs at 25 °C. Cold water (30 mL) was added and the filtered solid was redissolved in dichloromethane and dried with $MgSO_4$. The solvent was removed *in vacuo* and purification by silica gel column chromatography using dichloromethane:methanol (98:2 v/v) yielded the 3'-*O*-nicotinoyl nucleoside (33)(1.13 g, 93%) after recrystallization from ethyl acetate: mp 190-192 °C; ^{1}H NMR ($CDCl_3$) δ 0.17 (s, 6H, SiMe_2), 0.96 (s, 9H, Me_3C), 4.02-4.04 (m, 2H, H-5'), 4.21-4.23 (m, 1H, $J_{3',4'}$=3.4 Hz, H-4'), 5.27 (dd, 1H, $J_{2',F}$=50.3, $J_{1',2'}$=3.4 Hz, H-2'), 5.62 (dd,1H, $J_{3',F}$=19.1, $J_{3',4'}$=3.4 Hz, H-3'), 6.27 (dd, 1H, $J_{1',F}$=20.0, $J_{1',2'}$=3.4 Hz, H-1'), 7.46 (dd, 1H, $J_{4,5}$=8.3, $J_{5,6}$=4.9 Hz, pyridyl H-5), 8.04 (s, 1H, uracil H-6), 8.31 (ddd, 1H, $J_{4,5}$=8.3 Hz, $J_{4,6}$=2.0 Hz, $J_{2,4}$=2.0 Hz, pyridyl H-4), 8.62 (br s, 1H, NH), 8.86 (dd, 1H, $J_{5,6}$=4.9, $J_{4,6}$=2.0 Hz, pyridyl H-6), 9.25 (d, 1H, $J_{2,4}$=2.0 Hz, pyridyl H-2). Anal. calc'd for $C_{21}H_{27}FIN_3O_6Si$: C, 42.65; H, 4.60; N, 7.10. Found: C, 42.67; H, 4.64; N, 7.03.

5-Iodo-3'-*O*-(3-pyridylcarbonyl)-2'-fluoro-2'-deoxyarabinouridine (34). 5-Iodo-5'-*O*-*t*-butyldimethylsilyl-3'-*O*-(3-pyridylcarbonyl)-2'-fluoro-2'-deoxyarabinouridine (33)(1.0 g, 1.69 mmol) was dissolved in 20 ml THF. A 1 M solution of *n*-Bu_4N^+ F^- in THF (2.5 mL) was added with stirring. The

reaction was allowed to proceed for 90 minutes at 25 °C. The solvent was removed *in vacuo* and the residue purified by silica gel chromatography using dichloromethane:methanol (93:7 v/v). Recrystallization from methanol gave the deprotected compound as colorless crystals (**34**)(0.689 g, 85%): mp 203-205 °C; ^{1}H NMR (DMSO-d_6) δ 3.68-3.74 (m, 1H, H-5'), 3.78-3.83 (m, 1H, H-5''), 4.24-4.27 (m, 1H, H-4'), 5.35 (t, 1H, $J_{OH,5'}$=5.4 Hz, C-5' OH, exchanges with deuterium oxide), 5.52 (ddd, 1H, $J_{2',F}$=50.8, $J_{1',2'}$=3.9, $J_{2',3'}$=2.0 Hz, H-2'), 5.58 (ddd,1H, $J_{3',F}$=21.0, $J_{3',4'}$=3.4, $J_{2',3'}$=2.0 Hz, H-3'), 6.24 (dd, 1H, $J_{1',F}$=17.6, $J_{1',2'}$=3.9 Hz, H-1'), 7.61 (dd, 1H, $J_{4,5}$=7.8, $J_{5,6}$=4.9 Hz, pyridyl H-5), 8.25 (s, 1H, uracil H-6), 8.37 (ddd, 1H, $J_{4,5}$=7.8, $J_{2,4}$=1.9, $J_{4,6}$=1.5 Hz, pyridyl H-4), 8.86 (dd, 1H, $J_{5,6}$=4.9, $J_{4,6}$=1.5 Hz, pyridyl H-6), 9.18 (d, 1H, $J_{2,4}$=1.9 Hz, pyridyl H-2), 11.91 (br s, 1H, NH, exchanges with deuterium oxide) Anal. calc'd for $C_{15}H_{13}FIN_3O_6$: C, 37.76; H, 2.74; N, 8.81. Found: C, 37.89; H, 2.83; N, 8.63.

(*E*)-5-(2-Trimethylsilylvinyl)-3'-O-(3-pyridylcarbonyl)-2'-fluoro-2'-deoxyarabinouridine (35). (*E*)-$Bu_3SnCH{=}CHSiMe_3$ (0.65 g, 1.67 mmol) was added to a solution of 5-iodo-3'-*O*-(3-pyridylcarbonyl)-2'-fluoro-2'-deoxyarabinouridine (**34**)(0.40 g, 0.839 mmol) and $(Ph_3P)_2Pd(II)Cl_2$ (60 mg, 0.085 mmol) in dry THF (30 mL) and the mixture was stirred at 50 °C for 16 hrs under an argon atmosphere. Removal of the solvent *in vacuo* and purification of the residue by silica gel column chromatography using dichloromethane:methanol (94:6 v/v) as eluant afforded the desired compound (**35**)(0.311 g, 82 %) as colorless crystals after recrystallization from ethyl acetate: mp 138-140 °C; ^{1}H NMR (DMSO-d_6) δ 0.11 (s, 9H, SiMe_3), 3.71-3.77 (m, 1H, H-5'), 3.81-3.86 (m, 1H, H-5''), 4.26-4.29 (m,1H, H-4'), 5.34 (t, 1H, $J_{OH,5'}$=5.4 Hz, C-5' OH, exchanges with

deuterium oxide), 5.57 (ddd, 1H, $J_{2',F}$=53.2, $J_{1',2'}$=3.9, $J_{2',3'}$=2.4 Hz, H-2'), 5.60 (ddd,1H, $J_{3',F}$=19.5, $J_{3',4'}$=3.7, $J_{2',3'}$=2.4 Hz, H-3'), 6.30 (dd, 1H, $J_{1',F}$=17.1, $J_{1',2'}$=3.9 Hz, H-1'),6.61 and 6.68 (two d, 1H each, J_{trans}=19.6 Hz, C*H*=C*H*SiMe$_3$), 7.61 (dd, 1H, $J_{4,5}$=7.8, $J_{5,6}$=4.9 Hz, pyridyl H-5), 8.04 (s, 1H, uracil H-6), 8.38 (ddd, 1H, $J_{4,5}$=7.8, $J_{4,6}$=2.0, $J_{2,4}$=1.5 Hz, pyridyl H-4), 8.86 (dd, 1H, $J_{5,6}$=4.9, $J_{4,6}$=2.0 Hz, pyridyl H-6), 9.18 (d, 1H, $J_{2,4}$=1.5 Hz, pyridyl H-2), 11.66 (s, 1H, NH, exchanges with deuterium oxide). Anal. calcd. for $C_{20}H_{24}FN_3O_6Si$: C, 53.44; H, 5.38; N, 9.35. Found: C, 53.45; H, 5.45; N, 9.18.

(*E*)-5-(2-Trimethylsilylvinyl)-3'-*O*-(1-methylpyridinium-3-carbonyl)-2'-fluoro-2'-deoxyarabinouridine iodide (36). Iodomethane (0.76 g, 5.339 mmol) was added to a solution of (*E*)-5-(2-trimethylsilylvinyl)-3'-*O*-(3-pyridylcarbonyl)-2'-fluoro-2'-deoxyarabinouridine (**35**)(0.12 g, 0.267 mmol) in acetone (2 mL) and the reaction mixture was refluxed for 10 hrs. Removal of the solvent *in vacuo* and trituration of the residue with ether (3 x 10 mL) gave the pyridinium salt (**36**)(0.12 g, 78 %) as yellow crystals: mp 170-172 °C; ^{1}H NMR (DMSO-d_6) d 0.11 (s, 9H, Si*Me*$_3$), 3.73-3.79 (m, 1H, H-5'), 3.83-3.88 (m, 1H, H-5''), 4.30-4.33 (m, 1H, H-4'), 4.44 (s, 3H, N*Me*), 5.39 (t, 1H, $J_{OH,5'}$=5.4 Hz, C-5' OH, exchanges with deuterium oxide), 5.57 (ddd, 1H, $J_{2',F}$=50.8, $J_{1',2'}$=3.9, $J_{2',3'}$=2.0 Hz, H-2'), 5.65 (ddd,1H, $J_{3',F}$=18.6, $J_{3',4'}$=4.9, $J_{2',3'}$=2.0 Hz, H-3'), 6.30 (dd, 1H, $J_{1',F}$=17.6, $J_{1',2'}$=3.9 Hz, H-1'), 6.61 and 6.69 (two d, 1H each, J_{trans}=19.1 Hz, C*H*=C*H*SiMe$_3$), 8.02 (s, 1H, uracil H-6), 8.30 (dd, 1H, $J_{4,5}$=7.8, $J_{5,6}$=5.8 Hz, pyridinium H-5), 9.05 (d, 1H, $J_{4,5}$=7.8 Hz, pyridinium H-4), 9.21 (d, 1H, $J_{5,6}$=5.8 Hz, pyridinium H-6), 9.65 (s, 1H, pyridinium H-2), 11.68 (s,1H, NH, exchanges with deuterium oxide). Anal.

calcd. for $C_{21}H_{27}FIN_3O_6Si$: C, 42.65; H, 4.60; N, 7.10. Found: C, 42.56; H, 4.54; N, 6.82.

(*E*)-5-(2-Trimethylsilylvinyl)-3'-*O*-(1-methylpyridinium-3-carbonyl)-2'-fluoro-2'-deoxyarabinouridine bromide (37). (*E*)-5-(2-Trimethylsilylvinyl)-3'-*O*-(3-pyridylcarbonyl)-2'-fluoro-2'-deoxyarabinouridine (35)(40 mg, 0.088 mmol) was dissolved in acetone (3 mL). A solution of 2N bromomethane in diethylether (0.88 mL, 167 mg, 1.76 mmol) was added and the reaction mixture stiirred at 50 °C for 12 hrs in a sealed stainless steel reaction vessel. An additional aliquot of bromomethane was added (167 mg, 1.76 mmol) and the mixture stirred for an additional 12 hrs at 50 °C. The solvent was evaporated and the residue triturated with acetone (3 x 10 ml) to yield the bromide salt (37)(46 mg, 96%) as colorless crystals: mp 174-176 °C; The ^1H NMR was identical to that observed for (*E*)-5-(2-trimethylsilylvinyl)-3'-*O*-(1-methylpyridinium-3-carbonyl)-2'-fluoro-2'-deoxyarabinouridine iodide. Anal. calcd. for $C_{21}H_{27}BrFN_3O_6Si$: C, 46.33; H, 5.00; N, 7.72. Found: C, 46.47; H, 5.18; N, 7.77.

(*E*)-5-(2-Iodovinyl)-3'-*O*-(1-methyl-1,4-dihydropyridine-3-carbonyl)-2'-fluoro-2'-deoxyarabinouridine (38). Iodine monochloride (11 mg, 0.0676 mmol) was added to a solution of (*E*)-5-(2-trimethylsilylvinyl)-3'-*O*-(1-methylpyridinium-3-carbonyl)-2'-fluoro-2'-deoxyarabinouridine iodide (36)(40 mg, 0.0676 mmol) in acetonitrile (2 mL) and the reaction mixture was stirred at 25 °C for 30 min. Removal of the solvent *in vacuo* gave the iodovinyl salt as a yellow solid which was dissolved in a two phase solvent system comprised of water: ethyl acetate (2 mL each). Sodium dithionite (82 mg, 0.47 mmol) and sodium bicarbonate (42 mg, 0.50 mmol) were added and the reaction was allowed to proceed at 25 °C with vigorous stirring for 15 min. The ethyl acetate fraction was washed with water (2

mL) and the ethyl acetate solution was dried over Na_2SO_4. The solvent was removed *in vacuo* and the product was purified by using a short neutral aluminum oxide column. Elution with chloroform:methanol (90:10, v/v) afforded the desired product (**38**)(15 mg, 43%) as yellow crystals after recrystallization from methanol: mp 148-152 °C; ^{1}H NMR (DMSO-d_6) d 2.97-3.00 (m, 4H, N*Me*, dihydropyridyl H-4), 3.60-3.75 (m, 2H, H-5'), 4.02-4.07 (m,1H, H-4'), 4.78 (dt, 1H, $J_{5,6}$=8.0, $J_{4,5}$=3.9 Hz, dihydropyridyl H-5), 5.15-5.25 (m, 2H, H-2', C-5' OH, exchanges with deuterium oxide), 5.30-5.31 (m, 1H, H-3'), 5.87 (d, 1H, $J_{5,6}$=8.0 Hz, dihydropyridyl H-6), 6.14 (dd, 1H, $J_{1',F}$=18.0, $J_{1',2'}$=3.8 Hz, H-1'), 7.18 (d, 1H, J_{trans}=14.8 Hz, C*H*=CHI), 7.21 (s, 1H, dihydropyridyl H-2), 7.26 (d, 1H, J_{trans}=14.8 Hz, CH=C*H*I), 7.98 (s, 1H, uracil H-6), 11.78 (bs,1H, NH, exchanges with deuterium oxide) . Anal. calcd. for $C_{18}H_{19}FIN_3O_6 \cdot H_2O$: C, 40.24; H, 3.94; N, 7.82. Found: C, 40.20; H, 3.57; N, 7.45.

F. Radiochemical Synthesis

(*E*)-5-(2-[^{125}I]Iodovinyl)-2'-deoxyuridine (**10a**). Na^{125}I (6.5 MBq) in 0.1 N NaOH solution (5 µL) was placed in a Wheaton vial and a solution of ICl (25 µg, 0.154 µmol) in 20% acetic acid in acetonitrile (10 µL) was added. A solution of (*E*)-5-2(trimethylsilylvinyl)-2'-deoxyuridine (**6**)(0.24 mg, 0.73 µmol) in 20% acetic acid in acetonitrile (10 µL) was added to the contents in the Wheaton vial and the reaction was allowed to proceed for 15 min at 25 °C. (*E*)-5-(2-[^{125}I]Iodovinyl)-2'-deoxyuridine ([^{125}I]IVDU) was purified by preparative reverse phase HPLC on a Whatman Partisil M9 10/25 C8 column using isocratic elution with acetonitrile:H_2O (3:7, v/v) at a flow rate of 1.5 mL/min and UV detection at 254 nm. The product (**10a**)(5.6 MBq, 86 % radiochemical yield, > 98 % radiochemical purity, specific

activity 38 GBq/mmol) had a HPLC retention time of 11.49 min whereas the unreacted trimethylsilylvinyl precursor had a retention time of 22.51 min.

(*E*)-5-(2-[^{125}I]Iodovinyl)-2'-fluoro-2'-deoxyuridine (11a) $Na^{125}I$ (6.5 MBq) in 0.1 N NaOH solution (5 μL) was placed in a Wheaton vial and a solution of ICl (25 μg, 0.154 μmol) in 20% acetic acid in acetonitrile (10 μL) was added. A solution of (*E*)-5-2(trimethylsilylvinyl)-2'-fluoro-2'-deoxyuridine (7)(0.25 mg, 0.73 μmol) in 20% acetic acid in acetonitrile (10 μL) was added to the contents in the Wheaton vial and the reaction was allowed to proceed for 15 min at 25 °C. The desired product was purified by preparative reverse phase HPLC on a Whatman Partisil M9 10/25 C8 column using isocratic elution with acetonitrile:H_2O (3:7, v/v) at a flow rate of 1.5 mL/min and UV detection at 254 nm. (*E*)-5-(2-[^{125}I]Iodovinyl)-2'-fluoro-2'-deoxyuridine ([^{125}I]IVFRU, **11a**) (5.5 MBq, 85 % radiochemical yield, > 98 % radiochemical purity, specific activity 41 GBq/mmol) had a HPLC retention time of 11.76 min whereas the unreacted trimethylsilylvinyl precursor had a retention time of 24.19 min.

(*E*)-5-(2-[^{131}I]Iodovinyl)-2'-fluoro-2'-deoxyuridine (11b). $Na^{131}I$ (74 MBq) in 0.1 N NaOH solution (5 μL) was placed in a Wheaton vial. ICl (124 μg, 0.765 μmol) dissolved in 20% acetic acid in acetonitrile (10 μL) was added. A solution of (*E*)-5-(2-trimethylsilylvinyl)-2'-fluoro-2'-deoxyuridine (7)(500 μg, 1.53 μmol) in 20% acetic acid in acetonitrile (10 μL) was added to the contents in the Wheaton vial and the reaction was allowed to proceed for 15 min at 25 °C. (*E*)-5-(2-[^{131}I]Iodovinyl)-2'-fluoro-2'-deoxyuridine (11b)(63 MBq, 85 % radiochemical yield, > 98 % radiochemical purity, specific activity 252 GBq/mmol) was isolated after purification by preparative reverse phase HPLC on a Whatman partisil M9 10/25 C8

column. Isocratic elution with acetonitrile:H_2O (7:3 v/v) at a flow rate of 1.5 mL/min with UV detection at 254 nm was employed.

"No Carrier Added" (*E*)-5-(2-[^{131}I]Iodovinyl)-2'-fluoro-2'-deoxyuridine (11b). (*E*)-5-(2-Trimethylsilylvinyl)-2'-fluoro-2'-deoxyuridine (7)(100 μg, 0.306 μmol) in 20% acetic acid in acetonitrile (10 μL) was added to a Wheaton vial containing Na^{131}I (11.3 MBq) in 0.1 N NaOH (5 μL). A solution of N-chlorosuccinimide (100 μg, 0.749 μmol) in 20% acetic acid in acetonitrile (10 μL) was added and the reaction allowed to proceed for 30 minutes at room temperature. The reaction was terminated by the addition of sodium thiosulfate (100 μg, 0.632 μmol) in 10 μL water. The radioactive product was purified in the same manner as carrier added material and (*E*)-5-(2-[^{131}I]iodovinyl)-2'-fluoro-2'-deoxyuridine (11b)(8.0 MBq, 71 % radiochemical yield, > 98 % radiochemical purity, specific activity > 5.29 TBq/mmol) was isolated as the no carrier added product.

(*E*)-5-(2-[^{125}I]Iodovinyl)-2'-fluoro-2'-deoxyarabinouridine (12a). Na^{125}I (6.5 MBq) in 0.1 N NaOH solution (5 μL) was placed in a Wheaton vial and a solution of ICl (25 μg, 0.154 μmol) in 20% acetic acid in acetonitrile (10 μL) was added. A solution of (*E*)-5-(2-trimethylsilylvinyl)-2'-fluoro-2'-deoxyarabinouridine (8)(0.25 mg, 0.73 μmol) in 20% acetic acid in acetonitrile (10 μL) was added to the contents in the Wheaton vial and the reaction was allowed to proceed for 15 min at 25 °C. (*E*)-5-(2-[^{125}I]Iodovinyl)-2'-fluoro-2'-deoxyarabinouridine([^{125}I]IVFAU) was purified by preparative reverse phase HPLC on a Whatman Partisil M9 10/25 C8 column using isocratic elution with acetonitrile:H_2O (3:7, v/v) at a flow rate of 1.5 mL/min and UV detection at 254 nm. The desired radiolabelled product (12a)(5.6 MBq, 86 % radiochemical yield, > 98 % radiochemical purity, specific activity 38 GBq/mmol) had a HPLC retention time of 13.21

min whereas the unreacted trimethylsilylvinyl precursor had a retention time of 27.59 min.

(*E*)-5-(2-[^{125}I]Iodovinyl)arabinouridine (13a). $Na^{125}I$ (6.5 MBq) in 0.1 N NaOH solution (5 μL) was placed in a Wheaton vial and a solution of ICl (25 μg, 0.154 μmol) in 20% acetic acid in acetonitrile (10 μL) was added. A solution of (*E*)-5-2(trimethylsilylvinyl)arabinouridine (9)(0.25 mg, 0.73 μ mol) in 20% acetic acid in acetonitrile (10 μL) was added to the contents in the Wheaton vial and the reaction was allowed to proceed for 15 min at 25 °C. The desired product was purified by preparative reverse phase HPLC on a Whatman Partisil M9 10/25 C8 column using isocratic elution with acetonitrile:H_2O (3:7, v/v) at a flow rate of 1.5 mL/min and UV detection at 254 nm. (*E*)-5-(2-[^{125}I]Iodovinyl)arabinouridine ([^{125}I]IVAU, 13a) (4.1 MBq, 63 % radiochemical yield, > 98 % radiochemical purity, specific activity 30 GBq/mmol) had a HPLC retention time of 10.24 min, whereas the unreacted trimethylsilylvinyl precursor had a retention time of 17.69 min.

(*E*)-5-(2-[^{131}I]Iodovinyl)-3'-*O*-(1-methyl-1,4-dihydropyridine-3-carbonyl)-2'-deoxyuridine (30a). (*E*)-5-(2-Trimethylsilylvinyl)-3-*O*-(1-methylpyridinium-3-carbonyl)-2'-deoxyuridine bromide (29)(1mg, 0.00190 mmol) was dissolved in 100 μL acetonitrile and added to a stirred solution of ICl (30 μg, 0.185 μmol) and $Na^{131}I$ (13.1 MBq) in 20 μL acetonitrile. After stirring the reaction mixture for 15 minutes at room temperature, the solvent was evaporated under a stream of nitrogen. The residue was then dissolved in degassed water (200 μL) and ethyl acetate (200 μL). Sodium dithionite (4 mg, 0.0229 mmol) and sodium bicarbonate (2 mg, 0.0238 mmol) were added and the reaction mixture was stirred for 20 minutes at room temperature. The ethyl acetate layer was then removed and the solvent

evaporated over a stream of nitrogen. The residue was then dissolved in methanol and purified by preparative reverse phase HPLC on a Whatman partisil M9 10/25 C8 column. Isocratic elution with acetonitrile:H_2O (60:40 v/v) at a flow rate of 2.0 mL/min gave (*E*)-5-(2-[^{131}I]iodovinyl-3-*O*-(1-methyl-1,4-dihydropyridyl-3-carbonyl)-2'-deoxyuridine (^{131}IVDU-CDS) with a retention time of 16.37 minutes. The desired product (**30a**) was isolated in 19% radiochemical yield (2.5 MBq) at a specific activity of 2.8 GBq/mmol and > 98% radiochemical purity after HPLC purification.

(*E*)-5-(2-[^{131}I]Iodovinyl)-3'-*O*-(1-methyl-1,4-dihydropyridine-3-carbonyl)-2'-fluoro-2'-deoxyuridine (22a). (*E*)-5-(2-Trimethylsilylvinyl)-3'-*O*-(1-methylpyridinium-3-carbonyl)-2'-fluoro-2'-deoxyuridine bromide (**21**)(1mg, 0.00184 mmol) was dissolved in 100 µL acetonitrile. The solution was immediately added to a stirred solution of ICl (30 µg, 0.185 µmol) and Na^{131}I (26.8 MBq) in 20 µL acetonitrile. After stirring the reaction mixture for 15 minutes at room temperature, the solvent was evaporated over a stream of nitrogen. The residue was then dissolved in degassed water (200 µL) and ethyl acetate (200 µL). Sodium dithionite (4 mg, 0.0229 mmol) and sodium bicarbonate (2 mg, 0.0238 mmol) were added and the reaction mixture was stirred for 20 minutes at room temperature. The ethyl acetate layer was then removed and the solvent evaporated over a stream of nitrogen. The residue was then dissolved in methanol and purified by preparative reverse phase HPLC on a Whatman partisil M9 10/25 C8 column. Isocratic elution with acetonitrile:H_2O (60:40 v/v) at a flow rate of 2.0 mL/min gave pure (*E*)-5-(2-[^{131}I]Iodovinyl)-3'-*O*-(1-methyl-1,4-dihydropyridine-3-carbonyl)-2'-fluoro-2'-deoxyuridine (^{131}IVFRU-CDS) with a retention time of 19.54 minutes. The desired product (**22a**) was isolated

in 14% radiochemical yield (3.8 MBq) at a specific activity of 4.3 GBq/mmol and > 98% radiochemical purity after HPLC purification.

Experiments G-J were performed by Dr. Jan Balzarini at the Rega Institute, Belgium.

G. Assay for Inhibition of Cell Proliferation

The methods for evaluating the cytostatic activity of the test compounds against murine mammary carcinoma FM3A cells have been reported previously.[172,175,178] Briefly, cells (4×10^4) suspended in growth medium were allowed to proliferate in 200 µL wells of microtitre plates in the presence of five-fold dilutions (ie. 500, 100, 20, 4, 0.8, 0.16, 0.032, 0.006, 0.0012, and 0.00025 µM) of the test compounds, at 37 °C in a humidified carbon dioxide-controlled atmosphere. Control FM3A cell cultures were grown without compound under the same experimental conditions. After 48 h, the number of cells were counted in a Coulter counter. The IC_{50} was defined as the drug concentration required to inhibit FM3A cell proliferation by 50%.

H. Tritium Release Assay from 5-^{3}H Deoxycytidine

Thymidylate synthase activity was measured in intact FM3A/0, FM3A TK^-, FM3A TK^-/HSV-1 TK^+, and FM3A TK^-/HSV-2 TK^+ cells by estimating tritium release from 5-^{3}H dUMP, which itself had been formed intracellularly from exogenous 5-^{3}H dCyd. The procedure has been described in detail previously.[213] Briefly, cells (0.75×10^6) in 300 µL medium were added to 60 µL of medium containing an appropriate amount of test compound and 40 µL of medium containing [5-^{3}H]dCyd (4 µCi). After incubation for 30

minutes, the suspensions were mixed with carbon black (160 mg/mL) in 5% trichloroacetic acid and then centrifuged. The supernatants were analyzed for radioactivity by scintillation counting.

I. Nucleoside Kinase Assay

Test compounds were evaluated in a competitive binding assay using purified HSV-1 TK as described previously.[175] Standard assay conditions were 50 mM Tris.HCl (pH=8.0), 2.5 mM $MgCl_2$, 10 mM dithiothreitol (DTT), 2.5 mM ATP, 1 mg/mL bovine seum albumin, 10 mM sodium fluoride, and 1 μM methyl-^{3}H dThd. Assays were performed at 37 ° C, with an incubation time of 15 min. Aliquots of 25 μL of the reaction mixtures were spotted on Whatman DEAE-81 filter paper disks. The filters were subsequently washed three times for 5 min with 1.5 mM ammonium formate and finally rinsed once with water and once with ethanol. The radioactivity on the filters was determined by scintillation counting.

J. Phosphorolysis by Human Deoxythymidine Phosphorylase

Phosphorolysis by dThd phosphorylase prepared from human blood platelets was measured by HPLC as described before.[175] One milliliter of the reaction mixture contained 10 mM Tris.HCl (pH=7.6), 1 mM EDTA, 2mM potassium phosphate, 150 mM NaCl, 0.1 mM concentrations of the test compounds, and 0.55 mg crude blood platelet protein extract. Reaction mixtures were incubated at 37 °C, and at different times 200 μL fractions were taken, rapidly cooled on ice, and centrifuged for 5 min at 4 °C. The supernatants were then precipitated with 400 μL of ice-cold methanol and analyzed by HPLC.

K. Partition Coefficients and Oxidation of CDS-derivatives

Partition coefficients (log P) were measured by determining the distribution of the test compound between a presaturated mixture of *n*-octanol and water (1:1, v/v). The analytical method consisted of a modified shake-flask technique and ultraviolet (UV) spectrometry quantitation after centrifugal separation of the two phases. The concentration of the test compound in the octanol phase prior to distribution was 0.5 mM. The dihydropyridine chromophore (λmax =360 nm) was used for quantitative UV analysis for IVDU-CDS, IVFRU-CDS, and IVFAU-CDS. IVDU, IVFRU, and IVFAU were analyzed at 254 nm. Partition coefficient (P) is defined as the ratio of the test compound concentrations in the octanol and water phases (o/w).

Pseudo-first order rate constants and half-lives for the oxidation of IVDU-CDS, IVFRU-CDS, and IVFAU-CDS were determined in 50% mouse blood, 20% mouse brain homogenate and 20% mouse liver homogenate. Tissue samples were obtained from a male Balb/c mouse immediately after sacrifice. A solution of the test compound dissolved in DMSO (10 mM) was added to each prewarmed (37 °C) matrix to give a final concentration of 0.5 mM and then incubated at 37 °C. At various times (5 min, 15 min, 30 min, 1 hr, 2hr, and 4 hr) after compound addition, an aliquot (25 µL) was removed and added to 100 µL acetonitrile. The samples were immediately centrifuged and the supernatant analyzed by reverse phase HPLC. The rate of disappearance of the 1-methyl-1,4-dihydropyridine-CDS was monitored by UV detection at 360 nm.

L. *In Vitro* Cellular Uptake in KBALB, KBALB-LNL and KBALB-STK Cells.

Cells (1 x 10^5) of each cell line (KBALB, KBALB-LNL, KBALB-STK) were grown in 24-well culture plates. Radiolabelled compound (38 pmol; specific activity = 30-41 GBq/mmol) was added to each well and incubated at 37 °C in Dulbecco's modified Eagles medium (0.5 mL). At varying times after exposure to the radiolabelled compounds, the supernatants were removed, the cells rinsed with phosphate buffered saline, and the adherant cells were then trypsinized and removed. Cellular uptake of radioactivity was determined by gamma counting in a Beckmann 8000 gamma counter. Each uptake experiment was performed four times for each compound in each cell line.

M. Transfection and Detection of Gene Expression

Two transfection methods were employed to introduce plasmid expression vectors carrying the HSV-1 TK and firefly luciferase genes into KBALB cells. Calcium phosphate co-precipitation was performed by mixing 4 μg DNA with 31 μL aqueous $CaCl_2$ (2 M) then co-precipitating with 250 μL 2x Tris buffered saline. After incubation for 30 min at room temperature, an aliquot (1 μg) was added to adherant KBALB cells (1 x 10^5) in DMEM. After incubation for 24 hours at 37°, the medium was removed, fresh growth medium added and the cells incubated for an additional 24 hours before analysis. Cationic liposome-mediated transfection was performed with DOTAP (Boehringer Mannheim) according to the manufacturer's recommended procedure. Briefly, DNA (4 μg) in 40 μL Hepes buffer was mixed with 30 μg DOTAP in 100 μL Hepes buffer and incubated at room temperature for 15 minutes. An aliquot (1 μg) was added to adherant

KBALB cells (1 x 10^5) in serum-free DMEM and incubated for 24 hours before replacement of media and further incubation for 24 hours before analysis. Co-transfections were performed in an identical manner with equal amounts (1 μg) of each plasmid. HSV-1 TK gene expression was detected by measuring [^{125}I]IVFRU uptake in transfected cells by gamma counting after 8 hours exposure to 80 pmol at a specific activity of 40 GBq/mmol. Luciferase gene expression was detected in cell lysates using a commercial assay kit (Boehringer Mannheim) and with single photon detection in a scintillation counter (Beckman LS9000). Each transfection experiment was performed three times. Transfection cocktails lacking DNA were used as controls for each experiment.

N. *In Vitro* Transduction and Cellular Uptake of [^{125}I]IVFRU

KBALB cells (1 x 10^5) were plated on 10-cm diameter culture plates. Growth medium (9 mL) and PA-317 producer cell supernatant containing pLSNtk retrovirus (1 mL, 1 x 10^6 colony-forming units) was added and incubated for 24 hr at 37 °C. The medium was removed and replaced with fresh growth medium containg 1 mg/mL G-418. Selection with antibiotic G-418 for 2 weeks after transduction isolated resistant cells that were successfully transduced with the retroviral vector. The transduced cell line (KBALB-LTK) was expanded *in vitro* and cultured in 24-well plates. Cellular uptake of [^{125}I]IVFRU in KBALB-LTK cells was evaluted in the same manner as uptake in the KBALB-STK cell line.

O. *In Vivo* HSV-1 TK Gene Transfer to KBALB Tumors

KBALB cells (1 x 10^5) were injected subcutaneously into the flank of male Balb/c mice (n = 12). Palpable tumors appeared 14 days after injection.

When the tumors reached a mean diameter of 5 mm, intratumoral injections of LSNtk retroviral vector was initiated. PA-317 producer cell supernatants (1×10^6 cfu/mL) were injected into 3 treatment groups. Two groups received single intratumoral injections of supernatant (200 μL and 400 μL). A third group received a daily injection of supernatant (400 μL) for three consecutive days. A control group received a single intratumoral injection of saline (200 μL). When the tumors reached a mean diameter of 10 mm, [^{131}I]IVFRU (370 KBq, sp. act. 59 GBq/mmol) was injected via the tail vein into each tumor bearing animal. The animals were sacrificed 8 hours after injection of [^{131}I]IVFRU. The radioactivity levels in blood and tumor were determined on a Beckman 8000 gamma counter.

P. Biodistribution of [^{131}I]IVFRU in Balb/c Mice Bearing KBALB or KBALB-STK Tumors

KBALB or KBALB-STK cells ($1 \times 10^{5)}$ were injected subcutaneously into the flank of male Balb/c mice (n = 24). Palpable tumors appeared 14 days after injection. [^{131}I]IVFRU (370 KBq, sp. act. 59 GBq/mmol) was injected via the tail vein into each tumor bearing animal when the tumors reached a mean diameter of 10 mm. Three animals were sacrificed at varying time intervals (1,2,4, and 8 hr) after injection of [^{131}I]IVFRU. The uptake of radioactivity in tissues of interest was determined on a Beckman 8000 gamma counter after dissection.

Q. Planar Scintigraphy of Balb/c Mice Bearing KBALB-STK Tumors During Ganciclovir Treatment

KBALB-STK cells (1×10^{5}) were injected subcutaneously into the flank of Balb/c mice (n = 12). All animals developed palpable tumors suitable

for imaging two weeks after inoculation. When the tumors were approximately 10 mm in diameter, static planar images were obtained following injection of [^{131}I]IVFRU (3.7 MBq, sp. act. = 252 GBq/mmol) via the tail vein. Anesthetized animals (inhaled methoxyfluorane) were placed in the prone position under a pinhole collimator on a Searle gamma camera (Scintiview) with data manipulated on an ADAC computer (DPS 3300). Images were acquired over 15 minutes using a 256 x 256 matrix. After initial imaging, a group of animals (n = 6) were subjected to i.p. ganciclovir injections of 100 mg/kg once daily for seven days. The control group (n = 6) received daily saline injections. After 4 days, [^{131}I]IVFRU was readministered as before (3.7 MBq) and the mice were imaged under the same acquisition protocol. The tumor diameter for each animal was measured each day until termination of the experiment.

III. Results and Discussion

A. Objective

Detecting gene expression during *in vivo* gene therapy is a critical issue for laboratory and clinical investigators. Until recently, the most sensitive and reliable techniques for detecting and quantitating *in vivo* gene transfer and expression have been invasive. Vector design and construction has often exploited the use of common reporter systems that invariably involve removal of host tissue for histochemical evaluation. In principle, generic reporter constructs encode for gene products that enzymatically alter exogenous substrates to easily detectable species. Similarly, tissue selective metabolic processing is a fundamental tenet for preferential radiopharmaceutical localization *in vivo*. Therefore, scintigraphic imaging techniques used routinely in nuclear medicine have potential applications in

gene therapy as a means of non-invasively detecting gene expression. The development of an efficient and highly selective reporter gene and ligand system is essential for non-invasive imaging studies.

Herpes simplex virus type-1 thymidine kinase (HSV-1 TK) is particularly promising as a target for scintigraphic detection with gamma-emitting nucleoside radiopharmaceuticals. Selective phosphorylation of anti-herpes nucleosides results in entrapment of phosphorylated derivatives in cells where HSV-1 TK is present. Metabolic entrapment via phosphorylation is a mechanism of localization that is very attractive for a putative nucleoside radiopharmaceutical. In contrast to receptor imaging agents, a high amount of labelled substrate can undergo phosphorylation and accumulate within a cell expressing HSV-1 TK.

Non-invasive imaging of gene expression during gene therapy could provide potentially useful information. The extent of gene delivery and expression may be assessed with a radiopharmaceutical selectively localizing in HSV-1 TK expressing tissue. This is particularly important in the HSV-1 TK/ganciclovir gene therapy paradigm since treatment failures in animal models are associated with inefficient gene delivery and expression prior to ganciclovir administration.[90] In addition, it is apparent that an imaging agent could be used as a reporter ligand for vector systems carrying other therapeutic genes in addition to the HSV-1 TK gene in order to assess gene transfer efficiency and expression.

The objective of this investigation was to synthesize and evaluate several radioiodinated nucleosides as non-invasive scintigraphic imaging agents to detect HSV-1 TK gene expression. New syntheses and radiosyntheses of (*E*)-5-(2-iodovinyl)-2'-deoxyuridine (IVDU), (*E*)-5-(2-iodovinyl)-2'-fluoro-2'-deoxyuridine (IVFRU), (*E*)-5-(2-iodovinyl)-2'-fluoro-2'-

deoxyarabinouridine (IVFAU) and (*E*)-5-(2-iodovinyl)arabinouridine (IVAU) were developed. Since IVDU, IVFRU, IVFAU, and IVAU display potent antiviral activity against HSV-1, these were considered promising candidates for evaluation as imaging agents. New 1-methyl-1,4-dihydropyridine prodrug derivatives of IVDU, IVFRU, and IVFAU were also investigated. The 1-methyl-1,4-dihydropyridyl chemical delivery system (CDS) is conjugated to the 3'-hydroxyl moiety of each nucleoside and is presumed to impart enhanced lipophilicity and tissue targeting to the CNS. Brain-targeting of putative HSV-1 TK imaging agents (IVDU-CDS, IVFRU-CDS, and IVFAU-CDS) would be advantageous for gene therapy protocols treating brain neoplasms.

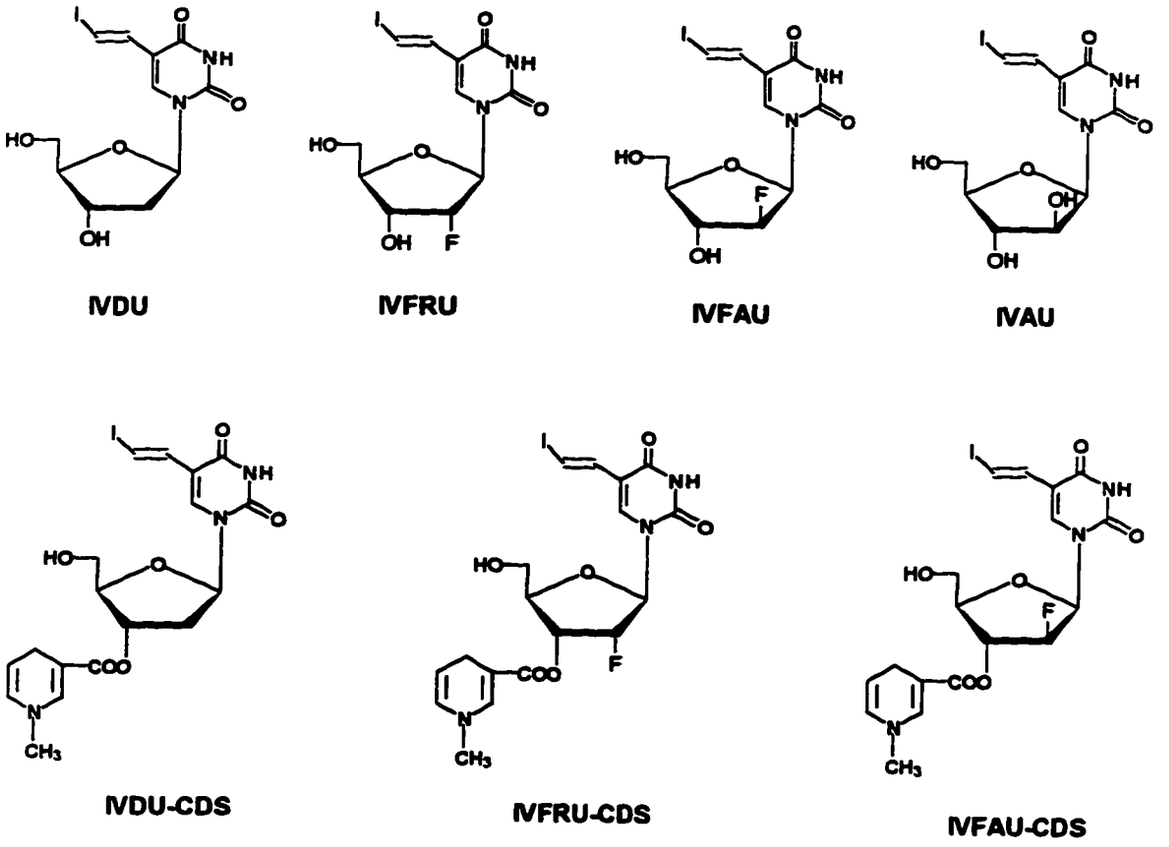

Fig. 14 Structures of nucleoside derivatives

B. Synthetic Strategies

Several strategies have been reported for the synthesis of radiolabelled IVDU. Radiohalogen exchange has been shown to be effective for the synthesis of lower specific activity product.[214] Similarly, carrier-added and high specific activity products have been isolated in respectable radiochemical yields using modified Hunsdiecker reactions.[185] Recent reports for the highly efficient radiosyntheses of labelled IVAU from vinylstannane and vinylsilane precursors under mild conditions is particularly appealing.[215,208] However, radioiodination of these precursors has only been attempted using protected nucleosides. Deprotection after radiohalogenation requires additional undesired laboratory handling of radioactive materials which results in some loss of radiolabelled product. A general radiosynthetic strategy where the final radiohalogenation is carried out using an unprotected (*E*)-5-(2-trimethylsilylvinyl) precursor was envisioned.

The introduction of an (*E*)-5-(2-trimethylsilylvinyl) functionality at the 5-position of 5-iodoarabinouridine has been reported using a reaction sequence which involved palladium-catalyzed coupling of (trimethylsilyl)acetylene followed by reduction over a Lindlar catalyst.[208] However, this procedure produces mixtures of reduced compounds that require HPLC separation. Direct coupling of (*E*)-2-tributylstannyl-1-trimethylsilylethene with protected 5-iodo-2'-deoxyuridine in the presence of a palladium catalyst gives protected (*E*)-5-(2-trimethylsilylvinyl)-2'-deoxyuridine in good yield.[216] It was therefore of interest to investigate whether a similar coupling reaction could be performed using unprotected nucleosides to simplify the subsequent radioiodination procedure.

Two general strategies were used for synthesis of IVDU-CDS, IVFRU-CDS, and IVFAU-CDS. Common features include 5'-silylether formation, 3'-ester formation, Pd-mediated coupling, N-alkylation, and the final one pot iodination and reduction reactions. However, the two strategies are divergent since C-5 iodination of 3'-*O*-(3-pyridylcarbonyl)-5'-*O*-*t*-butyldimethylsilyl-2'-fluoro-2'-deoxyuridine is performed midstream with simultaneous deprotection. In contrast, the synthetic strategy used for IVDU-CDS and IVFAU-CDS involves starting materials with a C-5 iodo functionality. An electrophilic iodination reaction was the method of choice for introduction of iodine. This step was carried out before reduction of the pyridinium salt because of facile oxidation of reduced dihydropyridine species.

C. (*E*)-5-(2-Iodovinyl)-2'-deoxyuridine (IVDU), (*E*)-5-(2-iodovinyl)-2'-fluoro-2'-deoxyuridine (IVFRU), (*E*)-5-(2-iodovinyl)-2'-fluoro-2'-deoxyarabinouridine (IVFAU), and (*E*)-5-(2-iodovinyl)arabinouridine (IVAU) (Fig. 15 and Fig. 16)

The palladium-catalyzed coupling reaction proceeded smoothly for 5-iodo-2'-deoxyuridine (3) and the 2'-fluorinated derivatives (4,5). Although the nucleoside precursors had a low solubilty in acetonitrile or THF, the reactions proceeded to completion providing yields ranging from 64-80%. The purification of the (*E*)-5-(2-trimethylsilylvinyl) products (6,7,8) was troublesome since trace impurities tended to co-elute with the desired products during silica gel column chromatography, and these impurities impeded subsequent crystallization attempts. Therefore, it was necessary to perform additional column chromatography purification of fractions containing small amounts of impurities prior to crystallization. The choice of

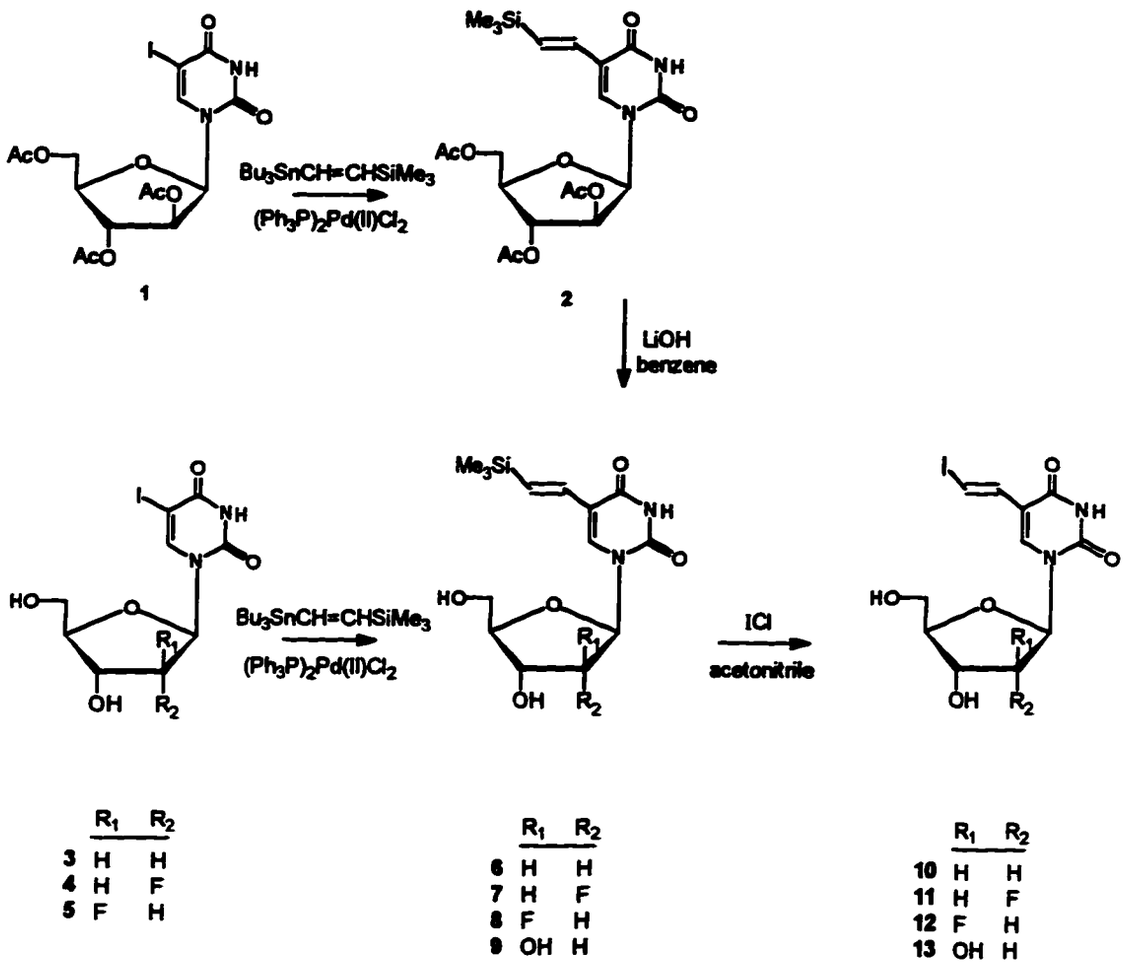

	R_1	R_2
3	H	H
4	H	F
5	F	H

	R_1	R_2
6	H	H
7	H	F
8	F	H
9	OH	H

	R_1	R_2
10	H	H
11	H	F
12	F	H
13	OH	H

Fig. 15 Synthesis of IVDU, IVFRU, IVFAU and IVAU.

recrystallization solvent was important since isomerization of vinylsilane nucleosides from the *E* to *Z* stereochemistry has been observed in polar solvents.[208] Recrystallization from ethyl acetate did not appear to induce this isomerization since only *E* isomer was recovered. The stereochemistry of the vinylsilane precursor is important since retention of stereochemistry is observed when these vinylsilane precursors are subjected to electrophilic iodination reactions.

Although the coupling reaction could be performed using the unprotected 5-iodo-2'-deoxy nucleosides (**3-5**), the extremely low solubility of 5-iodoarabinouridine in the reaction solvents necessitated the introduction of protecting groups. The reaction of (*E*)-2-tributylstannyl-1-trimethylsilylethene with 2',3',5'-tri-*O*-acetyl-5-iodoarabinouridine (**1**) in the presence of the palladium catalyst in dry acetonitrile gave the coupled product (**2**) in 64% yield. Several methods to remove the acetyl protecting groups, while retaining the reactive (*E*)-5-(2-trimethylsilylvinyl) moiety, were investigated. Selective deprotection of **2** was achieved after 80 hours at 25 °C by treatment with a suspension of 2% lithium hydroxide in dry benzene to give (*E*)-5-(2-trimethylsilylvinyl)arabinouridine (**9**, 39%).

Unlabelled iodination and carrier-added radioiodination reactions were performed using the unprotected (*E*)-5-(2-trimethylsilylvinyl) precursors (**6-9**). Thus, treatment with one equivalent of iodine monochloride in dry acetonitrile resulted in rapid formation of the desired (*E*)-5-(2-iodovinyl) products (**10,11,12,13**). It was noted that when the vinylsilane compounds were added to the iodine monochloride solution immediately after dissolution, only formation of the *E* isomer was observed. The *E*

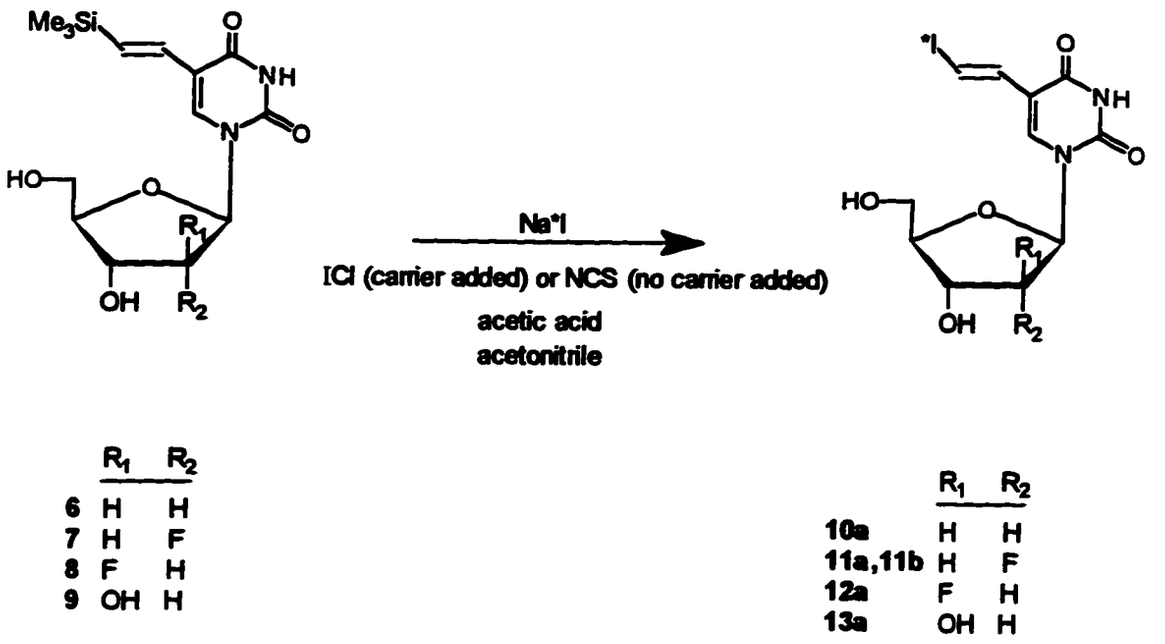

	R_1	R_2
6	H	H
7	H	F
8	F	H
9	OH	H

	R_1	R_2
10a	H	H
11a,11b	H	F
12a	F	H
13a	OH	H

Fig. 16 Synthesis of radioiodinated IVDU, IVFRU, IVFAU and IVAU.

stereochemistry was confirmed by the presence of large vinylic *trans* coupling constants (J_{trans} = 14-16 Hz). Isomers with *Z* stereochemistry display smaller *trans* coupling constants (J_{trans} = 9 Hz).[208] The retention of *E* stereochemistry is an important structural requirement for effective phosphorylation by HSV-1 TK since isomers with *Z* stereochemistry are much poorer substrates for HSV-1 TK.[236] Carrier-added radiolabelling was carried out by simply adding $Na^{125}I$ or $Na^{131}I$ to small scale reactions using iodine monochloride. However, radiochemical yields were improved when acetic acid (20%) was included in the reaction mixture. Radiochemical yields, after reverse-phase HPLC purification, were about 85% for all reactions except for [^{125}I]IVAU (13a) which was obtained in 63% radiochemical yield. The lower solubility of (*E*)-5-(2-trimethylsilylvinyl)arabinouridine (9) in acetonitrile may account for the lower

radiochemical yield obtained in this reaction. The specific activity of products obtained in carrier-added reactions, which ranged between 30-41 GBq/mmol, was acceptable for cellular uptake experiments. "No carrier added" radiosynthesis of [^{131}I]IVFRU (11b) was performed using *in situ* oxidation of Na^{131}I with N-chlorosuccinimide with 20 % acetic acid in acetonitrile as solvent. The radioiodination was complete after 30 min and yielded the product in 71 % radiochemical yield (specific activity > 5.29 TBq/mmol) after HPLC purification.

D. (*E*)-5-(2-iodovinyl)-3'-O-(1-methyl-1,4-dihydropyridyl-3-carbonyl)-2'-fluoro-2'-deoxyuridine (IVFRU-CDS) (Fig. 17).

The synthesis of IVFRU-CDS (22) was achieved using an eight step synthetic sequence using commercially available *O*^{2},2-anhydrouridine (14). 2'-Fluoro-2'-deoxyuridine (15) was prepared by reaction of 14 with HF in anhydrous dioxane as previously described.[206] The regiospecific reaction of 15 with *t*-butyldimethylsilyl chloride in the presence of imidazole in DMF gave 5'-*O*-*t*-butyldimethylsilyl-2'-fluoro-2'-deoxyuridine (16, 67%). The 3'-hydroxyl moiety of 16 was esterified with nicotinoyl chloride hydrochloride in pyridine to afford 3'-*O*-(3-pyridylcarbonyl)-5'-*O*-*t*-butyldimethylsilyl-2'-fluoro-2'-deoxyuridine (17, 73%).

The simultaneous cleavage of the silyl ether protecting group and C-5 iodination of the uracil ring was effected by treatment of 17 with iodine monochloride in methanol at reflux for 16 h which afforded 5-iodo-3'-*O*-(3-pyridylcarbonyl)-2'-fluoro-2'-deoxyuridine (18, 41%). However, the mother liquor was found to contain appreciable amounts of the 5-iodo-6-methoxy-5,6-dihydro adduct which , on further heating, eliminated methanol to give additional product (18).

The 5-iodo nucleoside derivative (**18**) was then subjected to a $(Ph_3P)_2Pd(II)Cl_2$ catalyzed coupling reaction using (*E*)-*n*-Bu_3Sn-CH=CH-TMS in THF under an argon atmosphere to give (*E*)-5-(2-trimethylsilylvinyl)-3'-O-(3-pyridylcarbonyl)-2'-fluoro-2'-deoxyuridine (**19**, 50%) after recrystallization from ethyl acetate. The C-5 2-trimethylsilylvinyl substituent of **6** possessed the desired *E*- stereochemistry (J_{trans} = 19 Hz). In contrast, recrystallization of **6** from methanol induced isomerization to the *Z*-isomer. Quaternization of **6** using an excess of iodomethane in acetone at reflux gave (*E*)-5-(2-trimethylsilylvinyl)-3'-O-(1-methylpyridinium-3-carbonyl)-2'-fluoro-2'-deoxyuridine iodide (**20**, 90%). The quaternary bromide salt (**21**) was obtained in 71 % yield by employing bromomethane as the alkylating reagent. The reactive vinylsilane iodide salt (**20**) was iodinated using iodine monochloride in acetonitrile which proceeded rapidly with retention of the *E*-stereochemistry. Since the iodide salt precursor (**20**) undergoes a slow isomerization to the (*Z*)-isomer in the acetonitrile solvent, iodine monochloride must be added immediately after dissolution of the salt (**20**).

Reduction of the pyridinium salt was performed immediately using sodium dithionite in the presence of sodium bicarbonate employing a two phase water/ethyl acetate solvent system. The residue from the ethyl acetate extract was chromatographed on a column of neutral alumina since silica gel column chromatography led to considerable decomposition. The compound, (*E*)-5-(2-iodovinyl)-3'-O-(1-methyl-1,4-dihydropyridyl-3-carbonyl)-2'-fluoro-2'-deoxyuridine (IVFRU-CDS) (**22**), obtained in this reaction, displayed a large *trans* coupling constant in the ^1H NMR spectrum for the iodovinyl protons confirming the presence of the desired (*E*)-iodovinyl stereochemistry (J_{trans} = 15 Hz). The iodination and reduction reactions were carried out using a one pot sequence which was readily amenable to a

radioiodination procedure. Radioiodination was performed with (*E*)-5-(2-trimethylsilylvinyl)-3'-O-(1-methylpyridinium-3-carbonyl)-2'-fluoro-2'-deoxyuridine bromide (**20**) as the salt precursor. Using the bromide salt in carrier added radioiodinations allows for a higher specific activity product compared to the iodide salt precursor. By simply adding $Na^{131}I$ in the iodination procedure, (*E*)-5-(2-[^{131}I]Iodovinyl)-3'-*O*-(1-methyl-1,4-dihydropyridine-3-carbonyl)-2'-fluoro-2'-deoxyuridine ([^{131}I]IVFRU-CDS, **22**) could be isolated in 14% radiochemical yield at a specific activity of 4.3 GBq/mmol and > 98% radiochemical purity after HPLC purification.

E. (*E*)-5-(2-iodovinyl)-3'-O-(1-methyl-1,4-dihydropyridyl-3-carbonyl)-2'-deoxyuridine (IVDU-CDS, 30) (Fig. 18)

Regiospecific reaction of 5-iodo-2'-deoxyuridine (**23**) with *t*-butyldimethylsilyl chloride in the presence of imidazole yielded the 5-iodo-5'-O-*t*-butyldimethylsilyl-2'-deoxyuridine (**24**) in 80% yield. Subsequent reaction with nicotinoyl chloride hydrochloride in pyridine afforded 5-iodo-3'-O-(3-pyridylcarbonyl)-5'-*O*-*t*-butyldimethylsilyl-2'-deoxyuridine (**25**, 76%). Deprotection with n-Bu_4N^+ F^- in THF yielded 5-iodo-3'-O-(3-pyridylcarbonyl)-2'-deoxyuridine (**26**) in 72% yield. Coupling with (*E*)-n-Bu_3Sn-CH=CH-$SiMe_3$ in the presence of $(Ph_3P)_2Pd(II)Cl_2$ gave (*E*)-5-(2-trimethylsilylvinyl)-3'-*O*-(3-pyridylcarbonyl)-2'-deoxyuridine (**27**) in 83% yield after recrystallization from ethyl acetate to circumvent isomerization to the (*Z*) stereochemistry. Quaternization with iodomethane yielded the (*E*)-5-(2-trimethylsilylvinyl)-3'-*O*-(1-methylpyridinium-3-carbonyl)-2'-deoxyuridine iodide (**28**) in 80% yield. Alternatively, N-alkylation of (*E*)-5-(2-trimethylsilylvinyl)-3'-*O*-(3-pyridylcarbonyl)-2'-deoxyuridine (**27**) with

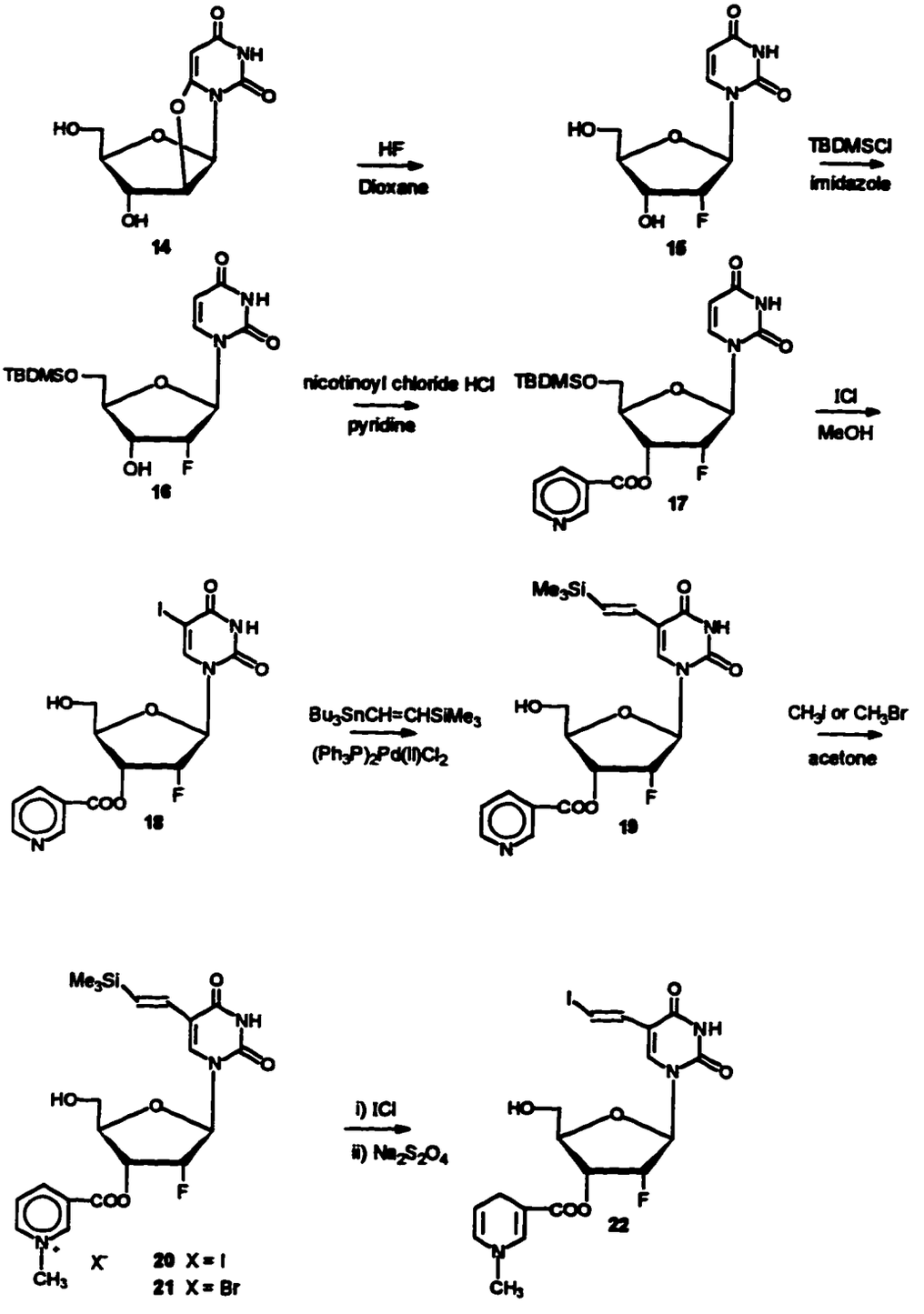

Fig. 17 Synthesis of IVFRU-CDS.

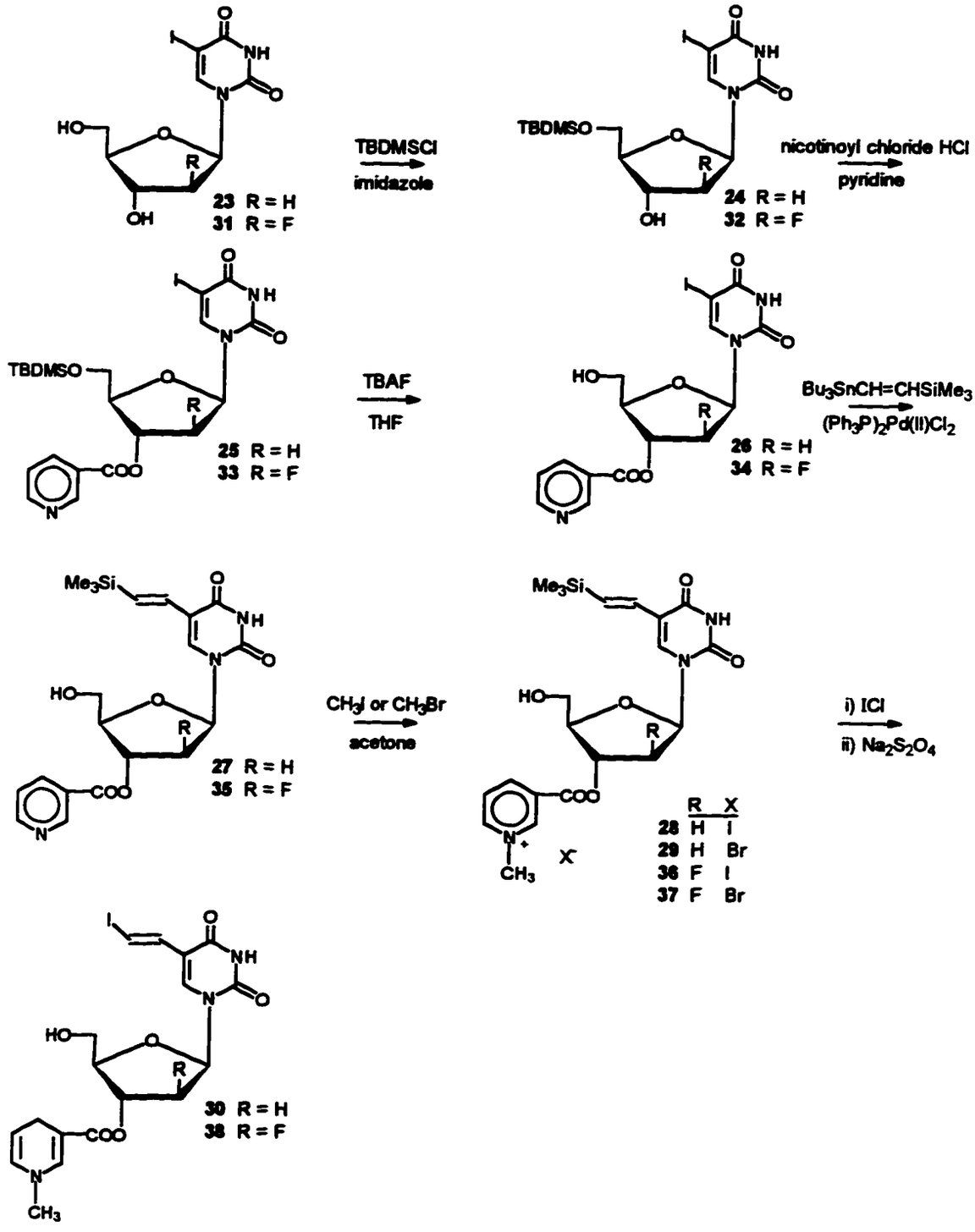

Fig. 18 Synthesis of IVDU-CDS and IVFAU-CDS.

bromomethane gave (*E*)-5-(2-trimethylsilylvinyl)-3'-*O*-(1-methylpyridinium-3-carbonyl)-2'-deoxyuridine bromide (**29**) in 72 % yield. Iodination of (*E*)-5-(2-trimethylsilylvinyl)-3'-*O*-(1-methylpyridinium-3-carbonyl)-2'-deoxyuridine iodide (**28**) with iodine monochloride and reduction with sodium dithionite in the presence of sodium bicarbonate was carried out as a one pot synthesis to afford (*E*)-5-(2-iodovinyl)-3'-O-(1-methyl-1,4-dihydropyridyl-3-carbonyl)-2'-deoxyuridine (IVDU-CDS, **30**) in 56% yield. This one-pot synthetic methodology was applied to the radiosynthesis of [^{131}I]IVDU-CDS (**30a**). Radiohalogenation was achieved by addition of Na^{131}I to the iodine monochloride solution during the one-pot procedure using (*E*)-5-(2-trimethylsilylvinyl)-3'-*O*-(1-methylpyridinium-3-carbonyl)-2'-deoxyuridine bromide (**29**) as the substrate. (*E*)-5-(2-[^{131}I]Iodovinyl)-3'-*O*-(1-methyl-1,4-dihydropyridine-3-carbonyl)-2'-deoxyuridine ([^{131}I]IVDU-CDS, **30a**) was isolated in 19% radiochemical yield (2.5 MBq) at a specific activity of 2.8 GBq/mmol and > 98% radiochemical purity after HPLC purification.

F. (*E*)-5-(2-iodovinyl)-3'-O-(1-methyl-1,4-dihydropyridyl-3-carbonyl)-2'-fluoro-2'-deoxyarabinouridine (IVFAU-CDS, 38) (Fig. 18).

The strategy for synthesis of IVFAU-CDS (**38**) was identical to that used for IVDU-CDS. However, 5-iodo-2'-fluoro-2'-deoxyarabinouridine (FIAU, **31**) was used as starting material. Protection of 5-iodo-2'-fluoro-2'-deoxyarabinouridine with *t*-butyldimethylsilyl chloride in the presence of imidazole yielded the 5'-*O*-*t*-butyldimethylsilyl derivative (**32**, 82%). Subsequent reaction with nicotinoyl chloride hydrochloride in pyridine afforded 5-iodo-3'-O-(3-pyridylcarbonyl)-5'-*O*-*t*-butyldimethylsilyl-2'-fluoro-2'-deoxyarabinouridine (**33**, 93%). Deprotection with *n*-Bu$_4$N$^+$ F$^-$ yielded the 3'-O-nicotinoyl nucleoside (**34**, 85%). Coupling with (*E*)-*n*-Bu$_3$Sn-

CH=CH-TMS in the presence of $(Ph_3P)_2Pd(II)Cl_2$ gave (*E*)-5-(2-trimethylsilylvinyl)-3'-O-(3-pyridylcarbonyl)-2'-fluoro-2'-deoxyarabinouridine (**35**, 82%). Quaternization with iodomethane or bromomethane yielded the 1-methylpyridinium iodide (**36**) or bromide salt (**37**) (80% and 96% yields respectively). Iodination with iodine monochloride and reduction of the quaternary iodide salt (**36**) with sodium dithionite in the presence of sodium bicarbonate afforded (*E*)-5-(2-iodovinyl)-3'-O-(1-methyl-1,4-dihydropyridyl-3-carbonyl)-2'-fluoro-2'-deoxyarabinouridine (IVFAU-CDS, **38**) in 43% yield.

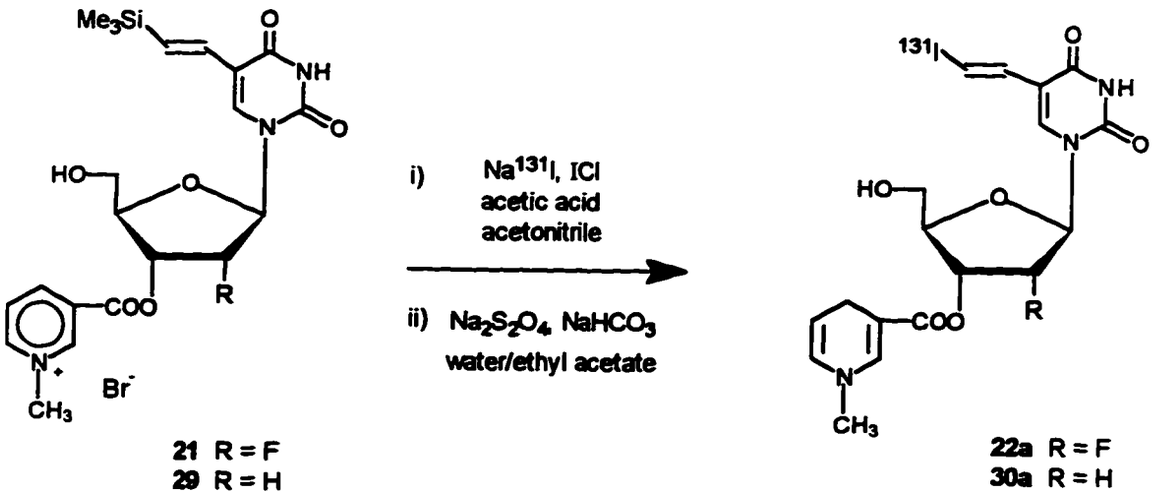

21 R = F
29 R = H

22a R = F
30a R = H

Fig. 19 Synthesis of radioiodinated IVDU-CDS and IVFRU-CDS

Table 1. Vinylic coupling constants, chemical and radiochemical yields of nucleoside derivatives

Compound	chemical yield (%)	radiochemical yield (%)	vinylic J_{trans} (Hz)
IVDU	77	86	14.3
IVFRU	78	85	16.0
IVFAU	64	86	14.8
IVAU	75	63	14.6
IVDU-CDS	56	19	15.0
IVFRU-CDS	59	14	15.0
IVFAU-CDS	43	-	14.8

G. Cytostatic Activity of Nucleoside Derivatives Against Murine Mammary Cell Lines

IVDU, its 2'-fluoro-substituted dervatives IVFRU and IVFAU, and the 3'-CDS-substituted derivatives IVDU-CDS, IVFRU-CDS, and IVFAU-CDS were evaluated for their cytostatic activity against wild-type FM3A/0 cells,

FM3A TK$^-$ cells deficient in cytosol TK, and the HSV-1 TK and HSV-2 TK gene transfected FM3A cells derived from the FM3A TK$^-$ cell line (Table 2). Whereas the test compounds were poorly cytostatic against wild-type FM3A/0 cells (IC_{50} 18-222 μM), they had a remarkably greater cytostatic activity against both the HSV-1 TK and HSV-2 TK gene transfected tumor cells. The test compounds inhibited tumor cell proliferation at concentrations in the nanomolar range (ie. 0.002-0.026 μM for IVDU and IVDU-CDS or 0.024-0.80 μM for IVFRU, IVFAU and their corresponding 3'-CDS derivatives) in the transfected tumor cells. The IC_{50} values obtained for IVDU, IVFRU and IVFAU in the transfected cells are in the same range as the IC_{50} values obtained previously against HSV-1 infected cells *in vitro*.[194,236]

There was approximately 5-10 fold higher cytostatic activity of IVFRU or IVFAU derivatives against FM3A TK$^-$/HSV-1 TK$^+$ cells as compared to activity against FM3A TK$^-$/HSV-2 TK$^+$ cells. This greater inhibitory effect in HSV-1 TK expressing cells most likely reflects a higher affinity of HSV-1 TK than HSV-2 TK for the test compounds. In addition, there appeared to be no significant differences in the cytostatic potential of the 3'-CDS derivatives as compared with the 3'-unsubstituted counterparts. IVDU and IVDU-CDS, but not the 2'-fluoro substituted derivatives, were 45-55 fold more inhibitory to FM3A TK$^-$ than to the wild-type FM3A/0 cells. A similar observation has been made previously for BVDU, which also proved more inhibitory to TK$^-$ cell lines as compared to wild-type cells with normal thymidine kinase activity. The biochemical basis of these observations has yet to be resolved, however specific inhibition of protein glycosylation in TK$^-$ cell lines by BVDU has been postulated as a mechanism leading to cytostatic effects.[217] Since protein glycosylation is dependent on

nucleotide cofactors it is possible that phosphorylated BVDU may be interfering with the function of normal nucleotide cofactors.

Table 2. Cytostatic activity of nucleoside derivatives against murine mammary carcinoma cell lines

	IC_{50} (μM)			
Compound	FM3A/0	FM3A TK$^-$	FM3A TK$^-$/ HSV-1 TK$^+$	FM3A TK$^-$/ HSV-2 TK$^+$
IVDU	18 ± 6.9	0.40 ± 0.11	0.005 ± 0.002	0.002 ± 0.001
IVFRU	143 ± 9	155 ± 12	0.027 ± 0.010	0.34 ± 0.23
IVFAU	222 ± 47	152 ± 25	0.024 ± 0.008	0.53 ± 0.17
IVDU-CDS	27 ± 2.6	0.48 ± 0.02	0.026 ± 0.004	0.004 ± 0.001
IVFRU-CDS	203 ± 13	132 ± 15	0.051 ± 0.026	0.80 ± 0.71
IVFAU-CDS	124 ± 63	60 ± 24	0.093 ± 0.075	0.49 ± 0.17

The selectivity index ratio of the IC_{50} for FM3A/0 to FM3A TK$^-$/HSV-1 TK$^+$ cells ranged between 1333 to 10423 for the test compounds demonstrating the exquisite cytostatic selectivity in cells expressing HSV-1 TK (Table 3). However, the selectivity index ratio of IC_{50} for FM3A TK$^-$ to FM3A TK$^-$/HSV-1 TK$^+$ cells was 70-80 fold higher for IVFRU and IVFAU than for IVDU. Similarly, the selectivity index for IVFRU-CDS and IVFAU-CDS were higher than IVDU-CDS (3.5-4 fold higher) but less pronounced than the 3'-unsubstituted compounds. Thus, IVFRU and IVFAU appear to be the most selective cytostatic compounds against the HSV-1 TK gene transfected tumor cells. However, for HSV-2 TK gene transfected tumor

cells, the superior selectivity of IVFRU and IVFAU was virtually lost, due to the markedly lower cytostatic activity of the test compounds against FM3A TK$^-$/HSV-2 TK$^+$ cells.

Table 3. Selectivity index of the cytostatic activity of nucleosides against murine mammary carcinoma cell lines

	Selectivity Index	
Compound	$\frac{IC_{50}\ FM3A/0}{IC_{50}\ FM3A\ TK^-/HSV\text{-}1\ TK^+}$	$\frac{IC_{50}\ FM3A\ TK^-}{IC_{50}\ FM3A\ TK^-/HSV\text{-}2\ TK^+}$
IVDU	3461	77
IVFRU	5296	5740
IVFAU	9250	6333
IVDU-CDS	10423	184
IVFRU-CDS	3980	2588
IVFAU-CDS	1333	642

H. Inhibitory Effect of Nucleosides on Tritium Release from 5-^{3}H Deoxycytidine

Upon conversion of 5-^{3}H dCyd to 5-^{3}H dUMP via deamination to 5-^{3}H dUrd and phosphorylation to 5-^{3}H dUMP, or via phosphorylation to 5-^{3}H dCMP and deamination to 5-^{3}H dUMP, the tritium atom at the C-5 position of the uracil ring of 5-^{3}H dUMP is replaced by a methyl group in the thymidylate synthase reaction. It has been demonstrated that tritium

release from 5-^{3}H dCyd in intact tumor cells can be considered as a valuable parameter for thymidylate synthase activity *in vivo*.[173,217] All test compounds proved to be poor inhibitors of tritium release from 5-^{3}H dCyd in intact FM3A/0 and FM3A TK^{-} cells deficient in cytosolic TK (Table 4). However, all compounds were found to be inhibitory to tritium release in both HSV-1 TK and HSV-2 TK gene transfected FM3A tumor cells. IVDU, IVFRU, and IVFAU were at least 1000 to 4000-fold more inhibitory to tritium release from 5-^{3}H dCyd in the HSV-TK gene transfected tumor cells than in FM3A/0 and FM3A TK^{-} cells. The inhibitory effect of IVFRU and IVFAU on tritium release from 5-^{3}H dCyd in FM3A TK^{-}/HSV-2 TK^{+} cells was less pronounced than in FM3A TK^{-}/HSV-1 TK^{+} cells. Also, the CDS derivatives of IVDU, IVFRU, and IVFAU were approximately 5 to 10-fold less inhibitory to HSV-2 TK gene transfected tumor cells than to FM3A TK^{-}/HSV-1 TK^{+} cells. There was a correlation between the cytostatic activity of the test compounds and their inhibitory effect on tritium release from 5-^{3}H dCyd (r=0.78 for FM3A/0, FM3A TK^{-}/HSV-1 TK^{+} and FM3A TK^{-}/HSV-2 TK^{+} cells). The correlation between inhibitory effect on tritium release and cytostatic activity implies that thymidylate synthase inhibition after initial phosphorylation is a likely mechanism of cytostatic effect. However, there was a poor correlation between the cytostatic activity and tritium release from 5-^{3}H dCyd in the FM3A TK^{-} cells. Unlike IVFRU, IVFAU, IVFRU-CDS, or IVFAU-CDS, IVDU and IVDU-CDS are much more inhibitory to FM3A TK^{-} than wild-type cells. Thus, the cytostatic effect in FM3A TK^{-} cells is most likely due to interaction with an intracellular target different from thymidylate synthase.

Table 4. Inhibitory effect of nucleosides on tritium release from 5-^{3}H dCyd in murine mammary carcinoma cell lines.

	IC_{50} (μM)			
Compound	FM3A/0	FM3A TK$^-$	FM3A TK$^-$/ HSV-1 TK$^+$	FM3A TK$^-$/ HSV-2 TK$^+$
IVDU	8.8 ± 1.3	18 ±12	0.005 ± 0.0005	0.007 ± 0.0004
IVFRU	109 ± 59	196 ± 13	0.087 ± 0.013	0.61 ± 0.03
IVFAU	135 ± 55	78 ± 1.5	0.060 ± 0.002	0.50 ± 0.03
IVDU-CDS	175 ± 120	61 ± 3.6	0.044 ± 0.024	0.078 ± 0.005
IVFRU-CDS	275 ± 59	275 ± 54	0.62 ± 0.06	7.3 ± 0.32
IVFAU-CDS	28 ± 31	34 ± 6.9	0.36 ± 0.04	1.6 ± 1.0

I. Interaction of Nucleosides with Purified HSV-1 TK.

When the nucleoside derivatives were evaluated for their affinity for purified HSV-1 TK, with the natural substrate thymidine (dThd) being present in the reaction mixture at 1 μM, IVDU inhibited the HSV-1 TK-catalysed dThd phosphorylation by 50% at 0.56 μM (Table 5). The 2'-fluoro-substituted IVFRU and IVFAU derivatives inhibited the enzyme activity at 1.0 and 1.8 μM, respectively. The 3'-CDS-substituted derivatives IVFRU-CDS and IVFAU-CDS were only 4 to 7-fold less inhibitory than the 3'-unsubstituted derivatives. However, IVDU-CDS was 45-fold less inhibitory to HSV-1 TK than IVDU. These results suggest that although the 3'-CDS derivatives are assumed to act as prodrugs of IVDU, IVFRU, and IVFAU, they may be first phosphorylated intracellularly before releasing the 3'-promoiety by hydrolysis. However, competitive inhibition of dThd phosphorylation is possible without phosphorylation of the competitive

substrate. Moreover, there have been no previous reports of 3′-ester derivatives of pyrimidine nucleosides that undergo selective 5′-phosphorylation by HSV-1 TK. However, cleavage of the 3'-ester linkage is expected to occur *in vivo*. An assay that directly quantifies phosphorylated metabolites of the 3′-CDS derivatives would be useful to further investigate these results.

J. Phosphorolysis by Human dThd Phosphorylase

IVDU undergoes > 90% conversion to its free base (*E*)-5-(2-iodovinyl)uracil within 25 min incubation at 37 °C with human platelet dThd phosphorylase (Table 5). In contrast, when hydrolysis of IVFRU, IVFAU and their corresponding CDS derivatives were evaluated as substrates for phosphorylase under identical experimental conditions, they proved to be completely stable in the presence of the enzyme for 18 h. No breakdown products (ie. (*E*)-5-(2-iodovinyl)uracil) could be detected by high performance liquid chromatography (HPLC). The dramatic enhancement of stability of IVFRU, IVFAU and their CDS-derivatives toward phosphorolysis is a desirable property for retaining biological activity after *in vivo* administration.

K. Log P and Oxidation of CDS-derivatives in Mouse Tissues.

All of the compounds evaluated can be considered to be lipophilic based on their partition coefficients. The log P values obtained for IVDU and IVFRU were identical to those observed in a previous study.[194] All test compounds displayed log P values which are in the range considered optimal for permeability of radiopharmaceuticals across the BBB (0.9 to 2.5).[218] As expected, the CDS-derivatives demonstrated substantially higher log P

values than their corresponding 3'-unsubstituted derivatives. The increased log P values of the CDS-derivatives indicate that these compounds are more likely to enter the CNS by diffusion than the 3'-unsubstituted compounds after *in vivo* administration.

Table 5. Interaction with HSV-1 TK, phosphorolysis and log P of nucleoside derivatives

Compound	IC_{50} (μM) [a]	% phosphorolysis [b]	log P [c]
IVDU	0.56 ± 0.0	> 90	1.10
IVFRU	1.0 ± 0.2	0	1.21
IVFAU	1.8 ± 1.2	0	1.20
IVDU-CDS	23.0 ± 12.0	0	1.77
IVFRU-CDS	7.1 ± 0.6	0	1.83
IVFAU-CDS	7.0 ± 0.6	0	1.83

a inhibition of HSV-1 TK-catalysed dThd phosphorylation by 50%

b phosphorolysis by human dThd phosphorylase

c log of the partition coefficient between octanol and water

The relatively facile oxidation of the CDS-derivatives to the pyridinium salt derivatives is evident in the determination of the psuedo-first order oxidation process in blood, brain, and liver homogenates (Table 6). The half-lives of the oxidation to the pyridinium salt derivatives were shortest in liver homogenates and ranged from 23-63 min. In brain homogenates, the half-lives were between 61-72 min. All CDS-derivatives displayed their longest oxidation half-lives in blood, ranging between 127-133 min. These

results are similar to those observed for related CDS-nucleoside analogues and support the concept that lipophilic 1-methyl-1,4-dihydropyridine prodrugs undergo oxidation in biological tissues to highly polar pyridimium salt derivatives.[219] The short half-life of these prodrugs in brain homogenate is desirable for metabolic imaging of HSV-1 TK expression in brain tumors receiving gene therapy since the lipophilic compounds are expected to be widely distributed following *in vivo* administration. Rapid oxidation, as observed with CDS-derivatives *in vitro*, can be expected to trap the pyridinium salt species in the brain leading to a sustained release of parent nucleoside after hydrolysis of the oxidized promoiety. If the CDS-derivatives are phosphorylated directly before hydrolysis, then one could expect efficient metabolic trapping in HSV-1 TK-expressing cells since initial entry by diffusion would be facilitated by enhanced lipophilicity.

Table 6. Psuedo-first order oxidation rate constants and half-lives of CDS-derivatives in mouse tissues.

	$k \times 10^{-3}$ min^{-1}			oxidation t 1/2 (min)		
Compound	blood	brain	liver	blood	brain	liver
IVDU-CDS	5.22	9.61	10.81	133	72	63
IVFRU-CDS	5.71	11.26	17.47	121	62	40
IVFAU-CDS	5.46	11.36	30.13	127	61	23

L. *In Vitro* Cellular Uptake in KBALB, KBALB-LNL and KBALB-STK Cells

The KBALB cell line is a Kirsten virus-transformed sarcoma tumor cell line.[220] KBALB-STK cells were derived from the KBALB cell line, express

HSV-1 TK and are sensitive to the cytotoxic effects of ganciclovir *in vitro* and *in vivo*.[77] The KBALB-STK cells have been transduced with the STK vector which is a replication-incompetent Moloney murine leukemia retrovirus vector containing the HSV-1 TK gene promoted by the SV40 early promoter-enhancer and the neomycin resistance gene driven by the viral long terminal repeat. In contrast, the KBALB-LNL cell line was transduced with the LNL6 vector that carries only the neomycin phosphotransferase gene driven by the 5'-LTR. Integration of the LNL6 or STK vector into the genome of KBALB cells results in stable, long term expression of neomycin phosphotransferase and allows *in vitro* selection by culturing in the presence of the neomycin analogue G-418 which ensures that resistant cells are propagated. In order to accurately compare cellular uptake, [^{125}I]IVDU, [^{125}I]IVFRU, [^{125}I]IVFAU, and [^{125}I]IVAU were assayed under identical molar concentration (0.076 μM) and cellular density (1 x 10^5 cells) in cell cultures of KBALB, KBALB-LNL and KBALB-STK cells.

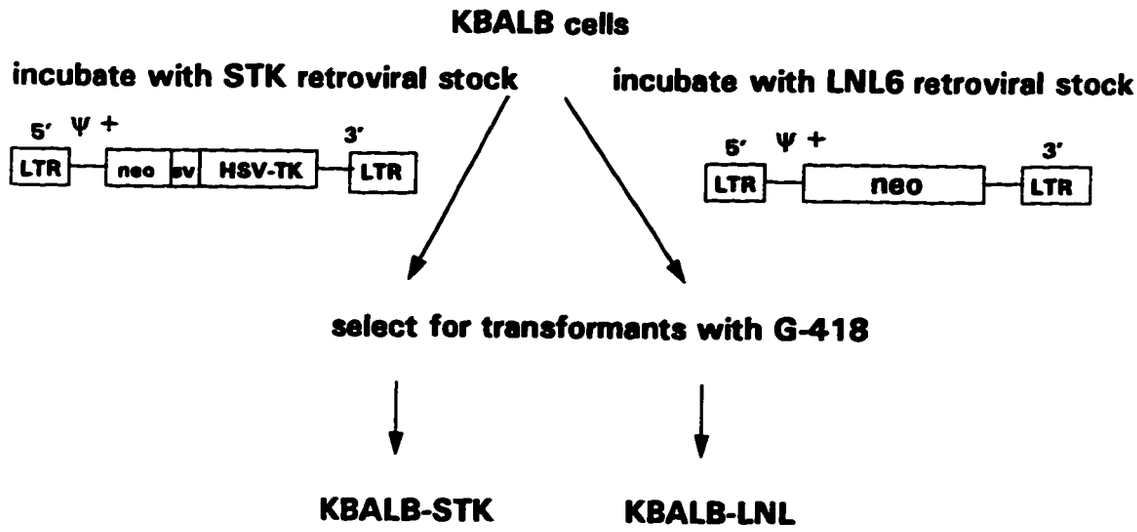

Fig. 20 Transduced cell lines derived from KBALB cells

A 10-fold higher concentration was used in assays for [^{131}I]IVDU-CDS and [^{131}I]IVFRU-CDS uptake since these compounds were synthesized in approximately 10-fold lower specific activity (2.8-4.3 GBq/mmol). The cellular uptake of the radiolabelled compounds in cell lines over a period of 8 hours is illustrated in Fig. 21-26. Minimal uptake of [^{125}I]IVDU, [^{125}I]IVFRU, [^{125}I]IVFAU, and [^{125}I]IVAU occurred in cells lacking the HSV-1 TK gene (KBALB or KBALB-LNL cell lines) since less than 0.3 pmol compound/10^5 cells was present at all time periods in these cells. Somewhat higher uptake of [^{131}I]IVDU-CDS and [^{131}I]IVFRU-CDS in KBALB-LNL cells was observed. However, this was probably a consequence of the higher concentration used in the assays for the CDS-derivatives. Approximately 1.5-2.3 pmol/10^5 cells of [^{131}I]IVDU-CDS and [^{131}I]IVFRU-CDS, respectively, accumulated in KBALB-LNL cells after 8 h exposure to the radiolabelled compounds. Interestingly, the uptake of either CDS-derivative in KBALB-LNL cells after 8 h was relatively unchanged from that observed at 15 min when uptake was approximately 1.2-2.0 pmol/10^5 cells.

The uptake of [^{131}I]IVDU-CDS and [^{131}I]IVFRU-CDS in KBALB-STK cells paralleled the uptake in KBALB-LNL cells with no apparent difference in uptake between the two cell lines. The absence of any preferential uptake of [^{131}I]IVDU-CDS or [^{131}I]IVFRU-CDS in KBALB-STK cells provides evidence that direct phosphorylation of the CDS-derivatives by HSV-1 TK probably does not occur *in vitro*. If these derivatives were phosphorylated directly, then increased uptake by metabolic trapping in the KBALB-STK cells would occur within the 8 h incubation period. Therefore, it is likely that the cytostatic activity of the CDS-derivatives previously observed in FM3A TK$^-$/HSV-1 TK$^+$ cells occurs after release of the 3'-promoiety. After

hydrolysis, the 3-unsubstituted compounds can be efficiently phosphorylated by HSV-1 TK. This hypothesis is supported by the fact that, in contrast to the KBALB or KBALB-LNL cells which lack HSV-1 TK expression, the KBALB-STK cell line was capable of accumulating the 3'-unsubstituted compounds to varying degrees. [^{125}I]IVDU was metabolically trapped to the greatest extent, with cellular radioactivity increasing up to 8 hours after exposure (see Fig. 21). At 8 hours after exposure, 66% of the radioactivity (25 pmol/10^5 cells) was intracellularly trapped. The kinetic profile of the uptake process is qualitatively similar to that observed previously with [^{131}I]IVDU in TK+ HSV-1 infected rabbit kidney cells.[188] [^{125}I]IVFRU also accumulated rapidly in KBALB-STK cells, with increasing cellular radioactivity over time (see Fig. 22). However, the presence of a 2'-fluorine substituent in the ribofuranosyl configuration appears to affect cellular nucleoside uptake, since there was substantially lower cellular uptake of [^{125}I]IVFRU relative to [^{125}I]IVDU. After 8 hours exposure to [^{125}I]IVFRU, KBALB-STK cells accumulated 8.2 pmol/10^5 cells or 21.6% of the total activity added to the culture.

Unexpected uptake kinetics were observed for both [^{125}I]IVFAU (see Fig. 23) and [^{125}I]IVAU (see Fig. 24) which possess 2'-fluoro and 2'-hydroxy substituents in the arabinofuranosyl configuration, respectively. In both cases, rapid uptake of radioactivity was evident at the earliest time intervals. However, the influx of labelled compounds was minimal after 30 minutes exposure. In the case of [^{125}I]IVFAU, initial uptake at 15 minutes was 2.4 pmol/10^5 cells, which is comparable to [^{125}I]IVFRU at this early time point. However, after 8 hours exposure to [^{125}I]IVFAU, only 2.7 pmol/10^5 cells had accumulated in the KBALB-STK cells. This represents a 3-fold decrease in uptake relative to [^{125}I]IVFRU, which differs structurally

from [^{125}I]IVFAU only in that [^{125}I]IVFRU has a 2'-fluoro substituent in the ribofuranosyl configuration. A similar time-response profile with substantially lower uptake of activity was observed for [^{125}I]IVAU. Preferential uptake in HSV-1 TK expressing cells was evident at 15 minutes in KBALB-STK cells relative to KBALB cells lacking HSV-1 TK. However, less than 1 pmol/10^5 cells had accumulated at the earliest time point in the KBALB-STK cells. Exposure to [^{125}I]IVAU for up to 8 hours did not substantially increase its influx into KBALB-STK cells. After 8 hours, cellular uptake of [^{125}I]IVAU was only 0.9 pmol/10^5 cells representing a 3-fold decrease in uptake relative to [^{125}I]IVFAU where the 2'-substituent in the arabino configuration is fluorine.

Structure-activity correlations for a variety of 2'-fluoro-2'-deoxyuridine analogs have indicated that the sugar 2'-configuration results in differential antiviral effects.[221] Moreover, 5-substituted-2'-fluoro-2'-deoxyuridine analogs possessing the arabinofuranosyl configuration are generally more potent against HSV-1 than similar compounds possessing the ribofuranosyl configuration.[222] Similarly, in a previous study, there was a correlation between nucleoside uptake in rabbit kidney cells infected with HSV-1 (TK $^+$) and antiviral effect, since radiolabelled 5-iodo-2'-fluoro-2'-deoxyarabinouridine (FIAU) accumulated to a greater extent than 5-iodo-2'-fluoro-2'-deoxyuridine (FIRU) in HSV-1 infected cells over a 24 hour period.[193] However, a comparative uptake investigation revealed that [^{125}I]IVDU and [^{125}I]IVFRU had significantly higher cellular uptake than [^{125}I]IVFAU in HSV-1 (TK$^+$) infected rabbit kidney cells despite the comparable antiviral activity of IVFAU.[194] Interestingly, this latter study indicated that the change in cellular uptake of [^{125}I]IVFAU between 4 and 24 hours was quite low compared to [^{125}I]IVDU and [^{125}I]IVFRU. The

pattern of uptake in HSV-1 TK expressing tumor cells is in agreement with the previous observations since [^{125}I]IVDU and [^{125}I]IVFRU accumulated to a greater degree than [^{125}I]IVFAU and [^{125}I]IVAU, with the latter two compounds showing very little change in uptake between 15 minutes and 8 hours. In addition, the extent of [^{125}I]IVAU uptake in KBALB-STK cells is similar to that previously observed in HSV-1 (TK+) infected rabbit kidney cells.[208]

The reasons for the different time-response profiles are not directly apparent. Uncompromised cytoplasmic membrane integrity due to an absence of cytopathic viral infection imply that facilitated nucleoside transport mechanisms may be of increased importance relative to HSV-1 cell infection. It is known that NBMPR-sensitive, equilibrative nucleoside transporters are capable of accepting a variety of nucleoside substrates which are relatively insensitive to modifications at the 2'-position of uracil nucleosides.[223,224] Thus, it is likely that other biochemical processes are affecting metabolic trapping of [^{125}I]IVFAU and [^{125}I]IVAU. IVDU, IVFRU and IVFAU are effective substrates for HSV-1 TK, display comparable cytostatic activity against HSV-1 TK gene-transfected murine mammary carcinoma, and appear to evoke this cytostatic effect primarily through inhibition of thymidylate synthase. However, the observation that the structurally related (*E*)-5-(2-bromovinyl)-2'-arabinouridine completely lacks cytostatic and thymidylate synthase inhibitory activity in HSV-1 TK expressing tumor cells whereas (*E*)-5-(2-bromovinyl)-2'-deoxyuridine is one the most potent cytostatic agents in these cells, demonstrates that a small modification in structure can have dramatic biochemical consequences even though both compounds exhibit potent antiviral activity against HSV-1.[173,225]

The structure-uptake relationship indicates that for these 2'-substituted-2'-deoxyuridine derivatives possessing an (*E*)-5-(2-iodovinyl) substituent, the presence of a 2'-fluoro substituent in the ribo configuration confers a superior ability to accumulate in tumor cells expressing HSV-1 TK. Radiolabelled IVFRU was selected as the most promising compound for further study among those synthesized and evaluated *in vitro* because it was accumulated to the greatest extent in HSV-1 TK-expressing cells and because it was stable to phosphorylytic degradation which is an absolute requirement for an effective *in vivo* imaging agent.

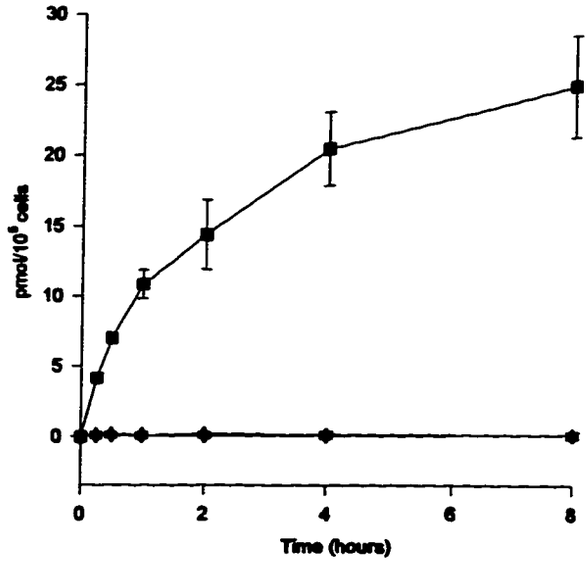

Fig. 21. *In vitro* uptake of [^{125}I]IVDU in KBALB-STK (■), KBALB-LNL (▼) and KBALB (▲) cells.

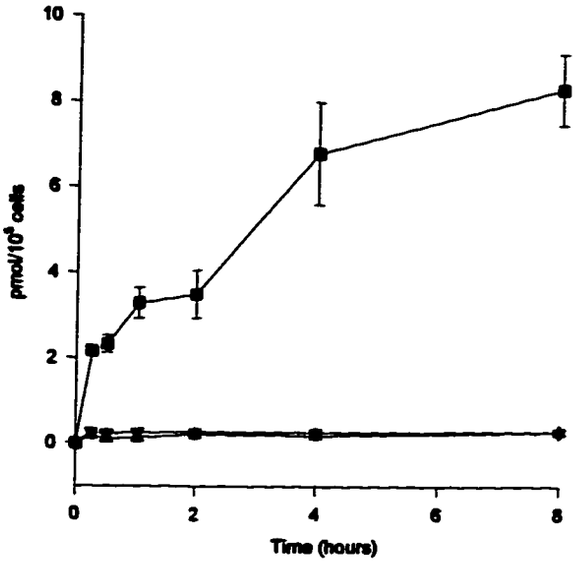

Fig. 22. *In vitro* uptake of [^{125}I]IVFRU in KBALB-STK (■), KBALB-LNL (▼) and KBALB (▲) cells.

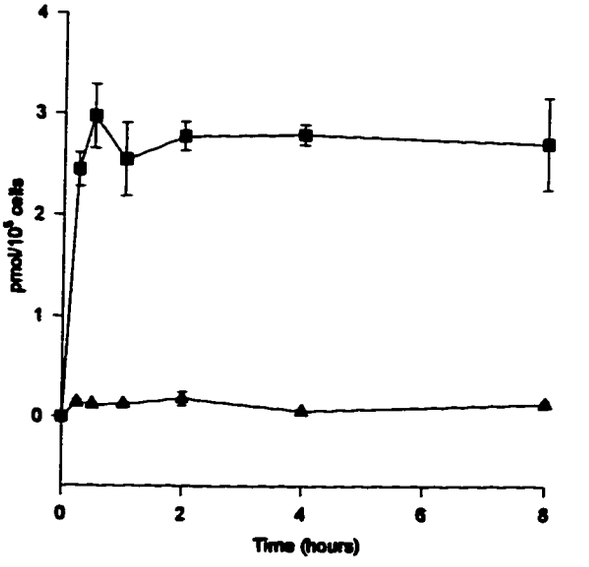

Fig. 23. *In vitro* uptake of [^{125}I]IVFAU in KBALB-STK (■) and KBALB (▲) cells.

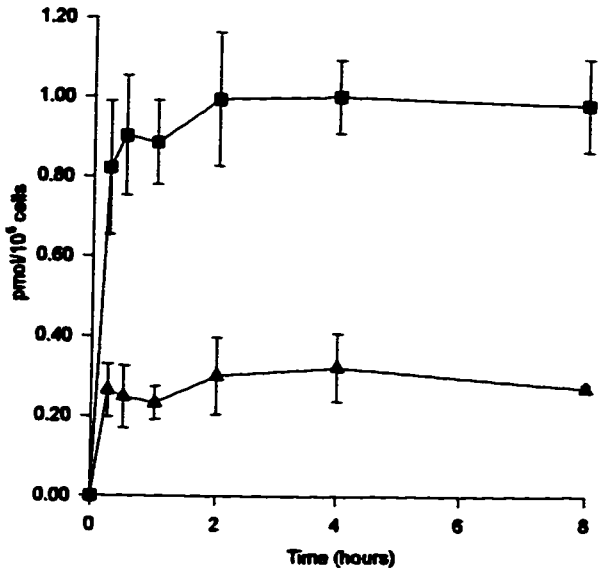

Fig. 24. *In vitro* uptake of [^{125}I]IVAU in KBALB-STK (■) and KBALB (▲) cells.

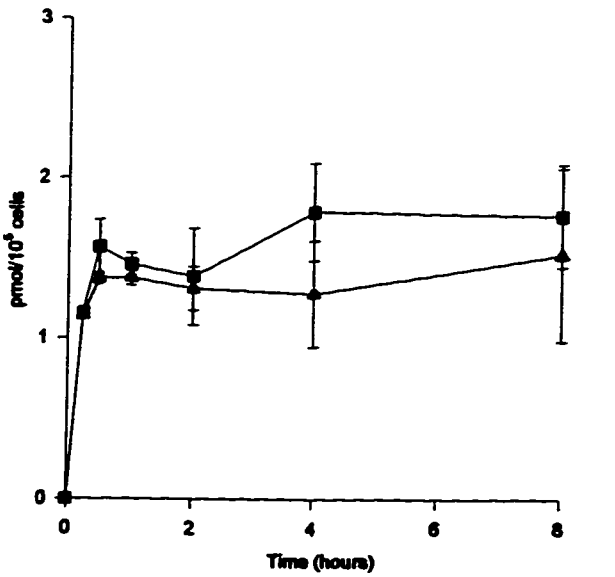

Fig. 25. *In vitro* uptake of [^{131}I]IVDU-CDS in KBALB-STK (■) and KBALB-LNL (▲) cells.

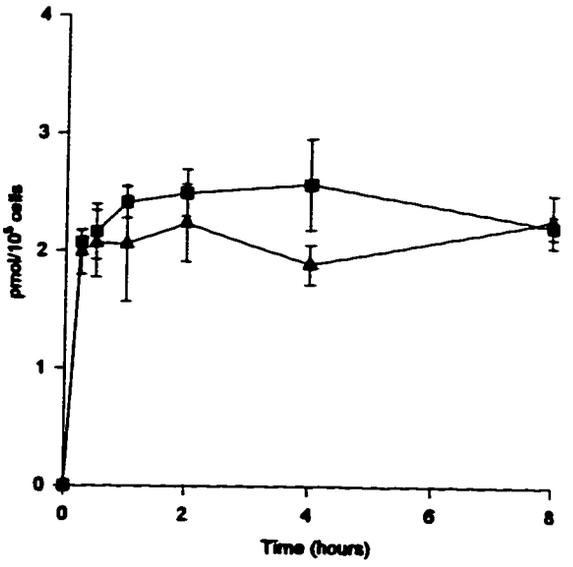

Fig. 26. *In vitro* uptake of [^{131}I]IVFRU-CDS in KBALB-STK (■) and KBALB-LNL (▲) cells.

M. Transfection and Detection of Gene Expression

Introduction of the HSV-1 TK gene into KBALB cells was achieved by transfection using the eukaryotic expression vector, pMLBKTK. This vector contains a *Bam*HI fragment of the HSV-1 genome encoding the HSV-1 TK gene and the upstream promoter sequences allowing constitutive expression in eukaryotic cells. In addition, pMLBKTK contains virtually the entire genome of human papovavirus BK isolated from the urine of a renal transplant recipient receiving immunosuppressive therapy.[226] The BK virus is ubiquitous in the human population and is the human homologue of the SV-40 virus.[227] When introduced into eukaryotic cells, an early gene product (large T antigen) stimulates the BK virus origin of replication in a manner analogous to SV-40 T-antigen-dependent replication. Episomal replication of the plasmid results in a high copy number in transfected cells and long-term persistence of gene expression in the absence of selective

pressure.[228,229] BK virus propagation is avoided through a 107 base pair deletion disrupting late viral capsid gene transcription and rendering the virus replication incompetent.[230] Therefore, pMLBKTK was considered to be an ideal plasmid vector to introduce the HSV-1 TK gene into KBALB cells *in vitro*. Co-transfections with a plasmid vector carrying the firefly luciferase gene was used to confirm gene transfer and correlate luciferase and HSV-1 TK activity *in vitro*. The pSluc2 vector contains the luciferase gene promoted by an enhancerless SV-40 early promoter.[231]

The uptake of [^{125}I]IVFRU in transfected cells was evaluated 48 h after transfection of KBALB cells with plasmid pMLBKTK by calcium phosphate coprecipitation or by using cationic liposomes (DOTAP reagent). Cellular uptake was quantitated after 8 h exposure to 80 pmol [^{125}I]IVFRU. Basal uptake of radioactivity in controls lacking DNA and transfecting reagent was observed to be 3.5 pmol/10^6 cells. Similarly, when calcium phosphate or liposomes were used in the absence of vector, only 2.6-4.2 pmol/10^6 cells was accumulated. In contrast, when the pMLBKTK vector was introduced into KBALB cells by calcium phosphate co-precipitation, there was a 3-fold increase in [^{125}I]IVFRU uptake (11.8 pmol/10^6 cells) compared to controls. Liposomal delivery of pMLBKTK lead to enhanced [^{125}I]IVFRU uptake in transfected cells. Cellular uptake of [^{125}I]IVFRU in cells transfected with cationic liposomes was similar to cells transfected by the calcium phosphate co-precipitation method.

Co-transfection of KBALB cells with pMLBKTK and pSluc2 by either calcium phosphate coprecipitation or DOTAP lipofection lead to transfected cells that could be detected by a standard luciferase assay and by gamma counting following exposure to [^{125}I]IVFRU. The magnitude of [^{125}I]IVFRU uptake in co-transfected cells was similar (8.7-9.1 pmol/10^6 cells) to that

observed after transfections using only pMLBKTK as the vector. High levels of luciferase activity were detected 48 h after co-transfection. The sensitivity of the luciferase/luciferin reporter system can allow accurate quantitation of luciferase levels *in vitro*.[232] When each co-transfection data point is plotted with chemiluminescence on the ordinate and [^{125}I]IVFRU uptake on the abscissa, then a trend towards correlation was observed. However, despite the relatively sparse number of data points, a correlation coefficient of $r=0.63$ was obtained. The detection of luciferase in co-transfectants confirms that the transfection methods are capable of transferring genes carried on the vectors. Efficiency of transfection is highly dependent on a variety of factors. Amount of input DNA, concentration of reagents, time of exposure and cell type are all factors that can affect efficiency of gene transfer.[233] These parameters were not optimized in this study, therefore uptake of [^{125}I]IVFRU or luciferase activity after transfection may be altered by varying experimental conditions during transfection.

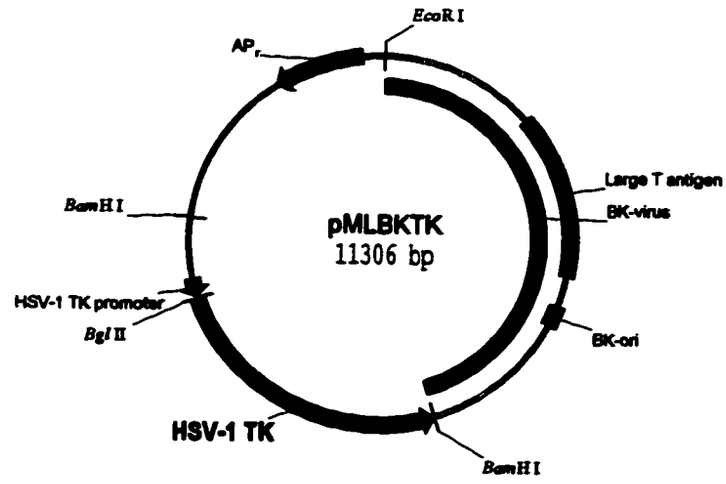

Fig. 27 pMLBKTK expression vector.

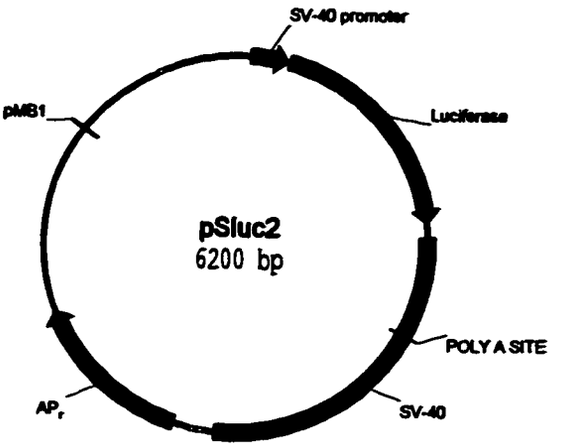

Fig. 28 pSluc2 plasmid vector.

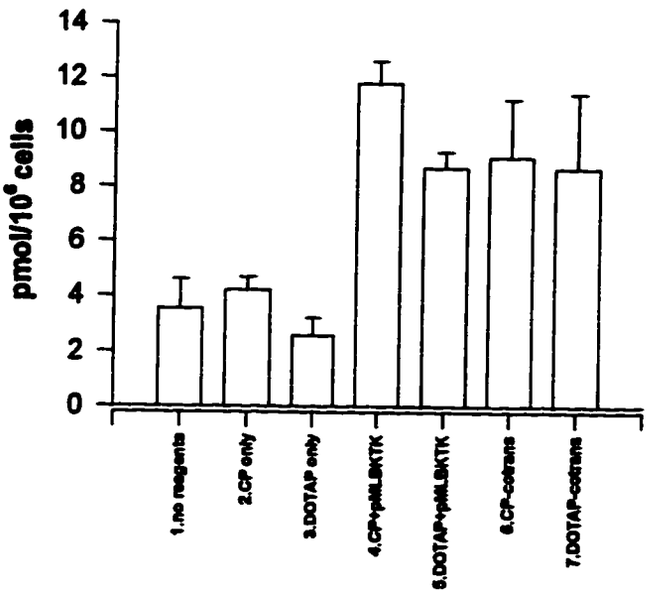

Fig. 29 Transfection and detection of HSV-1 TK gene expression with [^{125}I]IVFRU. Co-transfections were performed with both pMLBKTK and pSluc2.

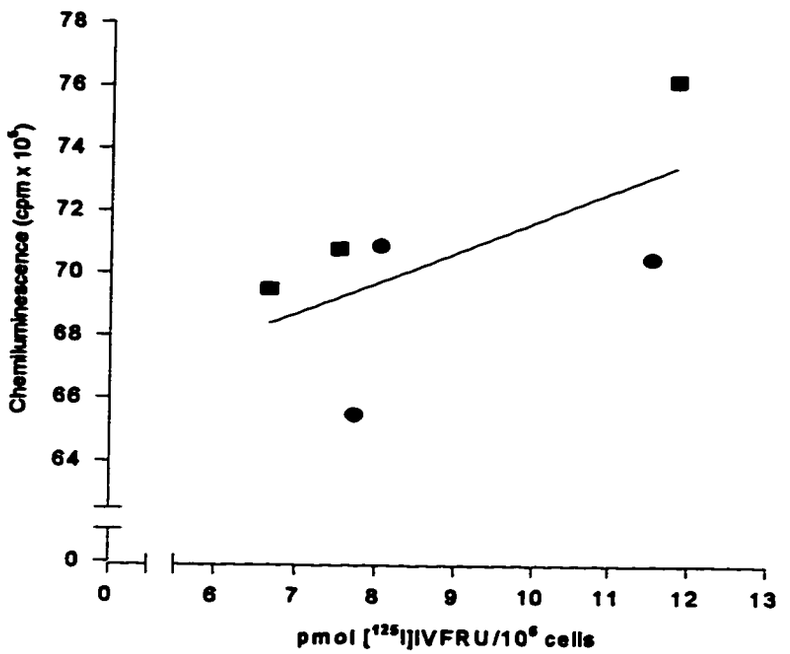

Fig. 30 Co-transfection of KBALB cells by calcium phosphate coprecipitation (●) and DOTAP liposomes (■) with pMLBKTK and pSluc2 followed by detection with luciferin or [^{125}I]IVFRU.

N. *In Vitro* Transduction and Uptake of [^{125}I]IVFRU.

The amphotropic PA-317 packaging cell line secretes replication-incompetent retroviral particles when transfected with a construct containing the ψ packaging signal. After transfection with the plasmid pLSNtk, the resulting amphotropic particles are capable of transducing a wide variety of cells including those of murine origin. After exposing KBALB cells to producer cell supernatants containing LSNtk vector, cells became resistant to the cytotoxic effects of the neomycin analogue G-418. Culturing cells for 2 weeks in the presence of G-418 selected the transduced cells and provided the KBALB-LTK cell line. The ability of this transduced cell line and its parental cell line (KBALB cells) to accumulate [^{125}I]IVFRU was evaluated *in vitro* over a period of 8 h.

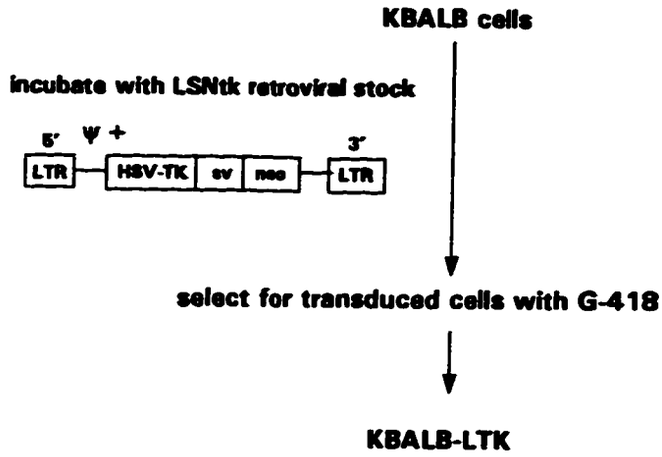

Fig. 31 *In vitro* transduction of KBALB cells with the LSNtk vector

In KBALB cells, [^{125}I]IVFRU uptake was limited to less than 0.4 pmol/10^5 cells for all time periods. In contrast, rapid uptake of [^{125}I]IVFRU was observed in the KBALB-LTK cells and continued to increase over 8 h. After 15 min, the KBALB-LTK cells accumulated 1.6 pmol/10^5 cells. The maximum level of [^{125}I]IVFRU influx was observed 8 h after exposure when 6.2 pmol/10^5 cells was intracellularly trapped. The cellular uptake of [^{125}I]IVFRU in KBALB-LTK cells was somewhat lower than that previously observed in KBALB-STK cells. After 8 h, approximately 8.2 pmol/10^5 cells accumulated in KBALB-STK cells. Thus, at this time point, the uptake of [^{125}I]IVFRU in KBALB-LTK was 24% lower than the uptake KBALB-STK cells.

The most likely explanation for the differential uptake of [^{125}I]IVFRU in KBALB-LTK and KBALB-STK cells is due to the different regulatory elements driving expression of HSV-1 TK in each cell line. In the LSNtk

vector, the 5'-LTR is promoting expression of HSV-1 TK. However, the STK vector relies on the SV-40 early promoter/enhancer element to drive HSV-1 TK expression. Both elements can have varying degrees of promoter efficiency depending on cell type.[234] However, the SV-40 early promoter/enhancer is thought to promote transcription to a greater degree than the Moloney murine leukemia virus 5'-LTR in some murine cells.[235] Thus, expression of HSV-1 TK may be greater in KBALB-STK cells leading to somewhat higher uptake of [^{125}I]IVFRU as compared to KBALB-LTK cells. Although less effective in accumulating [^{125}I]IVFRU, the preferential uptake in KBALB-LTK cells relative to KBALB cells indicates that the 5'-LTR is capable of promoting HSV-1 TK gene expression.

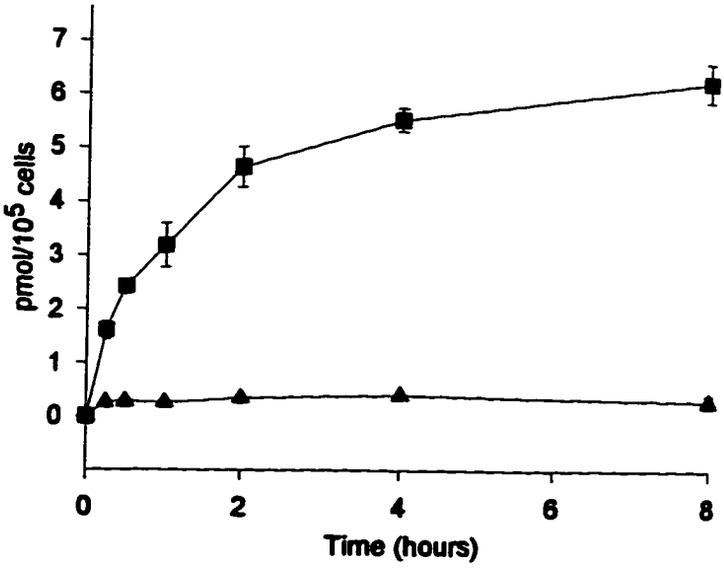

Fig. 32 *In vitro* uptake of [^{125}I]IVFRU in KBALB-LTK (■) and KBALB (▲) cells.

O. *In Vivo* HSV-1 TK Gene Transfer to KBALB Tumors.

The uptake of [^{125}I]IVFRU in KBALB-LTK cells indicates that the amphotropic LSNtk vector is capable of transferring the HSV-1 TK gene to KBALB cells. Therefore, it was of interest to examine if the LSNtk vector was capable of mediating HSV-1 TK gene transfer *in vivo*. Balb/c mice bearing KBALB tumors were injected with PA-317 supernatants containing the LSNtk vector when the tumors were 5 mm in diameter. After the tumors measured 10 mm in diameter, radiolabelled [^{131}I]IVFRU was administered by tail vein injection and the animals were sacrificed 8 h after injection. Blood and tumor radioactivity were evaluated and the results illustrated in Fig. 33.

Control animals receiving intratumoral saline injection demonstrated low [^{131}I]IVFRU uptake where approximately 0.25 % dose/g was present in the tumor 8 h after injection. Mice receiving a single intratumoral injection of 200 µL producer cell supernatant appeared to have slighly enhanced tumor uptake of [^{131}I]IVFRU (0.48 % dose/g). However, the enhancement of activity in the group receiving 200 µL was not statistically significant compared to controls. In contrast, a statistically significant difference was observed in animals receiving 400 µL supernatant ($p<0.05$, Student's t-test). The mean uptake of [^{131}I]IVFRU in animals receiving 400 µL supernatant was 0.62 % dose/g of tumor. The enhanced uptake of [^{131}I]IVFRU in tumors receiving larger volumes of supernatant is consistent with the idea that intratumoral transduction efficiency is dependent on the number of vector particles administered. However, when three consecutive injections of 400 µL supernatant were administered intratumorally, there was a decrease in [^{131}I]IVFRU uptake compared to tumors receiving a single injection. [^{131}I]IVFRU uptake in tumors receiving three consecutive

injections of 400 µL was 0.40 % dose/g. At necropsy, the tumors receiving multiple retrovirus administrations displayed some hemorrhaging and small areas of necrosis.

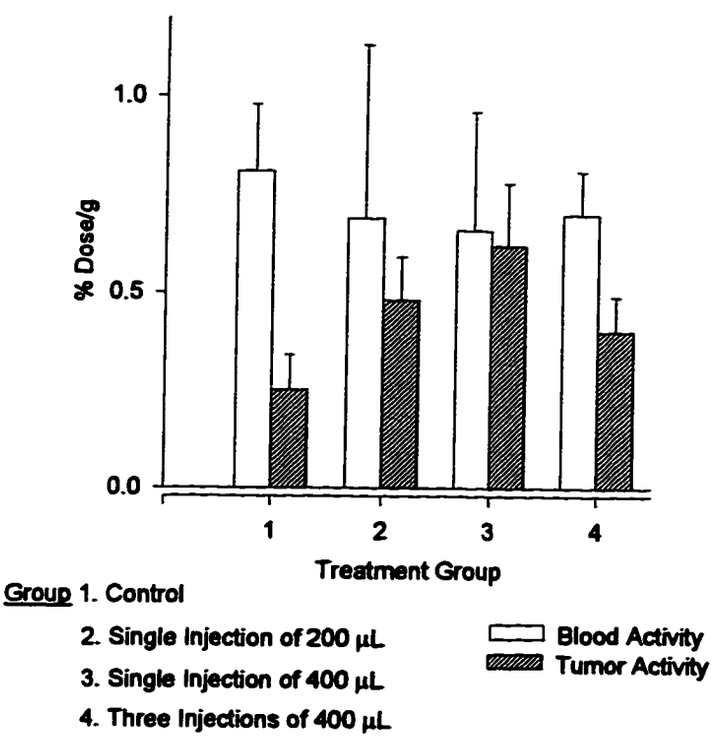

Fig. 33 Blood and tumor radioactivity 8 h after [^{131}I]IVFRU administration (n = 3).

Multifocal hemorrhage after PA-317 producer cell engraftment has been observed previously.[93] Although the reasons for this effect are not completely understood, it has important implications for radiopharmaceutical delivery. Compromised intratumoral vasculature would lead to a decrease in [^{131}I]IVFRU uptake despite transduction of a larger proportion of tumor cells. In this study, it is likely that large volumes of injected supernatant resulted in local trauma to vasculature that decreases tumor perfusion. Therefore, an ideal vector for intratumoral gene delivery should be administered in a small volume to avoid vascular damage.

The retrovirus titres in PA-317 producer cell supernatants have been shown to be sufficient to transduce tumors *in vivo*.[142] However, the extent of transduction is low after producer cell supernatant administration. The limited uptake of [^{131}I]IVFRU in tumors receiving LSNtk vectors confirms these previous results and indicates that other high titre viral vectors (ie. adenovirus) may be more appropriate as a delivery system. Although the results for the treatment group receiving 400 µL supernatant was statistically significant, the tumor to blood ratios for all groups were less than unity. Therefore, further imaging studies with [^{131}I]IVFRU were precluded in this HSV-1 TK gene transfer model.

P. Biodistribution of [^{131}I]IVFRU in Balb/c Mice Bearing KBALB or KBALB-STK Tumors

Biodistribution studies in Balb/c mice bearing subcutaneous KBALB or KBALB-STK tumors demonstrated that the HSV-1 TK expressing tumors were capable of selectively accumulating radiolabelled IVFRU *in vivo*. KBALB or KBALB-STK cells were injected subcutaneously into the flank of

male Balb/c mice (n=24). After the tumors reached 8-10 mm in diameter, [^{131}I]IVFRU (370 kBq, sp. act. 59 GBq/mmol) was injected via the tail vein into each tumor bearing animal. The concentration of radioactivity in sampled tissues and in KBALB and KBALB-STK tumors at 1,2,4 and 8 hours after intravenous administration of [^{131}I]IVFRU is depicted in Fig. 34 and Fig. 35. Up to 2 h after injection, it is apparent that the biodistribution of [^{131}I]IVFRU is similar in mice bearing either KBALB or KBALB-STK tumors. Radioactivity present in the blood accounts for the largest proportion of the injected dose in both animal groups. Approximately 4.12-4.21 % dose/g in blood was observed 2 h after administration of [^{131}I]IVFRU. Most tissues examined in both groups exhibited similar levels of radioactivity at the 1 and 2 hour time points with the exception of the tumors. Animals with KBALB tumors accumulated 2.35 % dose/g which was substantially lower than the blood activity at this time point. KBALB-STK tumor-bearing mice had a higher proportion of the dose (4.12 % dose/g) within the tumor and this level was similar to the blood radioactivity 2 h after injection of [^{131}I]IVFRU.

At the 4 h time period, the biodistribution of [^{131}I]IVFRU in animals bearing KBALB-STK tumors differs from the KBALB model. KBALB-STK tumor uptake 4 h after injection of [^{131}I]IVFRU is 2.03 % dose/g while the blood radioactivity in these same animals is 0.93 % dose/g. In contrast, KBALB tumor uptake at 4 h was 1.02 % dose/g and blood radioactivity was 2.51 % dose/g. Clearance of radioactivity from the blood of KBALB-STK tumor-bearing animals is more rapid than in animals bearing KBALB tumors. Preferential uptake of [^{131}I]IVFRU in KBALB-STK tumors appears to decrease the radioactivity circulating in the blood. However, in contrast to well perfused organs in KBALB tumor-bearing animals, the different levels of

radioactivity in the blood in each tumor model does not appear to perturb the thyroid uptake of radioactivity. At the 4 h time point, thyroid accumulation of radioactivity is virtually identical in both tumor models (0.52-0.54% dose/g). This observation suggests that, although deiodination of [^{131}I]IVFRU and accumulation of radioiodide in the thyroid occurs in both models, the levels of free iodide in both models is probably similar. Thyroid uptake increased to approximately 0.60-0.64% dose/organ at 8 h after administration. Negligible differences in thyroid uptake in animals bearing either KBALB or KBALB-STK tumors was observed at this latter time period.

Differences in the levels of radioactivity in the blood became less pronounced 8 h after [^{131}I]IVFRU administration. In animals bearing KBALB tumors, the blood radioactivity is slightly higher than in animals bearing KBALB-STK tumors at 8 h post-injection. An average of 0.81% dose/g of blood was present in KBALB tumor-bearing mice while animals bearing KBALB-STK tumors had radioactivity in the blood that accounted for approximately 0.62% dose/g. Similarly, major organs of interest displayed relatively low uptake of [^{131}I]IVFRU in both KBALB and KBALB-STK tumor-bearing animals. In KBALB tumor-bearing mice, tumor radioactivity accounts for only 0.23% dose/g. The lack of tumor uptake leads to a low (0.28) tumor to blood ratio for animals bearing the non-transduced KBALB tumors. In contrast, the KBALB-STK tumors accumulated 1.77% of the injected dose per gram of tissue; a concurrent decrease in mean blood activity results in a 10-fold increase in tumor/blood ratio compared to animals bearing KBALB tumors.

The preferential uptake of [^{131}I]IVFRU in the KBALB-STK tumors is a consequence of metabolic trapping of the radiolabelled nucleoside after selective phosphorylation by HSV-1 TK. Since the KBALB tumors did not

accumulate radioactivity, it is apparent that expression of HSV-1 TK is an absolute requirement for selective uptake *in vivo*. The biodistribution results indicate that [^{131}I]IVFRU retains its selective capability of accumulating in HSV-1 TK-expressing tissue after *in vivo* administration. However, even after 8 hours, there was a fair amount of residual radioactivity in the blood and major organs. High background radioactivity can be an impediment to effective scintigraphic imaging of HSV-1 TK-expressing tissue. However, it is possible that prolonging the interval between administration of [^{131}I]IVFRU and subsequent scintigraphic measurement may be advantageous. Tjuvajev and coworkers have shown that by allowing a 36 h washout period, HSV-1 TK gene-transduced tumors retain radioactivity (>1% dose/g) while extremely low levels of background radioactivity (<0.01% dose/g) is present in the blood and major organs after administration of [^{131}I]FIAU.[199] Although longer washout periods may allow clearance of radioactivity from non-transduced tissue, it is not favorable for higher resolution SPECT imaging with [^{123}I]IVFRU due to the shorter half-life of the isotope (13.3 h). The uptake of [^{131}I]IVFRU in KBALB-STK tumors and favorable tumor/blood ratio 8 h after administration suggests that scintigraphic imaging may be possible at this early time period. Therefore, we investigated whether early planar scintigraphy can delineate HSV-1 TK expressing tumors with [^{131}I]IVFRU.

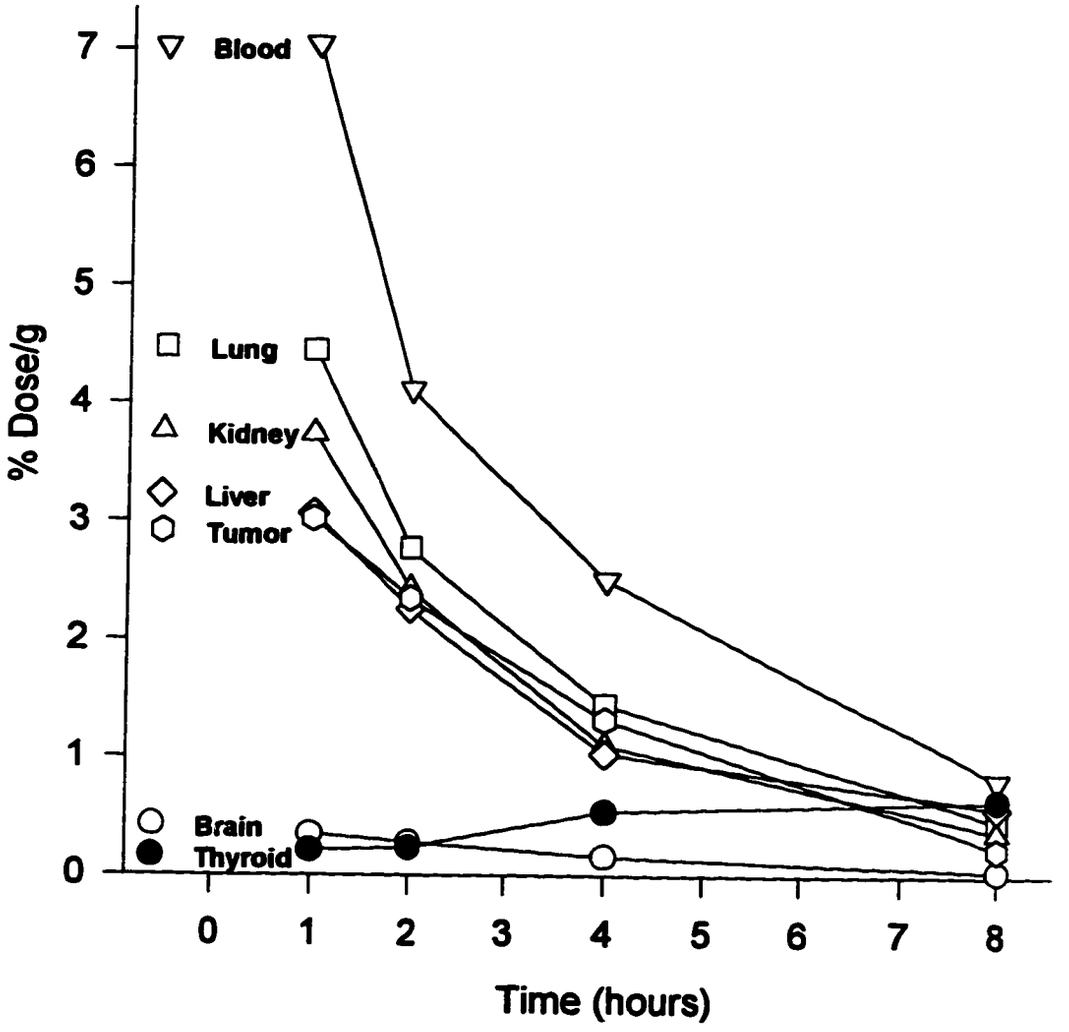

Fig. 34 Biodistribution of [^{131}I]IVFRU in Balb/c mice bearing KBALB tumors. Thyroid radioactivity (●) is represented as % dose/organ.

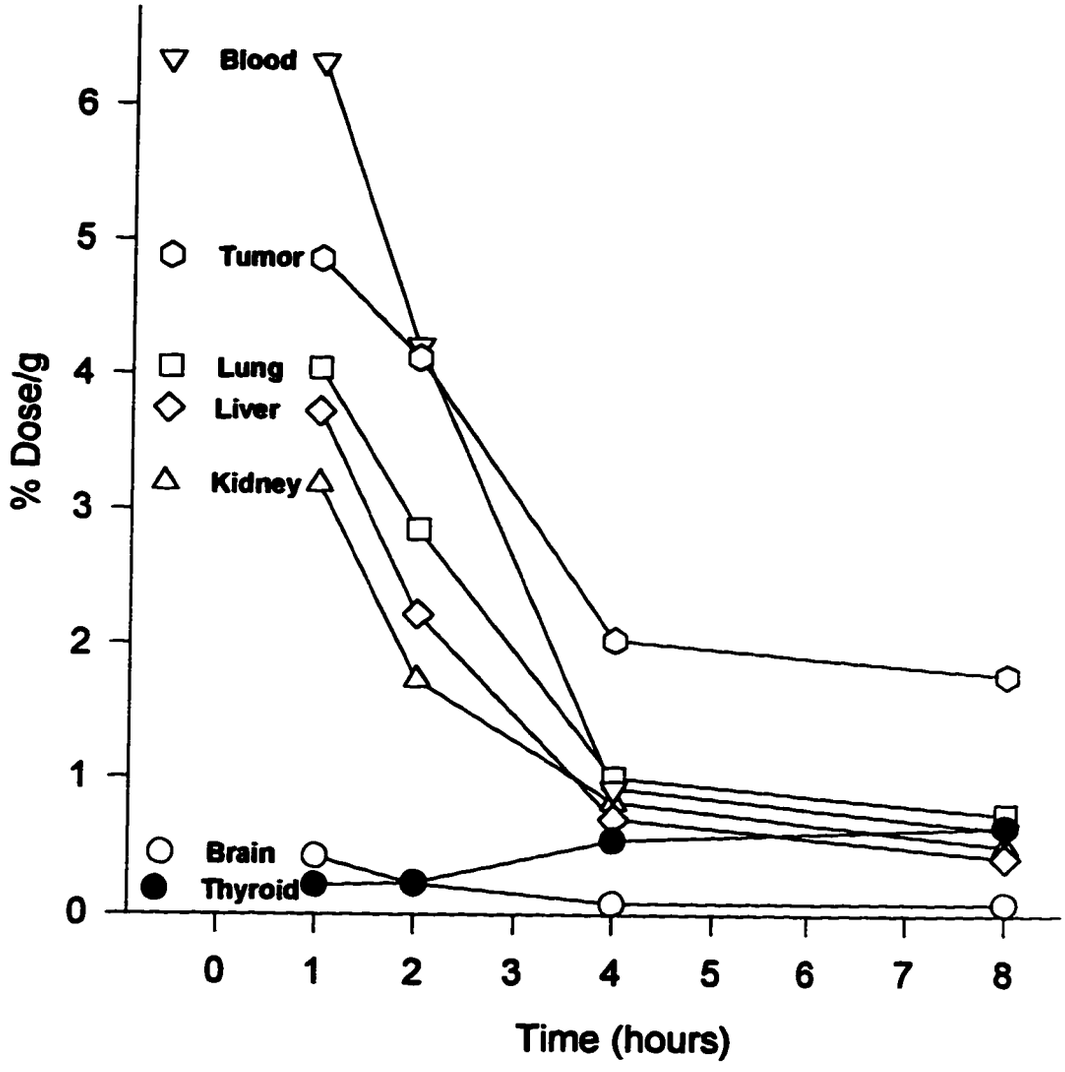

Fig. 35 Biodistribution of [^{131}I]IVFRU in Balb/c mice bearing KBALB-STK tumors. Thyroid radioactivity (●) is represented as % dose/organ.

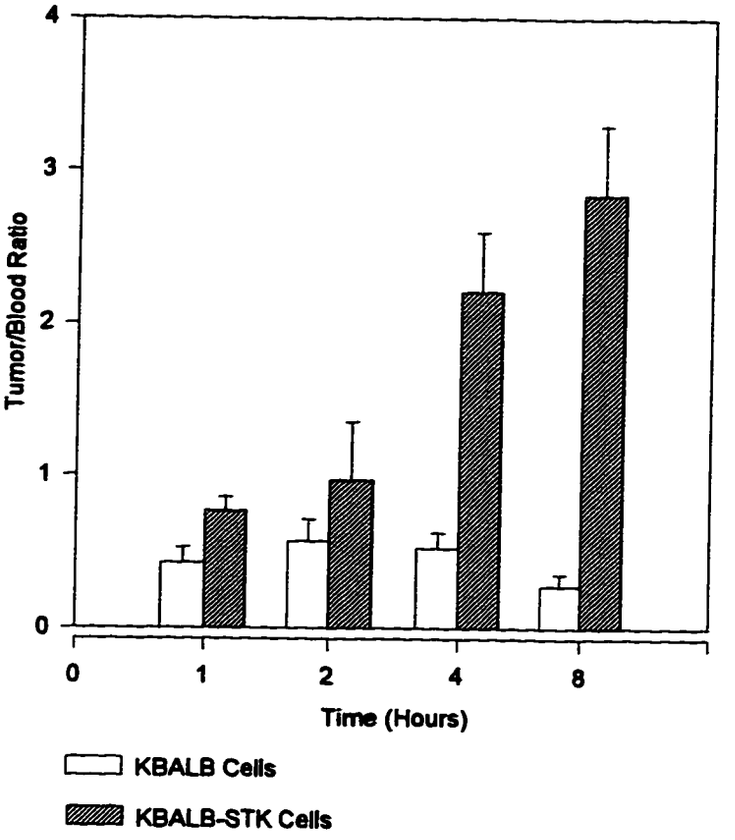

Fig. 36 Tumor to blood Ratios in Balb/c mice bearing KBALB or KBALB-STK tumors following injection of [^{131}I]IVFRU.

Q. Planar Scintigraphy of Balb/c Mice Bearing KBALB-STK Tumors During Ganciclovir Treatment

Two groups of Balb/c mice (6 animals in each group) were inoculated with KBALB-STK cells and tumor size was monitored (Fig. 37). When the tumors were approximately 10 mm in diameter, static planar images were

obtained following injection of 3.7 MBq of [^{131}I]IVFRU (sp. act. = 252 GBq/mmol) via the tail vein. After initial imaging, a group of animals (n = 6) were subjected to intraperitoneal ganciclovir injections of 100 mg/kg once daily for seven days. The control group (n = 6) received daily intraperitoneal saline injections. After 4 days, the animals were administered [^{131}I]IVFRU as before and imaged under the same acquisition protocol. It was noted that the treatment group tumor size had shrunk to an average diameter of 4.5 mm. Following the course of ganciclovir treatment, the KBALB-STK tumors had regressed in all treated animals. The tumors in the saline-control animals continued to grow reaching a mean diameter of 19 mm at termination of the experiment. The experiment was terminated due to tumor burden in these control animals.

In all of the mice imaged before ganciclovir treatment, specific tumor uptake was marked. Planar scintigraphic images of mice with KBALB-STK tumors implanted subcutaneously in the flank revealed the HSV-1 TK expressing tumors 8 hours after intravenous injection of [^{131}I]IVFRU. Radioactivity in thyroid was observed, indicating that some deiodination of [^{131}I]IVFRU had occurred. Variable amounts of radioactivity in the bladder implicate urinary excretion as a major route of elimination. However, it was noted that the animal in Fig. 38 had voided immediately prior to image acquisition leading to superior image quality. The scintigraphic image of the same animal, after 4 days of ganciclovir treatment, is shown in Fig. 39. In contrast to the image before ganciclovir treatment, the image acquired during ganciclovir treatment demonstrates that there is a complete absence of [^{131}I]IVFRU in the tumor. At this stage, there was a residual palpable tumor mass, but it was reduced to approximately half the original pre-treatment tumor size. Ganciclovir treatment precluded [^{131}I]IVFRU uptake

in all animals studied. Bladder radioactivity gave rise to the highest counts per pixel (Fig. 39). All animals receiving ganciclovir for 7 consecutive days (including the animal illustrated in Fig. 38 and Fig. 39) had nearly complete tumor regressions.

The scintigraphic imaging of ganciclovir-treated KBALB-STK tumors show that the mechanisms of cellular death are evoked early in a treatment regimen consisting of a once daily intraperitoneal injection of 100 mg/kg ganciclovir. The lack of [^{131}I]IVFRU uptake at 4 days after initiation of ganciclovir treatment is consistent with earlier evidence that KBALB-STK cells undergo rapid apoptosis following exposure to ganciclovir.[77] Although the mechanisms responsible for tumor regression remain unclear, tumor ischemia may result following ganciclovir therapy.[164] It is possible that induction of ischemia may affect delivery of [^{131}I]IVFRU to the tumor. A perfusion defect during ganciclovir treatment is a potential mechanism explaining the exclusion of [^{131}I]IVFRU from KBALB-STK tumors after 4 days of treatment. However, before ganciclovir treatment, it is clear that HSV-1 TK expressing tumors can be visualized by gamma scintigraphic imaging with [^{131}I]IVFRU.

During gene therapy with *in situ* implantation of retroviral vector secreting producer cells or intratumoral injection of high titer adenovirus vectors, the desired outcome is maximum tumoral transduction and expression of the HSV-1 TK gene before cell killing with ganciclovir. Radiolabelled IVFRU is promising as a diagnostic agent that can provide valuable information pertaining to the localization and extent of HSV-1 TK expression within a tumor. The use of the HSV-1 TK gene as a reporter on viral or plasmid vectors delivering other therapeutic genes is a potential application of this imaging technique. Moreover, the incorporation of the

HSV-1 TK gene on vectors as a "suicide gene" to enhance vector safety could also serve as a reporter for non-invasive detection with radioiodinated IVFRU.[168] This study illustrates that HSV-1 TK-expressing tissue can be clearly delineated using planar scintigraphy before ganciclovir treatment. Conceivably, incorporating ^{123}I as the isotope would result in an enhancement of resolution and allow three dimensional imaging of transduced tissue using SPECT. Alternatively, labelling IVFRU with positron-emitting ^{124}I (t 1/2 = 4.2 days) could yield even higher resolution using PET imaging. Non-invasive scintigraphic imaging during gene therapy with the HSV-1 TK gene clearly deserves further investigation.

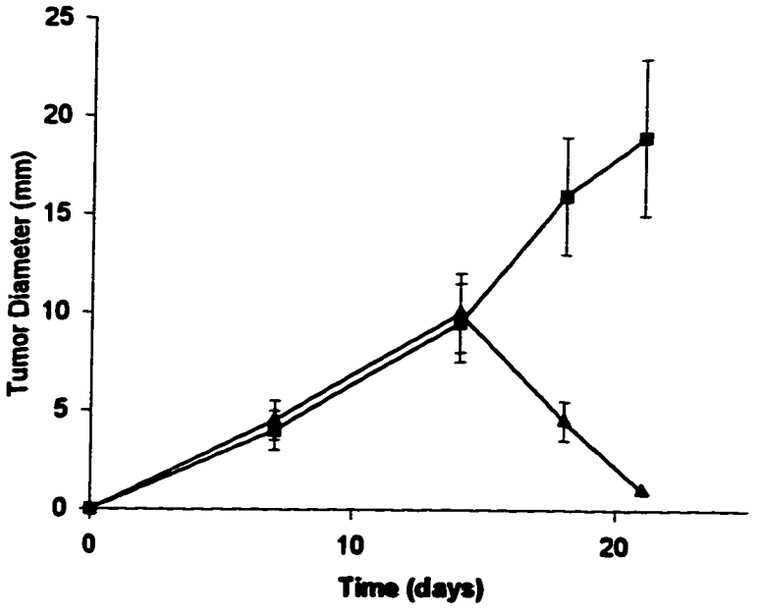

Fig. 37 Effect of administration of ganciclovir (▲) or saline (■) on KBALB-STK tumors. Daily administration begins on day 14.

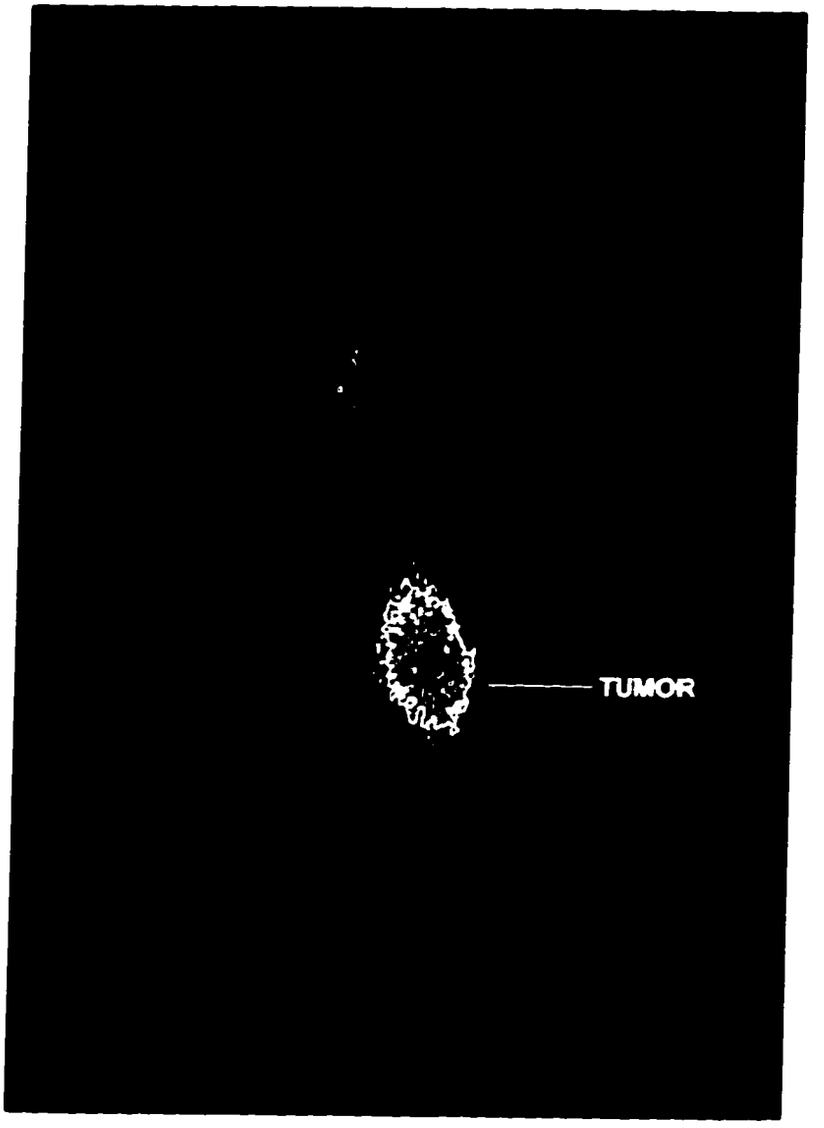

Fig. 38 Planar image of a KBALB-STK tumor-bearing mouse before ganciclovir treatment and 8 h after intravenous injection of [^{131}I]IVFRU.

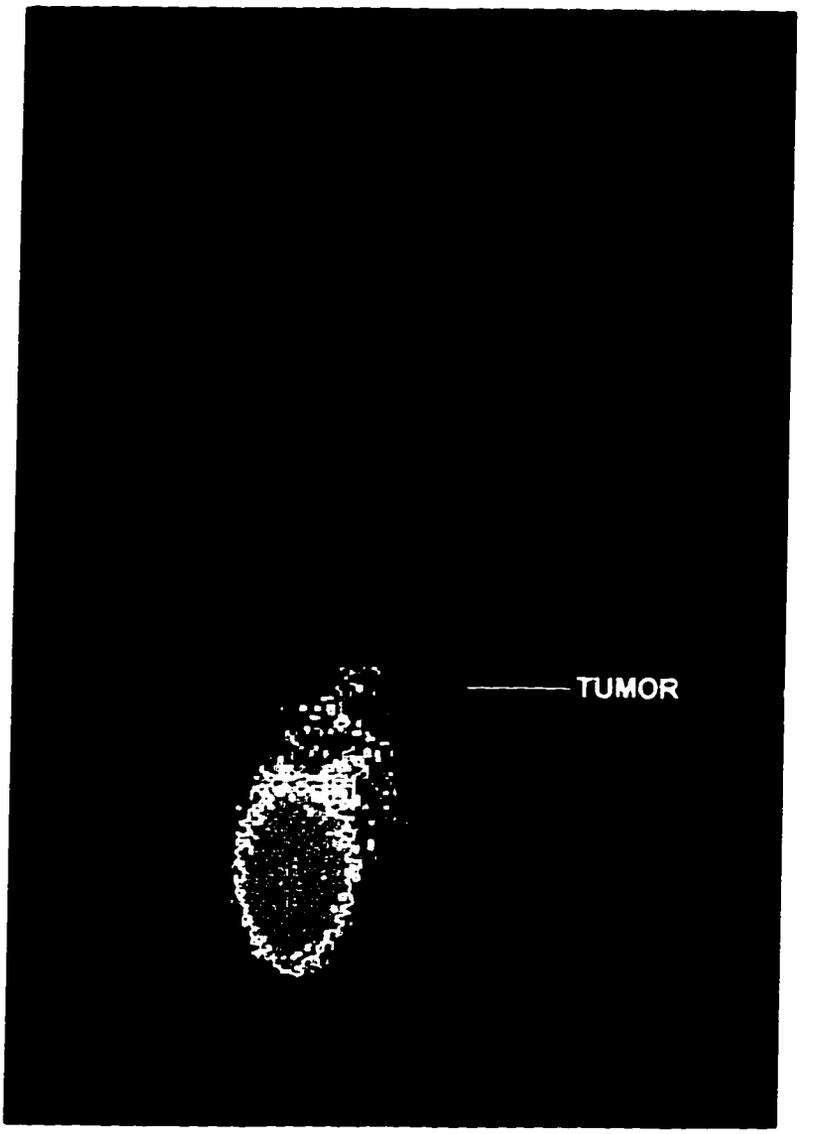

Fig. 39 Planar image of the same Balb/c mouse (as in Fig. 38) with KBALB-STK tumor after 4 days of ganciclovir treatment (100 mg/kg day) and 8 h after intravenous injection of [^{131}I]IVFRU.

IV. Summary and Conclusions

The objective of this work was to develop new synthetic and radiosynthetic methods for a series of compounds that may have utility as scintigraphic imaging agents for the detection of HSV-1 TK. Cytostatic activity and interaction with thymidylate synthase were evaluated in HSV-TK expressing cells *in vitro*. Interactions with HSV-1 TK and human phosphorylase were biochemically evaluated using purified enzymes. Evidence obtained from experiments suggested that radiolabelled IVFRU was worthy of further investigation. Cellular uptake of [^{125}I]IVFRU was performed *in vitro* after HSV-1 TK gene transfer with plasmid and retroviral vectors. *In vivo* transfer of the HSV-1 TK gene into tumors was performed with a retroviral vector and tumor uptake of [^{131}I]IVFRU was evaluated. Biodistribution and imaging experiments were performed in tumor-bearing animals with [^{131}I]IVFRU.

The synthetic strategies developed for synthesis of IVDU, IVFRU, IVFAU, IVAU, IVDU-CDS, IVFRU-CDS and IVFAU-CDS were readily amenable to radiosynthetic application. An electrophilic radiodination procedure using trimethylsilylvinyl precursors resulted in radiochemical yields of carrier added product that varied between 63-85% for 3'-unsubstituted compounds. A "no carrier added" radiosynthesis of [^{131}I]IVFRU was carried out in 71% radiochemical yield. [^{131}I]IVDU-CDS and [^{131}I]IVFRU-CDS were radioiodinated in 19 and 14% yields, respectively.

The cytostatic activities of IVDU, IVFRU, IVFAU, IVDU-CDS, IVFRU-CDS and IVFAU-CDS in FM3A TK$^-$/HSV-1 TK$^+$ cells were substantially higher than in FM3A TK$^-$ or FM3A/0 cells. In the HSV-1 TK expressing cells the iodovinyl nucleoside derivatives displayed IC_{50} values varying from

0.005-0.093 μM. The cytostatic activity in FM3A TK$^-$/HSV-1 TK$^+$ cells was 1333-10423 times higher than in FM3A/0 cells which lack HSV-1 TK expression. Selective but somewhat diminished cytostatic activity was also observed in HSV-2 TK expressing cells (FM3A TK$^-$/HSV-2 TK$^+$ cells). It was found that the iodovinyl nucleoside derivatives were more inhibitory to tritium release from 5-^{3}H dCyd in HSV-TK expressing cells than in cells lacking HSV-TK. A correlation between the cytostatic activity of these compounds and their inhibitory effect on tritium release from 5-^{3}H dCyd was observed implicating thymidylate synthase as a target for cytostatic activity.

The interaction of IVDU, IVFRU, IVFAU, IVDU-CDS, IVFRU-CDS and IVFAU-CDS with HSV-1 TK inhibited the ability of the enzyme to phosphorylate thymidine. The 3'-unsubstituted compounds exhibited IC_{50} values between 0.56-1.8 μM. The 3'-CDS-substituted derivatives were 4-45 fold less inhibitory (7.0-23.0 μM) than the 3'-unsubstituted compounds. All compounds except IVDU were completely stable to phosphorolysis by human platelet dThd phosphorylase. Greater than 90% degradation of IVDU was observed when incubated with this enzyme.

The log P values obtained for IVDU, IVFRU, IVFAU, IVDU-CDS, IVFRU-CDS and IVFAU-CDS indicate that these are all lipophilic compounds. For 3'-unsubstituted compounds, the log P values ranged from 1.10 to 1.21. The 3'-CDS derivatives had higher log P values (1.77-1.83) indicating that these compounds are more likely to enter the CNS by diffusion. In addition, the CDS compounds were rapidly oxidized in mouse blood, liver and brain homogenates. Half-lives for the 3'-CDS derivatives were shortest in the liver homogenate and ranged from 23 to 63 min. These derivatives were more stable in blood with half-lives between 127-133 min.

Cellular uptakes of [^{125}I]IVDU, [^{125}I]IVFRU, [^{125}I]IVFAU, [^{125}I]IVAU, [^{131}I]IVDU-CDS and [^{131}I]IVFRU-CDS were evaluated *in vitro*. All compounds showed minimal uptake in the cell lines lacking HSV-1 TK expression (KBALB or KBALB-LNL cells). However, increased uptake was observed for 3'-unsubstituted compounds in KBALB-STK cells which are transduced with a replication incompetent Moloney murine leukemia virus vector encoding the HSV-1 TK gene. Over a period of 8 h, [^{125}I]IVDU accumulated to the greatest extent in KBALB-STK cells. Of the 2'-substituted compounds, [^{125}I]IVFRU uptake in KBALB-STK cells was highest after 8 h exposure. In contrast, the 3'-CDS derivatives did not display any preferential uptake in KBALB-STK cells.

Transfection of KBALB cells with the pMLBKTK plasmid vector carrying the HSV-1 TK gene using calcium phosphate coprecipitation or cationic liposomes results in transfectants that are capable of accumulating [^{125}I]IVFRU. There was a 3-fold increase in [^{125}I]IVFRU uptake in cells transfected with the pMLBKTK vector compared to non-transfected KBALB cells. Co-transfection with a vector possessing the firefly luciferase gene (pSluc2) and subsequent detection with luciferin confirmed that the transfection methods were effective at delivering the vector. In addition, there was a correlation between luciferase activity and [^{125}I]IVFRU uptake in co-transfected cells.

In vitro transduction of KBALB cells with the LSNtk retroviral vector resulted in cells that were selected with antibiotic G-418. These transduced cells (KBALB-LTK cell line) were capable of accumulating [^{125}I]IVFRU to a greater extent than non-transduced KBALB cells indicating that the retroviral vector is capable of transferring the HSV-1 TK gene to KBALB cells. Intratumoral injection of LSNtk producer cell supernatant resulted in a

statistically significant increase in tumor uptake of [^{131}I]IVFRU at 8 h after administration. However, multiple intratumoral injections of producer cell supernatant appeared to induce vascular damage and decreased [^{131}I]IVFRU uptake after intravenous injection.

Biodistribution studies in Balb/c mice bearing subcutanous KBALB or KBALB-STK tumors demonstrated that the HSV-1 TK-expressing tumors were capable of selectively accumulating radiolabelled IVFRU *in vivo*. The biodistribution in sampled tissues at 8 h after intravenous administration of [^{131}I]IVFRU indicated that this compound was widely distributed after injection. In animals bearing KBALB tumors, mean tumor radioactivity accounts for only 0.23% dose/g while the blood radioactivity represented 0.81% dose/g 8 h after i.v. injection. The lack of tumor uptake leads to a low tumor to blood concentration ratio for animals bearing the non-transduced KBALB tumors. In contrast, the KBALB-STK tumors accumulated much more radioactivity than the KBALB tumors 8 h after administration of [^{131}I]IVFRU. A mean uptake of 1.77% dose/g of tissue in the HSV-1 TK-expressing tumors and a concurrent decrease in mean blood radioactivity resulted a 10-fold increase in tumor/blood ratio compared to animals bearing KBALB tumors.

Planar scintigraphic images of mice with subcutaneous KBALB-STK tumors revealed the HSV-1 TK expressing tumors 8 h after intravenous injection of [^{131}I]IVFRU. Daily treatment with ganciclovir (100 mg/kg day) for 7 days resulted in regression of KBALB-STK tumors in all treated animals. Scintigraphic imaging of KBALB-STK tumor-bearing animals after 4 days of ganciclovir treatment failed to delineate the treated tumors which were approximately 4.5 mm in diameter. In contrast to the images obtained before ganciclovir treatment, there is a complete absence of [^{131}I]IVFRU in

the tumor after 4 days of ganciclovir treatment. This study illustrates that HSV-1 TK-expressing tissue can be clearly delineated using planar scintigraphy before ganciclovir treatment. Non-invasive scintigraphic imaging with radiolabelled IVFRU clearly deserves further investigation in other animal models of gene therapy.

References

1. Illing, E.M.; Gaudette, L.A.; McLaughlin, J.; McBride, M. 1992 Canadian cancer statistics. *Health Reports* **1992**, *4*, 161-174.

2. Morsy, M. A.; Mitani, K.; Clemens, P.; Caskey, C. T. Progress toward human gene therapy. *JAMA* **1993**, *270*, 2338-2345.

3. Anonymous, Clinical protocol list. *Cancer Gene Ther.* **1995**, *2*, 225-234.

4. Mullen, C. A. Metabolic suicide genes in gene therapy. *Pharmacol. Ther.* **1994**, *63*, 199-207.

5. Moolten, F. L. Drug sensitivity ("suicide") genes for selective cancer chemotherapy. *Cancer Gene Ther.* **1994**, *1*, 279-287.

6. Mullen, C. A.; Kilstrup, M.; Blaese, R. M. Transfer of the bacterial gene for cytosine deaminase to mammalian cells confers lethal sensitivity to 5-fluorocytosine: a negative selection system. *Proc. Natl. Acad. Sci. USA* **1992**, *89*, 33-37.

7. Deonarain, M. P.; Spooner, R. A.; Epenetos, A. A. Genetic delivery of enzymes for cancer therapy. *Gene Ther.* **1995**, *2*, 235-244.

8. Austin, E. A.; Huber, B. E. A first step in the development of gene therapy for colorectal carcinoma: cloning, sequencing, and expression of Escherichia coli cytosine deaminase. *Mol. Pharmacol.* **1993**, *43*, 380-387.

9. Huber, B. E.; Austin, E. A.; Good, S. S.; Knick, V. C.; Tibbels, S.; Richards, C. A. In vivo antitumor activity of 5-fluorocytosine on

human colorectal carcinoma cells genetically modified to express cytosine deaminase. *Cancer Res.* **1993**, *53*, 4619-4626.

10. Rowley, S.; Lindauer, M.; Gebert, J. F.; Haberkorn, U.; Oberdorfer, F.; Moebius, U.; Herfarth, C.; Schackert, H. K. Cytosine deaminase gene as a potential tool for the genetic therapy of colorectal cancer. *J. Surg. Oncol.* **1996**, *61*, 42-48.

11. Huber, B. E.; Austin, E.A.; Richards, C. A.; Davis, S. T.; Good, S. S. Metabolism of 5-fluorocytosine to 5-fluorouracil in human colorectal tumor cells transduced with the cytosine deaminase gene: significant antitumor effects when only a small percentage of tumor cells express cytosine deaminase. *Proc. Natl. Acad. Sci. USA* **1994**, *91*, 8302-8306.

12. Hoganson, D. K.; Batra, R. K.; Olsen, J. C.; Boucher, R. C. Comparison of the effects of three different toxin genes and their levels of expression on cell growth and bystander effect in lung adenocarcinoma. *Cancer Res.* **1996**, *56*, 1315-1323.

13. Trinh, Q. T.; Austin, E. A.; Murray, D. M.; Knick, V. C.; Huber, B. E. Enzyme/prodrug gene therapy: comparison of cytosine deaminase/5-fluorocytosine versus thymidine kinase/ganciclovir enzyme/prodrug systems in a human colorectal carcinoma cell line. *Cancer Res.* **1995**, *55*, 4808-4812.

14. Haberkorn, U.; Oberdorfer, F.; Gebert, J.; Morr, I.; Haack, K.; Weber, K.; Lindauer, M.; van Kaick, G.; Schackert, H. K. Monitoring gene therapy with cytosine deaminase: in vitro studies using tritiated-5-fluorocytosine. *J. Nucl. Med.* **1996**, *37*, 87-94.

15. Mullen, C. A.; Coale, M. M.; Lowe, R.; Blaese, R. M. Tumors expressing the cytosine deaminase suicide gene can be eliminated in vivo with 5-fluorocytosine and induce protective immunity to wild type tumor. *Cancer Res.* **1994**, *54*, 1503-1506.

16. Consalvo, M.; Mullen, C. A.; Modesti, A.; Musiani, P.; Allione, A.; Cavallo, F.; Giovarelli, M.; Forni, G. 5-Fluorocytosine-induced eradication of murine adenocarcinomas engineered to express the cytosine deaminase suicide gene requires host immune competence and leaves an efficient memory. *J. Immunol.* **1995**, *154*, 5302-5312.

17. Kim, J.; Faye, F. J.; Henslee, J. G.; Shively, J. E.; Park, J.; Lai, S.; Linnoila, R. I.; Mulshine, J. L.; Gazdar A. F. Expression of

carcinoembryonic antigen and related genes in lung and gastrointesitinal cancers. *Int. J. Cancer*, **1992**, *52*, 718-725.

18. Richards, C. A.; Austin, E. A.; Huber, B. E. Transcriptional regulatory sequences of carcinoembryonic antigen: identification and use with cytosine deaminase for tumor-specific gene therapy. *Hum. Gene Ther.* **1995**, *6*, 881-893.

19. Harris, J. D.; Gutierrez, A. A.; Hurst, H. C.; Sikora, K.; Lemoine, N. R. Gene therapy for cancer using tumour-specific prodrug activation. *Gene Ther.* **1994**, *1*, 170-175.

20. Judde, J. G.; Spangler, G.; Magrath, I.; Bhatia, K. Use of Epstein-Barr virus nuclear antigen-1 in targeted therapy of EBV-associated neoplasia. *Hum. Gene Ther.* **1996**, *7*, 647-653.

21. Michael, N. P.; Brehm, J. K.; Anlezark, G. M.; Minton, N. P. Physical characterisation of the Escherichia coli B gene encoding nitroreductase and its over-expression in Escherichia coli K12. *FEMS Micro. Lett.* **1994**, *124*, 195-202.

22. Knox, R. J.; Friedlos, F.; Sherwood, R. F.; Melton, R. G.; Anlezark, G. M. The bioactivation of 5-(aziridin-1-yl)-2,4-dinitrobenzamide (CB1954)--II. A comparison of an Escherichia coli nitroreductase and Walker DT diaphorase. *Biochem. Pharmacol.* **1992**, *44*, 2297-2301.

23. Anlezark, G. M.; Melton, R. G.; Sherwood, R. F.; Wilson, W. R.; Denny, W. A.; Palmer, B. D.; Knox, R. J.; Friedlos, F.; Williams, A. Bioactivation of dinitrobenzamide mustards by an E. coli B nitroreductase. *Biochem. Pharmacol.* **1995**, *50*, 609-618.

24. Bridgewater, J. A.; Springer, C. J.; Knox, R. J.; Minton, N. P.; Michael, N. P.; Collins, M. K. Expression of the bacterial nitroreductase enzyme in mammalian cells renders them selectively sensitive to killing by the prodrug CB1954. *Eur. J. Cancer* **1995**, *31A*, 2362-2370.

25. Anlezark, G. M.; Melton, R. G.; Sherwood, R. F.; Coles, B.; Friedlos, F.; Knox, R. J. The bioactivation of 5-(aziridin-1-yl)-2,4-dinitrobenzamide (CB1954)--I. Purification and properties of a nitroreductase enzyme from Escherichia coli--a potential enzyme for antibody-directed enzyme prodrug therapy (ADEPT). *Biochem. Pharmacol.* **1992**, *44*, 2289-2295.

26. Sorscher, E. J.; Peng, S.; Bebok, Z.; Allan, P. W.; Bennett, L. L., Jr.; Parker, W. B. Tumor cell bystander killing in colonic carcinoma utilizing the Escherichia coli DeoD gene to generate toxic purines. *Gene Ther.* **1994**, *1*, 233-238.

27. Pendyala, L.; Smyth, J.; Wellman, A. M. Nature of 6-methylpurine inhibition and characterization of two 6-methylpurine-resistant mutants of Neurospora crassa. *J. Bacteriol.* **1979**, *137*, 248-255.

28. Kamatani, N.; Takeuchi, F.; Nishida, Y.; Yamanaka, H.; Nishioka, K.; Tatara, K.; Fujimori, S.; Kaneko, K.; Akaoka, I.; Tofuku, Y. Severe impairment in adenine metabolism with a partial deficiency of adenine phosphoribosyltransferase. *Metabol. Clin. Exp.* **1985**, *34*, 164-168.

29. Hughes, B. W.; Wells, A. H.; Bebok, Z.; Gadi, V. K.; Garver, R. I., Jr.; Parker, W. B.; Sorscher, E. J. Bystander killing of melanoma cells using the human tyrosinase promoter to express the Escherichia coli purine nucleoside phosphorylase gene. *Cancer Res.* **1995**, *55*, 3339-3345.

30. Leblanc, G. A.; Waxman, D. J. Interaction of anticancer drugs with hepatic monooxygenase enzymes. *Drug Metab. Rev.* **1989**, *20*, 395-439.

31. Chang, T. K. H.; Weber, G. F.; Crespi, C. L.; Waxman, D. J. Differential activation of of cyclophosphamide and ifosfamide by cytochromes P450 2B and 3A in human liver microsomes. *Cancer Res.* **1993**, *53*, 5629-5637.

32. Walker, D.; Flinois, J. P.; Monkman, S. C.; Beloc, C.; Boddy, A. V.; Cholerton, S.; Daly, A. K.; Lind, M. J.; Pearson, A. D. J.; Beaune P. H.; Idle, J. R. Identification of the major human hepatic cytochrome P450 involved in activation and N-dechloroethylation of ifosfamide. *Biochem. Pharmacol.* **1994**, *47*, 1157-1163.

33. Sladek, N. E. Metabolism of oxazaphosphorines. *Pharmacol. Ther.* **1988**, *37*, 301-355.

34. Clarke, L.; Waxman, D. J. Oxidative metabolism of cyclophosphamide: identification of the hepatic monooxygenase catalysts of drug activation. *Cancer Res.* **1989**, *49*, 2344-2350.

35. Wei, M. X.; Tamiya, T.; Chase, M.; Boviatsis, E. J.; Chang, T. K.; Kowall, N. W.; Hochberg, F. H.; Waxman, D. J.; Breakefield, X. O.; Chiocca, E. A. Experimental tumor therapy in mice using the

cyclophosphamide-activating cytochrome P450 2B1 gene. *Hum. Gene Ther.* **1994**, *5*, 969-978.

36. Chen, L.; Waxman, D. J. Intratumoral activation and enhanced chemotherapeutic effect of oxazaphosphorines following cytochrome P450 gene transfer: development of a combined chemotherapy/cancer gene therapy strategy. *Cancer Res.* **1995**, *55*, 581-589.

37. Chen, L.; Waxman, D. J.; Chen, D.; Kufe, D. W. Sensitization of human breast cancer cells to cyclophosphamide and ifosfamide by transfer of a liver cytochrome P450 gene. *Cancer Res.* **1996**, *56*, 1331-1340.

38. Mulligan, R. C.; Berg, P. Selection for animal cells that express the Escherichia coli gene coding for xanthine-guanine phosphoribosyltransferase. *Proc. Natl. Acad. Sci. USA* **1981**, *78*, 2072-2076.

39. Breter, H. J.; Zahn, R. K. Quantitation of intracellular metabolites of [35S]-6-mercaptopurine in L5178Y cells grown in time-course incubates. *Cancer Res.* **1979**, *39*, 3744-3748.

40. Besnard, C.; Monthioux, E.; Jami, J. Selection against expression of Escherichia coli gene gpt in hprt+ mouse teratocarcinoma and hybrid cells. *Mol. Cell. Biol.* **1987**, *7*, 4139-4141.

41. Mroz, P. J.; Moolten, F. L. Retrovirally transduced Escherichia coli gpt genes combine selectability with chemosensitivity capable of mediating tumor eradication. *Hum. Gene Ther.* **1993**, *4*, 589-595.

42. Koszalka, G. W.; Averett, D. R.; Fyfe, J. A.; Roberts, G. B.; Spector, T.; Biron, K.; Krenitsky, T. A. 6-N-substituted derivatives of adenine arabinoside as selective inhibitors of varicella-zoster virus. *Antimicrob. Agents Chemother.* **1991**, *35*, 1437-1443.

43. Averett, D. R.; Koszalka, G. W.; Fyfe, J. A.; Roberts, G. B.; Purifoy, D. J.; Krenitsky, T. A. 6-Methoxypurine arabinoside as a selective and potent inhibitor of varicella-zoster virus. *Antimicrob. Agents Chemother.* **1991**, *35*, 851-857.

44. de Miranda, P.; Burnette, T. C.; Biron, K. K.; Miller, R. L.; Averett, D. R.; Krenitsky, T. A. Anabolic pathway of 6-methoxypurine arabinoside in cells infected with varicella-zoster virus. *Antimicrob. Agents Chemother.* **1991**, *35*, 2121-2124.

45. Huber, B. E.; Richards, C. A.; Krenitsky, T. A. Retroviral-mediated gene therapy for the treatment of hepatocellular carcinoma: an innovative approach for cancer therapy. *Proc. Natl. Acad. Sci. USA* **1991**, *88*, 8039-8043.

46. De Clercq, E. Biochemical aspects of the selective antiherpes activity of nucleoside analogues. *Biochem. Pharmacol.* **1984**, *33*, 2159-2169.

47. Elion, G. B. The chemotherapeutic exploitation of virus-specified enzymes. *Adv. Enzyme Regul.* **1980**, *18*, 53-60.

48. Wild, K.; Bohner, T.; Aubry, A.; Folkers, G.; Schulz, G. E. The three-dimensional structure of thymidine kinase from herpes simplex virus type 1. *FEBS Lett.* **1995**, *368*, 289-292.

49. Brown, D. G.; Visse, R.; Sandhu, G.; Davies, A.; Rizkallah, P. J.; Melitz, C.; Summers, W. C.; Sanderson, M. R. Crystal structures of the thymidine kinase from herpes simplex virus type-1 in complex with deoxythymidine and ganciclovir. *Nature Struct. Biol.* **1995**, *10*, 876-881.

50. Chen, M. S.; Prusoff, W. H. Association of thymidylate kinase activity with pyrimidine deoxyribonucleoside kinase induced by herpes simplex virus. *J. Biol. Chem.* **1978**, *253*, 1325-1327.

51. Chen, M. S.; Summers W. P.; Walker, J.; Summers, W. C.; Prusoff, W. H. Characterization of pyrimidine deoxyribonucleoside kinase (thymidine kinase) and thymidylate kinase as a multifunctional enzyme in cells transformed by herpes simplex virus type 1 and in cells infected with mutant strains of herpes simplex virus. *J. Virol.* **1979**, *30*, 942-945.

52. Elion, G. B.; Furman, P. A.; Fyfe, J. A.; de Miranda, P.; Beauchamp, L.; Schaeffer, H. J. Selectivity of action of an antiherpetic agent, 9-(2-hydroxyethoxymethyl)guanine. *Proc. Natl. Acad. Sci. USA* **1977**, *74*, 5716-5720.

53. Fyfe, J. A.; Keller, P. M.; Furman, P. A.; Miller, R. I.; Elion, G. B. Thymidine kinase from herpes simplex virus phosphorylates the new antiviral compound, 9-(2-hydroxyethoxymethyl)guanine. *J. Biol. Chem.* **1978**, *253*, 8721-8727.

54. Miller, W. H.; Miller, R. L. Phosphorylation of acyclovir (acycloguanosine) monophosphate by GMP kinase. *J. Biol. Chem.* **1980**, *255*, 7204-7207.

55. Miller, W. H.; Miller, R. L. Phosphorylation of acyclovir diphosphate by cellular enzymes. *Biochem. Pharmacol.* **1982**, *31*, 3879-3884.

56. Furman, P. A.; St. Clair, M. H.; Fyfe, J. A.; Rideout, J. L.; Keller, P. M.; Elion, G. B. Inhibition of herpes simplex virus-induced DNA polymerase activity and viral DNA replication by 9-(2-hydroxyethoxymethyl)guanine and its triphosphate. *J. Virol.* **1979**, *32*, 72-77.

57. Furman, P. A.; St. Clair, M. H.; Spector, P. Acyclovir triphosphate is a suicide inactivator of herpes simplex virus DNA polymerase. *J. Biol. Chem.* **1984**, *259*, 9575-9579.

58. Furman, P. A.; McGuirt, P. V.; Keller, P. M.; Fyfe, J. A.; Elion, G. B. Inhibition by acyclovir of cell growth and DNA synthesis of cells biochemically transformed with herpesvirus genetic information. *Virology* **1980**, *102*, 420-430.

59. Smith, K. O.; Galloway, K. S.; Kennel, W. I.; Ogilvie, K. K.; Radatus, B. K. A new nucleoside analog, 9-[[2-hydroxy-1-(hydroxymethyl)ethoxy]methyl]guanine, highly active in vitro against herpes simplex virus type 1 and 2. *Antimicrob. Agents Chemother.* **1982**, *22*, 55-61.

60. Field, A. K.; Davies, M. E.; De Witt, C.; Perry, H. C.; Liou, R.; Germershausen, J.; Karkas, J. D.; Ashton, W. T.; Johnston, D. B. R.; Tolman, R. L. 9-[2-hydroxy-1 (hydroxymethyl)ethoxymethyl]guanine: a selective inhibitor of herpes group virus replication. *Proc. Natl. Acad. Sci. USA* **1983**, *80*, 4139-4143.

61. Oliver, S.; Bubley, G. Inhibition of HSV-transformed murine cells by nucleoside analogs, 2'-NDG and 2'-nor-cGMP: mechanisms of inhibition and reversal by exogenous nucleosides. *Virology*, **1985**, *145*, 84-93.

62. Nishiyama, Y.; Rapp, F. Anticellular effects of 9-(2-hydroxyethoxymethyl)guanine against herpes simplex virus-transformed cells. *J. Gen. Virol.* **1979**, *45*, 227-230.

63. Davidson, R. L.; Kaufman, E. R.; Crumpacker, C. S.; Schnipper, L. E. Inhibition of herpes simplex virus transformed and nontransformed

cells by acycloguanosine: mechanisms of uptake and toxicity. Virology, **1981**, 113, 9-19.

64. Moolten, F. L. Tumor sensitivity conferred by inserted herpes thymidine kinase genes: paradigm for a prospective cancer control strategy. *Cancer Res.* **1986**, *46*, 5276-5281.

65. Moolten, F. L. Mosaicism induced by gene insertion as a means of improving chemotherapeutic selectivity. *Immunology*, **1990**, *10*, 203-233.

66. Uckert, W.; Walther, W. Retrovirus-mediated gene transfer in cancer therapy. *Pharmacol. Ther.* **1994**, *63*, 323-347.

67. Mann, R.; Mulligan, R. C.; Balitimore D. Construction of a retrovirus packaging mutant and its use to produce helper-free defective retrovirus. Cell **1983**, 33, 153-159.

68. Cone, R. D.; Mulligan, R. C. High-efficiency gene transfer into mammalian cells: generation of helper-free recombinant retrovirus with broad mammalian host range. *Proc. Natl. Acad. Sci. USA* **1984**, *81*, 6349-6353.

69. Miller, A. D.; Law, M. F.; Verma, I. M. Generation of helper-free amphotropic retroviruses that transduce a dominant-acting, methotrexate-resistant dihydrofolate reductase gene. *Mol. Cell Biol.* **1985**, *5*, 431-437.

70. Miller, A. D.; Buttimore, C. Redesign of retrovirus packaging cell lines to avoid recombination leading to helper virus production. *Mol. Cell Biol.* **1986**, *6*, 2895-2902.

71. Markowitz, D.; Goff, S.; Bank, A. A safe packaging line for gene transfer: separating viral genes on two different plasmids. *J. Virol.* **1988**, *62*, 1120-1124.

72. Danos, O.; Mulligan, R. C. Safe and efficient generation of recombinant retroviruses with amphotropic and ecotropic host ranges. *Proc. Natl. Acad. Sci. USA* **1988**, *85*, 6460-6464.

73. Miller, D. G.; Adam, M. A.; Miller, A. D. Gene transfer by retrovirus vector occurs only in cells that are actively replicating at the time of infection. *Mol. Cell Biol.* **1990**, *10*, 4139-4142.

74. Moolten, F. L.; Wells, J. M. Curability of tumors bearing herpes thymidine kinase genes transferred by retroviral vectors. *J. Natl. Cancer Inst.* **1990**, *82*, 297-300.

75. Moolten, F. S.; Wells, J. M.; Mroz, P. J. Multiple transduction as a means of preserving ganciclovir chemosensitivity in sarcoma cells carrying retrovirally transduced herpes thymidine kinase genes. *Cancer Lett.* **1992**, *64*, 257-263.

76. Ezzeddine, Z. D.; Martuza, R. L.; Platika, D.; Short, M. P.; Malick, A.; Choi, B.; Breakefield, X. O. Selective killing of glioma cells in culture and in vivo by retrovirus transfer of the herpes simplex virus thymidine kinase gene. *New Biol.* **1991**, *3*, 608-614.

77. Freeman, S. M.; Abboud, C. N.; Whartenby, K. A.; Packman, C. H.; Koeplin, D. S.; Moolten, F. L.; Abraham, G. N. The "bystander effect": Tumor regression when a fraction of the tumor mass is genetically modified. *Cancer Res.* **1993**, *53*, 5274-5283.

78. Takenaga, K.; Tagawa, M.; Sakiyama, S. Therapeutic potency of transduction with herpes simplex virus thymidine kinase gene against multidrug resistant mouse leukemia cells. *Anticancer Res.* **1996**, *16*, 681-685.

79. Barba, D.; Hardin, J.; Ray, J.; Gage, F. H. Thymidine kinase-mediated killing of rat brain tumors. *J. Neurosurg.* **1993**, *79*, 729-735.

80. Abe, A.; Takeo, T.; Emi, N.; Tanimoto, M.; Ueda, R.; Yee, J. K.; Friedmann, T.; Saito, H. Transduction of a drug-sensitive toxic gene into human leukemia cell lines with a novel retroviral vector. *Proc. Soc. Exp. Biol. Med.* **1993**, *203*, 354-359.

81. Dilber, M. S.; Abedi, M. R.; Bjorkstrand, B.; Christensson, B.; Gahrton, G.; Xanthopoulos, K. G.; Smith, C. I. Suicide gene therapy for plasma cell tumors. *Blood* **1996**, *88*, 2192-2200.

82. Hasegawa, Y.; Emi, N.; Shimokata, K.; Abe, A.; Kawabe, T.; Hasegawa, T.; Kirioka, T.; Saito, H. Gene transfer of herpes simplex virus type I thymidine kinase gene as a drug sensitivity gene into human lung cancer cell lines using retroviral vectors. *Am. J. Resp. Cell Mol. Biol.* **1993**, *8*, 655-661.

83. Hasegawa, Y.; Emi, N.; Shimokata, K. Retroviral transfer of HSV1-TK gene into human lung cancer cell line. *J. Mol. Med.* **1995**, *73*, 107-112.

84. Kaneko, Y.; Tsukamoto, A. Gene therapy of hepatoma: bystander effects and non-apoptotic cell death induced by thymidine kinase and ganciclovir. *Cancer Lett.* **1995**, *96*, 105-110.

85. Vrionis, F. D.; Wu, J. K.; Qi, P.; Cano, W. G.; Cherington, V. Tumor cells expressing the herpes simplex virus-thymidine kinase gene in the treatment of Walker 256 meningeal neoplasia in rats. *J. Neurosurg.* **1996**, *84*, 250-257.

86. Wilson, K. M.; Stambrook, P. J.; Bi, W. L.; Pavelic, Z. P.; Pavelic, L.; Gluckman, J. L. HSV-tk gene therapy in head and neck squamous cell carcinoma. Enhancement by the local and distant bystander effect. *Arch. Otolaryng. Head Neck Surg.* **1996**, *122*, 746-749.

87. Yoshida, K.; Kawami, H.; Yamaguchi, Y.; Kuniyasu, H.; Nishiyama, M.; Hirai, T.; Yanagihara, K.; Tahara, E.; Toge, T. Retrovirally transmitted gene therapy for gastric carcinoma using herpes simplex virus thymidine kinase gene. *Cancer* **1995**, *75*, 1467-1471.

88. Beck, C.; Cayeux, S.; Lupton, S. D.; Dorken, B.; Blankenstein, T. The thymidine kinase/ganciclovir-mediated "suicide" effect is variable in different tumor cells. *Hum. Gene Ther.* **1995**, *6*, 1525-1530.

89. Short, M. P.; Choi, B. C.; Lee, J. K.; Malick, A.; Breakefield, X. O.; Martuza, R. L. Gene delivery to glioma cells in rat brain by grafting of a retrovirus packaging cell line. *J. Neurosci. Res.* **1990**, *27*, 427-433.

90. Culver, K. W.; Ram, Z.; Wallbridge, S.; Ishii, H.; Oldfield, E. H.; Blaese, R. M. In vivo gene transfer with retroviral vector-producer cells for treatment of experimental brain tumors. *Science* **1992**, *256*, 1550-1552.

91. Takamiya, Y.; Short, M. P.; Moolten, F. L.; Fleet, C.; Mineta, T.; Breakefield, X. O.; Martuza, R. L. An experimental model of retrovirus gene therapy for malignant brain tumors. *J. Neurosurg.* **1993**, *79*, 104-110.

92. Takamiya, Y.; Short, M. P.; Ezzeddine, Z. D.; Moolten, F. L.; Breakefield, X. O.; Martuza, R. L. Gene therapy of malignant brain tumors: a rat glioma line bearing the herpes simplex virus type 1-thymidine kinase gene and wild type retrovirus kills other tumor cells. *J. Neurosci. Res.* **1992**, *33*, 493-503.

93. Ram, Z.; Culver, K. W.; Walbridge, S.; Blaese, R. M.; Oldfield, E. H. In situ retroviral-mediated gene transfer for the treatment of brain tumors in rats. *Cancer Res.* **1993**, *53*, 83-88.

94. Rainov, N. G.; Kramm, C. M.; Aboody-Guterman, K.; Chase, M.; Ueki, K.; Louis, D. N.; Harsh, G. R. t.; Chiocca, A.; Breakefield, X. O. Retrovirus-mediated gene therapy of experimental brain neoplasms using the herpes simplex virus-thymidine kinase/ganciclovir paradigm. *Cancer Gene Ther.* **1996**, *3*, 99-106.

95. Izquierdo, M.; Cortes, M.; de Felipe, P.; Martin, V.; Diez-Guerra, J.; Talavera, A.; Perez-Higueras, A. Long-term rat survival after malignant brain tumor regression by retroviral gene therapy. *Gene Ther.* **1995**, *2*, 66-69.

96. Ram, Z.; Culver, K. W.; Walbridge, S.; Frank, J. A.; Blaese, R. M.; Oldfield, E. H. Toxicity studies of retroviral-mediated gene transfer for the treatment of brain tumors. *J. Neurosurg.* **1993**, *79*, 400-407.

97. Oldfield, E. H.; Ram, Z.; Culver, K. W.; Blaese, R. M.; DeVroom, H. L.; Anderson, W. F. Gene therapy for the treatment of brain tumors using intra-tumoral transduction with the thymidine kinase gene and intravenous ganciclovir. *Hum. Gene Ther.* **1993**, *4*, 39-69.

98. Culver, K. W.; Van Gilder, J.; Link, C. J.; Carlstrom, T.; Buroker, T.; Yuh, W.; Koch, K.; Schabold, K.; Doornbas, S.; Wetjen, B. Gene therapy for the treatment of malignant brain tumors with in vivo tumor transduction with the herpes simplex thymidine kinase gene/ganciclovir system. *Hum. Gene Ther.* **1994**, *5*, 343-379.

99. Raffel, C.; Culver, K.; Kohn, D.; Nelson, M.; Siegel, S.; Gillis, F.; Link, C. J.; Villablanca, J. G.; Anderson, W. F. Gene therapy for the treatment of recurrent pediatric malignant astrocytomas with in vivo tumor transduction with the herpes simplex thymidine kinase gene/ganciclovir system. *Hum. Gene Ther.* **1994**, *5*, 863-890.

100. Kun, L. E.; Gajjar, A.; Muhlbauer, M.; Heideman, R. L.; Sanford, R.; Brenner, M.; Walter, A.; Langston, J.; Jenkins, J.; Facchini, S. Stereotactic injection of herpes simplex thymidine kinase vector producer cells (PA317-G1Tk1SvNa.7) and intravenous ganciclovir for the treatment of progressive or recurrent primary supratentorial pediatric malignant brain tumors. *Hum. Gene Ther.* **1995**, *6*, 1231-1255.

101. Ram, Z.; Walbridge, S.; Oshiro, E. M.; Viola, J. J.; Chiang, Y.; Mueller, S. N.; Blaese, R. M.; Oldfield, E. H. Intrathecal gene therapy for malignant leptomeningeal neoplasia. *Cancer Res.* **1994**, *54*, 2141-2145.

102. Oshiro, E. M.; Viola, J. J.; Oldfield, E. H.; Walbridge, S.; Bacher, J.; Frank, J. A.; Blaese, R. M.; Ram, Z. Toxicity studies and distribution dynamics of retroviral vectors following intrathecal administration of retroviral vector-producer cells. *Cancer Gene Ther.* **1995**, *2*, 87-95.

103. Oldfield, E. H.; Ram, Z.; Chiang, Y.; Blaese, R. M. Intrathecal gene therapy for the treatment of leptomeningeal carcinomatosis. GTI 0108. A phase I/II study. *Hum. Gene Ther.* **1995**, *6*, 55-85.

104. Caruso, M.; Panis, Y.; Gagandeep, S.; Houssin, D.; Salzmann, J. L.; Klatzmann, D. Regression of established macroscopic liver metastases after in situ transduction of a suicide gene. *Proc. Natl. Acad. Sci. USA* **1993**, *90*, 7024-7028.

105. Moorman, D. W.; Butler, D. A.; Stanley, J. D.; Lamsam, J. L.; Ackermann, M. R.; Jacobson, C. D.; Culver, K. W. Survival and toxicity of xenogeneic murine retroviral vector producer cells in liver. *J. Surg. Oncol.* **1994**, *57*, 152-156.

106. Klatzmann, D. Gene therapy for metastatic malignant melanoma: evaluation of tolerance to intratumoral injection of cells producing recombinant retroviruses carrying the herpes simplex virus type 1 thymidine kinase gene, to be followed by ganciclovir administration. *Hum. Gene Ther.* **1996**, *7*, 255-267.

107. Link, C. J., Jr.; Kolb, E. M.; Muldoon, R. R. Preliminary in vitro efficacy and toxicities studies of the herpes simplex thymidine kinase gene system for the treatment of breast cancer. *Hybridoma* **1995**, *14*, 143-147.

108. Berkner, K. L. Development of adenovirus vectors for the expression of heterologous genes. *Biotechniques* **1988**, *6*, 616-629.

109. Graham, F. L.; Smiley, J.; Russell, W. C.; Nairn, R. Characteristics of a human cell line transformed by DNA from adenovirus type 5. *J. Gen. Virol.* **1977**, *36*, 59-72.

110. Yang, Y.; Li, Q.; Ertl, H. C.; Wilson, J. M. Cellular immunity to viral antigens limit E1-deleted adenoviruses for gene therapy. *Proc. Natl. Acad. Sci. USA*, **1994**, *91*, 4407-4411.

111. Engelhardt, J. F.; Ye, X.; Doranz, B.; Wilson, J. M. Abalation of E2A in recombinant adenoviruses improves transgene persistence and decreases inflammatory response in mouse liver. *Proc. Natl. Acad. Sci. USA*, **1994**, *91*, 6196-6200.

112. Perez-Cruet, M. J.; Trask, T. W.; Chen, S. H.; Goodman, J. C.; Woo, S. L.; Grossman, R. G.; Shine, H. D. Adenovirus-mediated gene therapy of experimental gliomas. *J. Neurosci. Res.* **1994**, *39*, 506-511.

113. Chen, S. H.; Shine, H. D.; Goodman, J. C.; Grossman, R. G.; Woo, S. L. Gene therapy for brain tumors: regression of experimental gliomas by adenovirus-mediated gene transfer in vivo. *Proc. Natl. Acad. Sci. USA* **1994**, *91*, 3054-3057.

114. Vincent, A. J.; Vogels, R.; Someren, G. V.; Esandi, M. C.; Noteboom, J. L.; Avezaat, C. J.; Vecht, C.; Bekkum, D. W.; Valerio, D.; Bout, A.; Hoogerbrugge, P. M. Herpes simplex virus thymidine kinase gene therapy for rat malignant brain tumors. *Hum. Gene Ther.* **1996**, *7*, 197-205.

115. Smythe, W. R.; Hwang, H. C.; Elshami, A. A.; Amin, K. M.; Albelda, S. M.; Kaiser, L. R. Differential sensitivity of thoracic malignant tumors to adenovirus-mediated drug sensitization gene therapy. *J. Thorac. Cardiovasc. Surg.* **1995**, *109*, 626-630.

116. Smythe, W. R.; Hwang, H. C.; Amin, K. M.; Eck, S. L.; Davidson, B. L.; Wilson, J. M.; Kaiser, L. R.; Albelda, S. M. Use of recombinant adenovirus to transfer the herpes simplex virus thymidine kinase (HSVtk) gene to thoracic neoplasms: an effective in vitro drug sensitization system. *Cancer Res.* **1994**, *54*, 2055-2059.

117. Smythe, W. R.; Hwang, H. C.; Elshami, A. A.; Amin, K. M.; Eck, S. L.; Davidson, B. L.; Wilson, J. M.; Kaiser, L. R.; Albelda, S. M. Treatment of experimental human mesothelioma using adenovirus transfer of the herpes simplex thymidine kinase gene. *Ann. Surg.* **1995**, *222*, 78-86.

118. Hwang, H. C.; Smythe, W. R.; Elshami, A. A.; Kucharczuk, J. C.; Amin, K. M.; Williams, J. P.; Litzky, L. A.; Kaiser, L. R.; Albelda, S. M. Gene therapy using adenovirus carrying the herpes simplex-thymidine kinase gene to treat in vivo models of human malignant mesothelioma and lung cancer. *Am. J. Resp. Cell Mol. Biol.* **1995**, *13*, 7-16.

119. Elshami, A. A.; Kucharczuk, J. C.; Zhang, H. B.; Smythe, W. R.; Hwang, H. C.; Litzky, L. A.; Kaiser, L. R.; Albelda, S. M. Treatment of pleural mesothelioma in an immunocompetent rat model utilizing adenoviral transfer of the herpes simplex virus thymidine kinase gene. *Hum. Gene Ther.* **1996**, *7*, 141-148.

120. Elshami, A. A.; Kucharczuk, J. C.; Sterman, D. H.; Smythe, W. R.; Hwang, H. C.; Amin, K. M.; Litzky, L. A.; Albelda, S. M.; Kaiser, L. R. The role of immunosuppression in the efficacy of cancer gene therapy using adenovirus transfer of the herpes simplex thymidine kinase gene. *Ann. Surg.* **1995**, *222*, 298-310.

121. Tong, X. W.; Block, A.; Chen, S. H.; Contant, C. F.; Agoulnik, I.; Blankenburg, K.; Kaufman, R. H.; Woo, S. L.; Kieback, D. G. In vivo gene therapy of ovarian cancer by adenovirus-mediated thymidine kinase gene transduction and ganciclovir administration. *Gynecol. Oncol.* **1996**, *61*, 175-179.

122. O'Malley, B. W.; Chen, S. H.; Schwartz, M. R.; Woo, S. L. Adenovirus-mediated gene therapy for human head and neck squamous cell cancer in a nude mouse model. *Cancer Res.* **1995**, *55*, 1080-1085.

123. Goebel, E. A.; Davidson, B. L.; Zabner, J.; Graham, S. M.; Kern, J. A. Adenovirus-mediated gene therapy for head and neck squamous cell carcinomas. *Ann. Otol. Rhinol. Laryngol.* **1996**, *105*, 562-567.

124. Bonnekoh, B.; Greenhalgh, D. A.; Bundman, D. S.; Eckhardt, J. N.; Longley, M. A.; Chen, S. H.; Woo, S. L.; Roop, D. R. Inhibition of melanoma growth by adenoviral-mediated HSV thymidine kinase gene transfer in vivo. *J. Invest. Dermatol.* **1995**, *104*, 313-317.

125. Colak, A.; Goodman, J. C.; Chen, S. H.; Woo, S. L.; Grossman, R. G.; Shine, H. D. Adenovirus-mediated gene therapy in an experimental model of breast cancer metastatic to the brain. *Hum. Gene Ther.* **1995**, *6*, 1317-1322.

126. Qian, C.; Bilbao, R.; Bruna, O.; Prieto, J. Induction of sensitivity to ganciclovir in human hepatocellular carcinoma cells by adenovirus-mediated gene transfer of herpes simplex virus thymidine kinase. *Hepatology* **1995**, *22*, 118-123.

127. Colak, A.; Goodman, J. C.; Chen, S. H.; Woo, S. L.; Grossman, R. G.; Shine, H. D. Adenovirus-mediated gene therapy for experimental

spinal cord tumors: tumoricidal efficacy and functional outcome. *Brain Res.* **1995**, *691*, 76-82.

128. Eastham, J. A.; Chen, S. H.; Sehgal, I.; Yang, G.; Timme, T. L.; Hall, S. J.; Woo, S. L.; Thompson, T. C. Prostate cancer gene therapy: herpes simplex virus thymidine kinase gene transduction followed by ganciclovir in mouse and human prostate cancer models. *Hum. Gene Ther.* **1996**, *7*, 515-523.

129. Kotin, R. M.; Linden, R. M.; Berns, K. I. Characterization of a preferred site on chromosome 19q for integration of adeno-associated virus DNA by non-homologous recombination. *EMBO J.* **1992**, *11*, 5071-5078.

130. Su, H.; Chang, J. C.; Xu, S. M.; Kan, Y. W. Selective killing of AFP-positive hepatocellular carcinoma cells by adeno-associated virus transfer of the herpes simplex virus thymidine kinase gene. *Hum. Gene Ther.* **1996**, *7*, 463-470.

131. Boviatsis, E. J.; Park, J. S.; Sena-Esteves, M.; Kramm, C. M.; Chase, M.; Efird, J. T.; Wei, M. X.; Breakefield, X. O.; Chiocca, E. A. Long-term survival of rats harboring brain neoplasms treated with ganciclovir and a herpes simplex virus vector that retains an intact thymidine kinase gene. *Cancer Res.* **1994**, *54*, 5745-5751.

132. Sugaya, S.; Fujita, K.; Kikuchi, A.; Ueda, H.; Takakuwa, K.; Kodama, S.; Tanaka, K. Inhibition of tumor growth by direct intratumoral gene transfer of herpes simplex virus thymidine kinase gene with DNA-liposome complexes. *Hum. Gene Ther.* **1996**, *7*, 223-230.

133. Shimizu, N.; Chen, J.; Gamou, S.; Takayanagi, A. Immunogene approach toward cancer therapy using erythrocyte growth factor receptor-mediated gene delivery. *Cancer Gene Ther.* **1996**, *3*, 113-120.

134. Miyao, Y.; Shimizu, K.; Moriuchi, S.; Yamada, M.; Nakahira, K.; Nakajima, K.; Nakao, J.; Kuriyama, S.; Tsujii, T.; Mikoshiba, K.; Hayakawa, T.; Ikenaka, K. Selective expression of foreign genes in glioma cells: use of the mouse myelin basic protein gene promoter to direct toxic gene expression. *J. Neurosci. Res.* **1993**, *36*, 472-479.

135. DiMaio, J. M.; Clary, B. M.; Via, D. F.; Coveney, E.; Pappas, T. N.; Lyerly, H. K. Directed enzyme pro-drug gene therapy for pancreatic cancer in vivo. *Surgery* **1994**, *116*, 205-213.

136. Tanaka, T.; Kanai, F.; Okabe, S.; Yoshida, Y.; Wakimoto, H.; Hamada, H.; Shiratori, Y.; Lan, K.; Ishitobi, M.; Omata, M. Adenovirus-mediated prodrug gene therapy for carcinoembryonic antigen-producing human gastric carcinoma cells in vitro. *Cancer Res.* **1996**, *56*, 1341-1345.

137. Osaki, T.; Tanio, Y.; Tachibana, I.; Hosoe, S.; Kumagai, T.; Kawase, I.; Oikawa, S.; Kishimoto, T. Gene therapy for carcinoembryonic antigen-producing human lung cancer cells by cell type-specific expression of herpes simplex virus thymidine kinase gene. *Cancer Res.* **1994**, *54*, 5258-5261.

138. Ido, A.; Nakata, K.; Kato, Y.; Nakao, K.; Murata, K.; Fujita, M.; Ishii, N.; Tamaoki, T.; Shiku, H.; Nagataki, S. Gene therapy for hepatoma cells using a retrovirus vector carrying herpes simplex virus thymidine kinase gene under the control of human alpha-fetoprotein gene promoter. *Cancer Res.* **1995**, *55*, 3105-3109.

139. Kanai, F.; Shiratori, Y.; Yoshida, Y.; Wakimoto, H.; Hamada, H.; Kanegae, Y.; Saito, I.; Nakabayashi, H.; Tamaoki, T.; Tanaka, T.; Lan, K. H.; Kato, N.; Shiina, S.; Omata, M. Gene therapy for alpha-fetoprotein-producing human hepatoma cells by adenovirus-mediated transfer of the herpes simplex virus thymidine kinase gene. *Hepatology* **1996**, *23*, 1359-1368.

140. Kaneko, S.; Hallenbeck, P.; Kotani, T.; Nakabayashi, H.; McGarrity, G.; Tamaoki, T.; Anderson, W. F.; Chiang, Y. L. Adenovirus-mediated gene therapy of hepatocellular carcinoma using cancer-specific gene expression. *Cancer Res.* **1995**, *55*, 5283-5287.

141. Wills, K. N.; Huang, W. M.; Harris, M. P.; Machemer, T.; Maneval, D. C.; Gregory, R. J. Gene therapy for hepatocellular carcinoma: chemosensitivity conferred by adenovirus-mediated transfer of the HSV-1 thymidine kinase gene. *Cancer Gene Ther.* **1995**, *2*, 191-197.

142. Vile, R. G.; Nelson, J. A.; Castleden, S.; Chong, H.; Hart, I. R. Systemic gene therapy of murine melanoma using tissue specific expression of the HSVtk gene involves an immune component. *Cancer Res.* **1994**, *54*, 6228-6234.

143. Kumagai, T.; Tanio, Y.; Osaki, T.; Hosoe, S.; Tachibana, I.; Ueno, K.; Kijima, T.; Horai, T.; Kishimoto, T. Eradication of Myc-overexpressing small cell lung cancer cells transfected with herpes simplex virus thymidine kinase gene containing Myc-Max response elements. *Cancer Res.* **1996**, *56*, 354-358.

144. Smith, M. J.; Rousculp, M. D.; Goldsmith, K. T.; Curiel, D. T.; Garver, R. I. Surfactant protein A-directed toxin gene kills lung cancer cells in vitro. *Hum. Gene Ther.* **1994**, *5*, 29-35.

145. Chen, L.; Chen, D.; Manome, Y.; Dong, Y.; Fine, H. A.; Kufe, D. W. Breast cancer selective gene expression and therapy mediated by recombinant adenoviruses containing the DF3/MUC1 promoter. *J. Clin. Invest.* **1995**, *96*, 2775-2782.

146. Manome, Y.; Abe, M.; Hagen, M. F.; Fine, H. A.; Kufe, D. W. Enhancer sequences of the DF3 gene regulate expression of the herpes simplex virus thymidine kinase gene and confer sensitivity of human breast cancer cells to ganciclovir. *Cancer Res.* **1994**, *54*, 5408-5413.

147. Ram, Z.; Walbridge, S.; Heiss, J. D.; Culver, K. W.; Blaese, R. M.; Oldfield, E. H. In vivo transfer of the human interleukin-2 gene: negative tumoricidal results in experimental brain tumors. *J. Neurosurg.* **1994**, *80*, 535-540.

148. O'Malley, B.W.; Cope, K. A.; Chen, S. H.; Li, D.; Schwarta, M. R.; Woo, S. L. Combination gene therapy for oral cancer in a murine model. *Cancer Res.* **1996**, *56*, 1737-1741.

149. Chen, S. H.; Chen, X. H.; Wang, Y.; Kosai, K.; Finegold, M. J.; Rich, S. S.; Woo, S. L. Combination gene therapy for liver metastasis of colon carcinoma in vivo. *Proc. Natl. Acad. Sci. USA* **1995**, *92*, 2577-2581.

150. Chen, S. H.; Kosai, K.; Xu, B.; Pham-Nguyen, K.; Contant, C.; Finegold, M. J.; Woo, S. L. Combination suicide and cytokine gene therapy for hepatic metastases of colon carcinoma: sustained antitumor immunity prolongs animal survival. *Cancer Res.* **1996**, *56*, 3758-3762.

151. Bi, W. L.; Parysek, L. M.; Warnick, R.; Stambrook, P. J. In vitro evidence that metabolic cooperation is responsible for the bystander effect observed with HSV tk retroviral gene therapy. *Hum. Gene Ther.* **1993**, *4*, 725-731.

152. Kuriyama, S.; Nakatani, T.; Masui, K.; Sakamoto, T.; Tominaga, K.; Yoshikawa, M.; Fukui, H.; Ikenaka, K.; Tsujii, T. Bystander effect caused by suicide gene expression indicates the feasibility of gene

therapy for hepatocellular carcinoma. *Hepatology* **1995**, *22*, 1838-1846.

153. Vrionis, F. D.; Wu, J. K.; Qi, P.; Cano, W.; Cherington, V. A more potent bystander cytocidal effect elicited by tumor cells expressing the herpes simplex virus-thymidine kinase gene than by fibroblast virus-producer cells in vitro. *J. Neurosurg.* **1995**, *83*, 698-704.

154. Wu, J. K.; Cano, W. G.; Meylaerts, S. A.; Qi, P.; Vrionis, F.; Cherington, V. Bystander tumoricidal effect in the treatment of experimental brain tumors. *Neurosurgery* **1994**, *35*, 1094-102.

155. Fick, J.; Barker, F. G. n.; Dazin, P.; Westphale, E. M.; Beyer, E. C.; Israel, M. A. The extent of heterocellular communication mediated by gap junctions is predictive of bystander tumor cytotoxicity in vitro. *Proc. Natl. Acad. Sci. USA* **1995**, *92*, 11071-11075.

156. Mesnil, M.; Piccoli, C.; Tiraby, G.; Willecke, K.; Yamasaki, H. Bystander killing of cancer cells by herpes simplex virus thymidine kinase gene is mediated by connexins. *Proc. Natl. Acad. Sci. USA* **1996**, *93*, 1831-1835.

157. Shinoura, N.; Chen, L.; Wani, M. A.; Kim, Y. G.; Larson, J. J.; Warnick, R. E.; Simon, M.; Menon, A. G.; Bi, W. L.; Stambrook, P. J. Protein and messenger RNA expression of connexin43 in astrocytomas: implications in brain tumor gene therapy. *J. Neurosurg.* **1996**, *84*, 839-845.

158. Freeman, S. M.; Whartenby, K. A.; Freeman, J. L.; Abboud, C. N.; Marrogi, A. J. In situ use of suicide genes for cancer therapy. *Sem. Oncol.* **1996**, *23*, 31-45.

159. Colombo, B. M.; Benedetti, S.; Ottolenghi, S.; Mora, M.; Pollo, B.; Poli, G.; Finocchiaro, G. The "bystander effect": association of U-87 cell death with ganciclovir-mediated apoptosis of nearby cells and lack of effect in athymic mice. *Hum. Gene Ther.* **1995**, *6*, 763-772.

160. Hamel, W.; Magnelli, L.; Chiarugi, V. P.; Israel, M. A. Herpes simplex virus thymidine kinase/ganciclovir-mediated apoptotic death of bystander cells. *Cancer Res.* **1996**, *56*, 2697-2702.

161. Barba, D.; Hardin, J.; Sadelain, M.; Gage, F. H. Development of anti-tumor immunity following thymidine kinase-mediated killing of experimental brain tumors. *Proc. Natl. Acad. Sci. USA* **1994**, *91*, 4348-4352.

162. Gagandeep, S.; Brew, R.; Green, B.; Christmas, S. E.; Klatzmann, D.; Poston, G. J.; Kinsella, A. R. Prodrug-activated gene therapy: involvement of an immunological component in the "bystander effect". *Cancer Gene Ther.* **1996**, *3*, 83-88.

163. Freeman, S. M.; Ramesh, R.; Shastri, M.; Munshi, A.; Jensen, A. K.; Marrogi, A. J. The role of cytokines in mediating the bystander effect using HSV-TK xenogeneic cells. *Cancer Lett.* **1995**, *92*, 167-174.

164. Ram, Z.; Walbridge, S.; Shawker, T.; Culver, K. W.; Blaese, R. M.; Oldfield, E. H. The effect of thymidine kinase transduction and ganciclovir therapy on tumor vasculature and growth of 9L gliomas in rats. *J. Neurosurg.* **1994**, *81*, 256-260.

165. Chang, M. W.; Ohno, T.; Gordon, D.; Lu, M. M.; Nabel, G. J.; Nabel, E. G.; Leiden, J. M. Adenovirus-mediated transfer of the herpes simplex virus thymidine kinase gene inhibits vascular smooth muscle cell proliferation and neointima formation following balloon angioplasty of the rat carotid artery. *Mol. Med.* **1995**, *1*, 172-181.

166. Guzman, R. J.; Hirschowitz, E. A.; Brody, S. L.; Crystal, R. G.; Epstein, S. E.; Finkel, T. In vivo suppression of injury-induced vascular smooth muscle cell accumulation using adenovirus-mediated transfer of the herpes simplex virus thymidine kinase gene. *Proc. Natl. Acad. Sci. USA* **1994**, *91*, 10732-10736.

167. Ohno, T.; Gordon, D.; San, H.; Pompili, V. J.; Imperiale, M. J.; Nabel, G. J.; Nabel, E. G. Gene therapy for vascular smooth muscle cell proliferation after arterial injury. *Science* **1994**, *265*, 781-784.

168. Plautz, G.; Nabel, E. G.; Nabel, G. J. Selective elimination of recombinant genes in vivo with a suicide retroviral vector. *New Biol.* **1991**, *3*, 709-715.

169. Drew, W. L.; Buhles, W.; Erlich, K. S. Herpes infection (cytomegalovirus, herpes simplex virus, varicella-zoster virus). How to use gancyclovir and acyclovir. *Infect. Dis. Clin. N. Am.* **1988**, *2*, 495-509.

170. Faulds, D.; Heels, R. C. Gancyclovir, a review of its antiviral activity, pharmacokinetic properties and therapeutic efficacy in cytomegalovirus infection. *Drugs*, **1990**, *39*, 597-638.

171. Balzarini, J.; Bohman, C.; Walker, R. T.; De Clercq, E. Comparative cytostatic activity of different antiherpetic drugs against herpes simplex virus thymidine kinase gene-transfected tumor cells. *Mol. Pharmacol.* **1994**, *45*, 1253-1258.

172. Balzarini, J.; De Clercq, E.; Ayusawa, D.; Seno, T. Murine mammary FM3A carcinoma cells transformed with the herpes simplex virus type 1 thymidine kinase gene are highly sensitive to the growth-inhibitory properties of (E)-5-(2-bromovinyl)-2'-deoxyuridine and related compounds. *FEBS Lett.* **1985**, *185*, 95-100.

173. Balzarini, J.; De Clercq, E. Inhibitory effects of (E)-5-(2-bromovinyl)-2'-deoxyuridine (BVDU) and related compounds on herpes simplex virus (HSV)-infected cells and HSV thymidine kinase gene-transformed cells. *Methods Find. Exp. Clin. Pharmacol.* **1989**, *11*, 379-389.

174. Balzarini, J. Herpes simplex virus thymidine kinase gene-transfected tumor cells: sensitivity to antiherpetic drugs. *Nucleosides Nucleotides* **1996**, *15*, 821-831.

175. Bohman, C.; Balzarini, J.; Wigerinck, P.; Van Aerschot, A.; Herdewijn, P.; De Clercq, E. Mechanism of cytostatic action of novel 5-(thien-2-yl)- and 5-(furan-2-yl)-substituted pyrimidine nucleoside analogues against tumor cells transfected by the thymidine kinase gene of herpes simplex virus. *J. Biol. Chem.* **1994**, *269*, 8036-8043.

176. Balzarini, J.; Bohman, C.; De Clercq, E. Differential mechanism of cytostatic effect of (*E*)-5-(2-bromovinyl)-2'-deoxyuridine, 9-(1,3-dihydroxy-2-propoxymethyl)guanine, and other antiherpetic drugs on tumor cells transfected by the thymidine kinase gene of herpes simplex virus type 1 or type 2. *J. Biol. Chem.* **1993**, *268*, 6332-6337.

177. Santi, D. V. Perspectives on the design and biochemical pharmacology of inhibitors of thymidylate synthetase. *J. Med. Chem.* **1980**, *23*, 103-111.

178. Balzarini, J.; De Clercq, E.; Verbruggen, A.; Ayusawa, D.; Seno, T. Highly selective cytostatic activity of (*E*)-5-(2-bromovinyl)-2'-deoxyuridine derivatives for murine mammary carcinoma (FM3A) cells transformed with the herpes simplex type 1 thymidine kinase gene. *Mol. Pharmacol.* **1985**, *28*, 581-587.

179. Balzarini, J.; De Clercq, E.; Verbruggen, A.; Ayusawa, D.; Shimizu, K.; Seno, T. Thymidylate synthase is the principle target enzyme for

the cytostatic activity of (*E*)-5-(2-bromovinyl)-2'-deoxyuridine against murine mammary carcinoma (FM3A) cells transformed with the herpes simplex type 1 or type 2 thymidine kinase gene. ***Mol. Pharmacol.*** **1987**, *32*, 410-416.

180. Hirota, Y.; Arao, Y.; Matsumoto, A.; Nii, S.; Wataya, Y. Different mechanisms of inhibition of DNA synthesis by (E)-5-(2-bromovinyl)-2'-deoxyuridine in cells transfected with gene for thymidine kinase of herpes simplex virus type 1 and in cells infected with the virus. *Nucleosides Nucleotides* **1995**, *14*, 2079-2087.

181. Saito, Y.; Price, R. W.; Rottenberg, D. A.; Fox, J. J.; Watanabe, K. A. Philips, F. A. Quantitative autoradiographic mapping of herpes simplex encephalitis with radiolabeled antiviral drug. *Science*, **1982**, *217*, 1151-1153.

182. Saito, Y.; Rubenstein, R.; Price, R. W.; Fox, J. J.; Watanabe, K. A. Diagnostic imaging of herpes simplex virus encephalitis using radiolabeled antiviral drug: autoradiographic assessment in an animal model. *Ann. Neurol.* **1984**, *15*, 548-559.

183. Price, R.; Cardle, K.; Watanabe, K. The use of antiviral drugs to image herpes encephalitis. *Cancer Res.* **1983**, *43*, 3619-3627.

184. Whitley, R. J. Herpes simplex virus infections of the central nervous system. *Drugs* **1991**, *42*, 406-427.

185. Samuel, J.; Knaus, E. E.; Wiebe, L. I.; Tyrrell, D.L. Synthesis of ^{131}I, ^{125}I, and ^{82}Br labelled (*E*)-5-(2-halovinyl)-2'-deoxyuridines. *Int. J. Appl. Radiat. Isot.* **1984**, *35*, 1049-1052.

186. De Clercq, E.; Descamps, J.; Verhelst, G.; Walker, R. T.; Jones, A. S.; Torrence, P. F.; Shugar, D. Comparative efficacy of antiherpes drugs against different strains of herpes simplex virus. *J. Infect. Dis.* **1980**, *141*, 563-574.

187. Descamps, J.; De Clercq, E. Specific phosphorylation of E-5-(2-iodovinyl)-2'-deoxyuridine by herpes simplex virus-infected cells. *J. Biol. Chem.* **1981**, *256*, 5973-5976.

188. Gill, M. J.; Samuel, J.; Wiebe, L. I.; Knaus, E. E.; Tyrrell, D. L. Quantitative uptake studies of ^{131}I-labeled (E)-5-(2-iodovinyl)-2'-deoxyuridine in herpes simplex virus-infected cells in vitro. *Antimicrob. Agents Chemother.* **1984**, *25*, 476-478.

189. Samuel, J.; Gill, M. J.; Knaus, E. E.; Wiebe, L. I.; Tyrrell, D.L. Radiohalogenated (E)-5-(2-halovinyl)-2'-deoxyuridines. *J. Label. Compd. Radiopharm.* **1984**, *21*, 1104-1106.

190. Samuel, J.; Gill, M. J.; Iwashina, T.; Tovell, D. R.; Tyrrell, D. L.; Knaus, E. E.; Wiebe, L. I. Pharmacokinetics and metabolism of (E)-5-(2-[^{131}I]iodovinyl)-2'-deoxyuridine in dogs. *Antimicrob. Agents Chemother.* **1986**, *29*, 320-324.

191. Klapper, P. E.; Cleator, G. M.; Bruce, J. M.; Longson, M. Penetration of the blood-brain barrier by the antiviral drug (E)-5-(2-iodovinyl)-2'-deoxyuridine in a rat model of herpes encephalitis. *Drug Des. Del.* **1988**, *3*, 57-68.

192. Cleator, G. M.; Klapper, P. E.; Lewis, A. G.; Sharma, H. L.; Longson, M. Specific neuro-radiological diagnosis of herpes encephalitis in an animal model. *Arch. Virol.* **1988**, *101*, 1-12.

193. Tovell, D. R.; Samuel, J.; Mercer, J. R.; Misra, H. K.; Xu, L.; Wiebe, L. I.; Tyrrell, D. L.; Knaus, E. E. The in vitro evaluation of nucleoside analogues as probes for use in the non-invasive diagnosis of herpes simplex encephalitis. *Drug Des. Del.* **1988**, *3*, 213-221.

194. Iwashina, T.; Tovell, D. R.; Xu, L.; Tyrrell, D. L.; Knaus, E. E.; Wiebe, L. I. Synthesis and antiviral activity of IVFRU, a potential probe for the non-invasive diagnosis of herpes simplex encephalitis. *Drug Des. Del.* **1988**, *3*, 309-321.

195. Schroth, G.; Gawehn, J.; Thron, A.; Vallbracht, A.; Voigt, K. Early diagnosis of herpes simplex encephalitis by MRI. *Neurology* **1987**, *37*, 179-183.

196. Schmidbauer, M.; Podreka, I.; Wimberger, D.; Oder, W.; Koch, G.; Wenger, S.; Goldenberg, G.; Asenbaum, S.; Deecke, L. SPECT and MR imaging in herpes simplex encephalitis. *J. Comput. Assist. Tomogr.* **1991**, *15*, 811-815.

197. Lane, R.; Kirkbride, V.; Hughes, P.; Jones, B.; Costa, D. Diagnosis of herpes simplex encephalitis by single photon emission tomography. *Lancet* **1989**, *1*, 778-779.

198. Tjuvajev, J. G.; Stockhammer, G.; Desai, R.; Uehara, H.; Watanabe, K.; Gansbacher, B.; Blasberg, R. G. Imaging the expression of transfected genes in vivo. *Cancer Res.* **1995**, *55*, 6126-6132.

199. Tjuvajev, J. G.; Finn, R.; Watanabe, K.; Joshi, R.; Oku, T.; Kennedy, J.; Beattie, B.; Koutcher, J.; Larson, S.; Blasberg, R. G. Noninvasive imaging of herpes virus thymidine kinase gene transfer and expression: a potential method for monitoring clinical gene therapy. *Cancer Res.* **1996**, *56*, 4087-4095.

200. Bodor, N.; Farag, H.; Brewster, M. E. Site-specific, sustained release of drugs to the brain. *Science* **1981**, *214*, 1370-1372.

201. Rand, K. H.; Bodor, N.; El Koussi, A. A.; Raad, I.; Miyake, A.; Houck, H.; Gildersleeve, N. Potential treatment of herpes simplex virus encephalitis by brain-specific delivery of trifluorothymidine using a dihydropyridine↔pyridinium salt type redox delivery system. *J. Med. Virol.* **1986**, *20*, 1-8.

202. El Koussi, A.; Bodor, N. Improved delivery through biological membranes XXV. Enhanced and sustained delivery of trifluorothymidine to the brain using a dihydropyridine↔pyridinium salt type redox delivery system. *Drug Des. Del.* **1987**, *1*, 275-283.

203. Brewster, M. E.; Raghavan, K.; Pop, E.; Bodor, N. Enhanced delivery of ganciclovir to the brain through the use of redox targeting. *Antimicrob. Agents Chemother.* **1994**, *38*, 817-823.

204. Chikhale, P.; Bodor, N. Improved delivery of acyclovir to the skin using a dihydrotrigonelline↔trigonelline redox carrier. *J. Pharm. Sci.* **1991**, *80*, 402-403.

205. Kumar, R.; Ji, G.; Wiebe, L. I.; Knaus, E. E. Synthesis of brain-targeted 5-iodo-, 5-vinyl- and (E)-5-(2-iodovinyl)-2'-deoxyuridines coupled to a dihydropyridine↔pyridinium salt redox chemical delivery system. *J. Heterocyclic Chem.* **1991**, *28*, 711-715.

206. Codington, J. F.; Doerr, I. L.; Fox J. J. Nucleosides. XVIII. Synthesis of 2'-fluorothymidine, 2'-fluorodeoxyuridine and other 2'-halogeno-2'-deoxynucleosides. *J. Org. Chem.* **1964**, *29*, 558-564.

207. Mercer, J. R.; Xu, L. H.; Knaus, E. E.; Wiebe, L. I. Synthesis and tumor uptake of 5-^{82}Br and 5-^{131}I-labeled 5-halo-1-(2-fluoro-2-deoxy-β-D-ribofuranosyl)uracils. *J. Med. Chem.* **1989**, *32*, 1289-1294.

208. Robins, M. J.; Manfredini, S.; Wood, S. G.; Wanklin, R. J.; Rennie, B. A.; Sacks, S. L. Nucleic acid related compounds. 65. New syntheses

of 1-(β-D-arabinofuranosyl)-5-(E)-(2-iodovinyl)uracil (IVAraU) from vinylsilane precursors. Radioiodine uptake as a marker for thymidine kinase positive herpes viral infections. *J. Med. Chem.* **1991**, *34*, 2275-2280.

209. Cunico, R. F.; Clayton, F. J. trans-β-Trimethylsilylvinyllithium. *J. Org. Chem.* **1976**, *41*, 1480-1482.

210. Ayusawa, D.; Shimizu, K.; Seno, T.; Balzarini, J.; De Clercq E. Establishment of mutant FM3A murine mammary carcinoma cell lines transformed with the herpes simplex virus type 1 thymidine kinase gene. *Jpn. J. Cancer Res.* **1985**, *76*, 984-988.

211. Shimizu, K. L.; Ren, L.; Ayusawa, D.; Seno, T.; Balzarini, J.; De Clercq, E. Establishment of mutant murine mammary carcinoma FM3A cell strains transformed with the herpes simplex virus type 2 thymidine kinase gene. *Cell Struct. Funct.* **1986**, *11*, 295-301.

212. Watanabe, K. A.; Su, T. L.; Reichman, U.; Greenberg, N.; Lopez, C.; Fox, J. J. Nucleosides. 129. Synthesis of antiviral nucleosides: 5-Alkenyl-1-(2-deoxy-2-fluoro-β-D-arabinofuranosyl)uracils. *J. Med. Chem.* **1984**, *27*, 91-94.

213. Balzarini, J.; De Clercq, E. Strategies for the measurements of the inhibitory effects of thymidine analogs on the activity of thymidylate synthase in intact murine leukemia L1210 cells. *Biochim. Biophys. Acta.* **1984**, *785*, 36-45.

214. Verbruggen, A.; Julien, C.; De Clercq, E.; De Roo, M. Simple quantitative radioiodination of (E)-5-(2-iodovinyl)-2'-deoxyuridine (IVDU) by exchange labelling. *Appl. Radiat. Isot.* **1986**, *37*, 355-357.

215. Dougan, H.; Rennie, B. A.; Lyster, D. M.; Sacks, S. L. No-carrier-added [^{123}I]-1-(β-D-arabinofuranosyl)-5-(E)-(2-iodovinyl)uracil (IVaraU): High yielding radiolabeling via organotin and exchange reactions. *Appl. Radiat. Isot.* **1994**, *45*, 795-801.

216. Crisp, G. T. Synthesis of 5-alkenyl-2'-deoxyuridines via organostannanes. *Synth. Commun.* **1989**, *19*, 2117-2123.

217. Balzarini, J.; De Clercq, E.; Verbruggen, A.; Crumpacker, C.; Ayusawa, D.; Seno, T. Inreased sensitivity of thymidine kinase-deficient (TK$^-$) tumor cell lines to the cell growth inhibitory effects of

(E)-5-(2-bromovinyl)-2'-deoxyuridine (BVDU) and related compounds. *Anticancer Res.* **1986**, *6*, 1077-1084.

218. Dischino, D. D.; Welch, M. J.; Kilbourn, M. R.; Raichle, M. E. Relationship between lipophilicity and brain extraction of C-11-labelled radiopharmaceuticals. *J. Nucl. Med.* **1983**, *24*, 1030-1038.

219. Little, R.; Bailey, D.; Brewster, M. E.; Estes, K. S.; Clemmons, R. M.; Saab, A.; Bodor, N. Improved delivery through biological membranes XXXIII. Brain-enhanced delivery of azidothymidine (AZT). *J. Biopharm. Sci.* **1990**, *1*, 1-18.

220. Aaronson, S. A.; Weaver, C. A. Characterization of murine sarcoma virus (Kirsten) transformation of mouse and human cells. *J. Gen. Virol.* **1971**, *13*, 245-252.

221. Perlman, M. E.; Watanabe, K. A.; Schinazi, R. F.; Fox, J. J. Nucleosides. 133. Synthesis of 5-alkenyl-1-(2-deoxy-2-fluoro-β-D-arabinofuranosyl)cytosines and related pyrimidine nucleosides as potential antiviral agents. *J. Med. Chem.* **1985**, *28*, 741-748.

222. Watanabe, K. A.; Su, T. L.; Klein, R. S.; Chu, C. K.; Matsuda, A.; Chun, M. W.; Lopez, C.; Fox, J. J. Nucleosides. 123. Synthesis of antiviral nucleosides: 5-Substituted 1-(2-deoxy-2-halogeno-β-D-arabinofuranosyl)cytosines and -uracils. Some structure-activity relationships. *J. Med. Chem.* **1983**, *26*, 152-156.

223. Gati, W. P.; Knaus, E. E.; Wiebe, L. I. Interaction of 2'-halogeno-2'-deoxyuridines with the human erythrocyte nucleoside transport mechanism. *Mol. Pharmacol.* **1983**, *23*, 146-152.

224. Gati, W. P.; Misra, H. K.; Knaus, E. E.; Wiebe, L. I. Structural modifications at the 2'- and 3'-positions of some pyrimidine nucleosides as determinants of their interaction with the mouse erythrocyte nucleoside transporter. *Biochem. Pharmacol.* **1984**, *33*, 3325-3331.

225. Machida, H.; Sakata, S. In vitro and in vivo antiviral activity of 1-β-D-arabinofuranosyl-*E*-5-(2-bromovinyl)uracil (BV-araU) and related compounds. *Antiviral Res.* **1984**, *4*, 135-141.

226. Gardner, S.; D.; Field, A. M.; Coleman, D. V.; Hulme, B. New papovavirus (BK) isolated from urine after renal transplantation. *Lancet* **1971**, *1*, 1253-1257.

227. Seif, I.; Khoury, G.; Dhar, R. The genome of human papovavirus BKV. *Cell* **1979**, *18*, 67-77.

228. Cooper, M. J.; Miron, S. M. Efficient episomal expression vector for human transitional carcinoma cells. *Hum Gene Ther.* **1993**, *4*, 557-566.

229. Thierry, A. R.; Iskandar, Y. L.; Bryant, J. L.; Rabinovich, P.; Gallo, R. C.; Mahan, L. C. Systemic gene therapy: biodistribution and long-term expression of a transgene in mice. *Proc. Natl. Acad. Sci. USA* **1995**, *92*, 9742-9746.

230. Milanesi, G.; Barbanti-Brodano, G.; Negrini, M.; Lee, D.; Corallini, A.; Caputo, A.; Grossi, M. P.; Ricciardi, R. P. BK virus-plasmid expression vector that persists episomally in human cells and shuttles into Escherichia coli. *Mol. Cell Biol.* **1984**, *4*, 1551-1560.

231. Nordeen, S. K. Luciferase reporter gene vectors for analysis of promoters and enhancers. *Biotechniques* **1988**, *6*, 454-457.

232. Nguyen, V. T.; Morange, M.; Bensaude, O. Firefly luciferase luminescence assays using scintillation counters for quantitation in transfected mammalian cells. *Anal. Biochem.* **1988**, *171*, 404-408.

233. Chen, C.; Okayama, H. High-efficiency transformation of mammalian cells by plasmid DNA. *Mol. Cell Biol.* **1987**, *7*, 2745-2752.

234. Guild, B. C.; Finer, M. F.; Housman, D. E.; Mulligan, R. C. Development of retroviral vectors useful for expressing genes in cultured embryonal and hematopoietic cells in vivo. *J. Virol.* **1988**, *62*, 3795-3801.

235. Wagner, E. F.: Vanek, M.; Vennstrom, B. Transfer of genes into early embryonal carcinoma cells by retrovirus infections: efficient expression from an internal promoter. *EMBO J.* **1985**, *4*, 663-666.

236. De Clercq, E.; Walker, R. T. Synthesis and antiviral properties of 5-vinylpyrimidine nucleoside analogs. *Pharmacol. Ther.* **1984**, *26*, 1-44.

237. Birnboim, H. C; Doly, J. A rapid alkaline extraction procedure for screening recombinant plasmid DNA. *Nucleic Acids Res.* **1979**, *7*, 1513-1523.